2013-12-09

Structural Analysis and Optimization of Skyscrapers Connected with Skybridges and Atria

Amy Jean Taylor McCall
Brigham Young University - Provo

Structural Analysis and Optimization of Skyscrapers Connected with Skybridges and Atria

Amy J. Taylor McCall

A dissertation submitted to the faculty of
Brigham Young University
in partial fulfillment of the requirements for the degree of

Doctor of Philosophy

Richard J. Balling, Chair
Matthew R. Jones
Alan R. Parkinson
Paul W. Richards
Grant G. Schultz

Department of Civil and Environmental Engineering

Brigham Young University

December 2013

ABSTRACT

Structural Analysis and Optimization of Skyscrapers
Connected with Skybridges and Atira

Amy J. Taylor McCall
Department of Civil and Environmental Engineering, BYU
Doctor of Philosophy

Skybridges and atria between buildings are becoming more and more popular. Most current skybridge connections are either roller or rigid-connections. This dissertation presents an investigation of the structural analysis and optimization of skyscraper systems with hinge-connected skybridges, and compares the results to skyscraper systems with roller-connected skybridges and to skyscraper systems without skybridges altogether. Also presented is an investigation of the structural analysis and optimization of skyscrapers both with and without atria between the buildings. It was assumed that the atria envelope was constructed with cushions made from lightweight, transparent, and flexible Ethylene Tetrafluoroethylene (ETFE).

A simplified skyscraper skybridge model (SSSM) was developed to approximate analysis of such systems. The SSSM identifies and includes only the dominant degrees of freedom (DOF's) when assembling the structure stiffness matrix. This greatly reduces computational time and computer memory compared to traditional finite element models (FEM). The SSSM is fast enough to be used with both gradient-based and genetic optimization algorithms. The steps of the SSSM consist of: 1) determination of megacolumn areas, 2) constructing the stiffness matrix, 3) evaluation of volume, weight, mass and period, 4) calculation of lateral force vectors, and 5) calculation of displacement and stress constraints.

Three skyscraper systems were analyzed using both the SSSM and a FEM to compare both the accuracy and efficiency of the SSSM. It was found that the SSSM was very accurate for displacements (translations and rotations), and core, megacolumn, outrigger, and skybridge stress. It was also found that the SSSM analysis time was significantly faster and used far less computer memory than FEM.

Four skyscraper systems were optimized for two different sites, with varying atria and skybridge conditions, using gradient-based and genetic optimization algorithms. The optimization strategy consisted of a series of executions of the sequential quadratic programming (SQP) algorithm, followed by executions of the generalized reduced gradient (GRG) algorithm, followed by executions of a discrete genetic algorithm. The genetic algorithm made significant progress for two of the systems. Optimal results showed that in some cases hinge skybridges and atria envelope produced significantly lighter systems compared to roller, no skybridge, or without atria envelope cases.

Keywords: Amy J. Taylor McCall, skyscrapers, skybridges, structural analysis, optimization, atria, gradient, genetic algorithms

ACKNOWLEDGEMENTS

My structural engineering doctoral studies at Brigham Young University has been a significant personal challenge and achievement. I am grateful for the solid encouragement, support and guidance of several people who have made this learning experience possible. I wish to acknowledge and thank them for their continual support.

I express gratitude to Dr. Richard J. Balling, my teacher, coach, and mentor throughout my engineering education. He has contributed to my growth as an engineer and a teacher. His guidance during the intensive research portion of my studies has been constructive and rewarding. His personal commitment to family and religious belief, along with his professional example is inspiring and motivating to me. I am grateful to have worked with such a qualified professor and exemplar.

I also thank other professors who have had a significant influence on me during my education. They have set an example of effective instructional principles and have provided opportunities for me to teach other students. I thank Dr. Paul W. Richards, Dr. Alan R. Parkinson, and Dr. Steven E. Benzley.

I appreciate the generous financial support I have received from the BYU Civil and Environmental Engineering Department and other donors. Particularly, I am grateful to the Leslie Youd Family, Joseph Layne Black, and King Hussein.

Lastly, I acknowledge my devout appreciation to my husband, Steven A. McCall and both his and my family, who have ever been supportive and encouraging. They have demonstrated persistence, diligence, and sacrifice. I will always be grateful for my husband's smile and positive attitude when I needed it most during this endeavor.

TABLE OF CONTENTS

LIST OF TABLES

LIST OF FIGURES

CHAPTER 1. INTRODUCTION

There is a need to build sustainable cities that are friendly to people, planet, and prosperity. Skybridges and atria satisfy this need. Skybridges and atria between buildings are becoming popular, and there is a need to understand their effect on structural behavior and design.

Skybridges between skyscrapers are appearing more frequently in architectural design. Skybridges increase walkability and reduce ground level congestion by providing more levels for horizontal movement. Wood (2013) underscores the need for skybridges, "It seems completely nonsensical that cities are making a push for ever-denser, ever-taller urban form, but allowing only the ground plane to be the sole physical plane of connection." Skybridges can also save lives by providing multiple emergency escape routes for tall buildings subject to fire or terrorist attack (NewScientist 2006).

The first skybridges between skyscrapers, such as the famous skybridge between the Petronas Towers in Malaysia, were connected to the skyscrapers with roller or slider connections. Such connections allow the skyscrapers to sway independently under lateral loading as shown in Figure 1-1a. Axially stiff skybridges that are hinge-connected to the skyscrapers constrain the skyscrapers to sway in unison as shown in Figure 1-1b. Flexurally stiff skybridges that are rigid-connected to the skyscrapers constrain the skyscrapers to deflect as a cantilever unit as shown in Figure 1-1c. Examples of flexurally-stiff, rigid-connected skybridges that are multiple stories deep exist throughout the world, but examples of hinge-connected skybridges are

rare. There is a need to investigate the structural analysis and optimization of skyscraper systems with hinge-connected skybridges at multiple levels, and to compare the results to skyscraper systems with roller-connected skybridges at multiple levels, and to skyscraper systems without skybridges altogether.

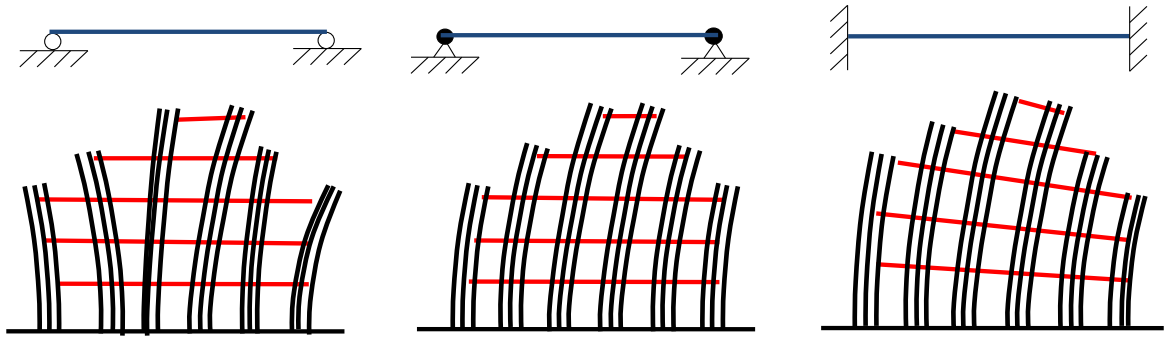

a) Roller b) Hinge c) Rigid

Figure 1-1: Roller, Hinge & Rigid-Connected Skybridges Between Skyscrapers

Atria between buildings are also appearing frequently in architectural design. Atria provide comfortable open space that is protected from adverse weather conditions and has access to natural lighting. Although atria between low-rise buildings are common, atria between high-rise buildings are rare. Atria between skyscrapers have the potential to significantly reduce energy costs for heating and air-conditioning by significantly reducing exposed surface area (Roaf et al. 2005). If the space between buildings is enclosed to create atria, then it becomes difficult to adequately ventilate emissions from gas-powered cars. The car-free environment would have reduced noise, congestion, air pollution, traffic accidents, fossil fuel consumption, and even obesity and stress. Walkability is enhanced by multilevel skybridges, and the comfort is enhanced by enclosed atria as shown in Figure 1-2.

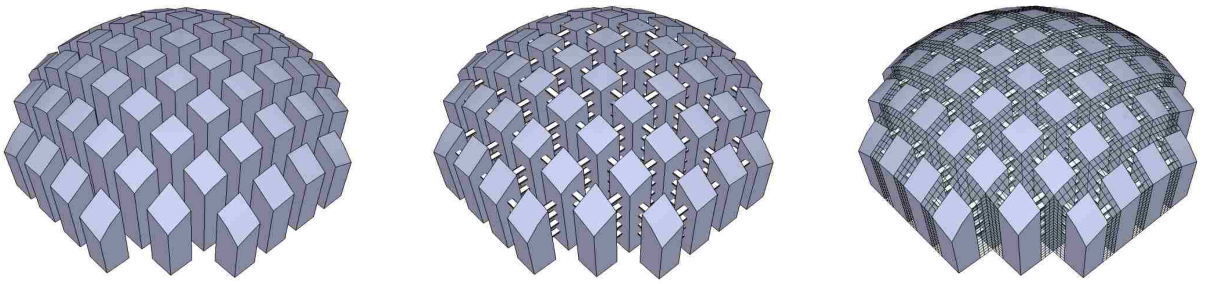

a) Skyscrapers b) Skyscrapers + Skybridges c) Skyscrapers + Skybridges + Atria

Figure 1-2: Car-Free System

The purpose of this work is to understand the behavior and design of skyscrapers connected with skybridges and atria. To do so, it was necessary to develop a fast and accurate approximate linear static model for analyzing connected skyscraper systems. It was also necessary to formulate appropriate optimization problems, and to develop an efficient optimization strategy. A specific objective was to understand the effect of hinge-connected skybridges on optimal design. Another specific objective was to investigate whether it is possible to reduce total structural material with skybridges and atria.

It is assumed that the atrium envelope is constructed with cushions made from lightweight, transparent, and flexible Ethylene Tetrafluoroethylene (ETFE). It is also assumed that the ETFE cushions are supported between the buildings with a cable-spring system that allows the buildings to displace independently. Such a system is shown in Figure 1-3 (Bessey 2012) complete with ventilation and rainwater collection capability. The biggest structural impact of the envelope on the buildings involves wind loading. Wind pressure on the envelope is transferred to the buildings. However, the envelope may actually reduce the total wind load acting on the system because of the reduction of wind load acting directly on interior buildings. Nevertheless, the lateral stiffness of interior buildings would not contribute to the resistance of the total wind load unless skybridges are hinge-connected rather than roller-connected. Thus,

skyscrapers, skybridges, and envelope have been analyzed and optimized simultaneously in the work reported herein.

The number of degrees of freedom (DOF's) in a system of 100 70-story skyscrapers, each with core, megacolumns, and outrigger trusses could easily overwhelm both the memory and computational speed of the fastest computers. The approximate model identifies and includes only the dominant DOF's, and is fast enough to be used with both gradient-based and genetic optimization algorithms.

Four skyscraper systems are optimized for two different sites, with and without envelope, and with varying skybridge connection types. The four systems are:

1) 16-Skyscraper Box

2) 64-Skyscraper Box

3) 25-Skyscraper Pyramid

4) 100-Skyscraper Pyramid

All skyscrapers are the same height in box systems, while the skyscrapers vary in height in the pyramid systems. The 16 and 25-skyscraper systems are considered small systems, while the 64 and 100-skyscraper systems are considered large systems.

Chapter 2 reviews the literature on skybridges, atria between buildings, ETFE atria, analysis models for connected buildings, and optimization methods for tall buildings. Chapter 3 explains the steps of the approximate model. Chapter 4 compares the accuracy of the approximate model to a finite element model (FEM). Chapter 5 presents the four skyscraper systems optimized in this research. Chapter 6 discusses the optimization strategy used in the investigation. Chapter 7 presents optimization results and Chapter 8 presents conclusions.

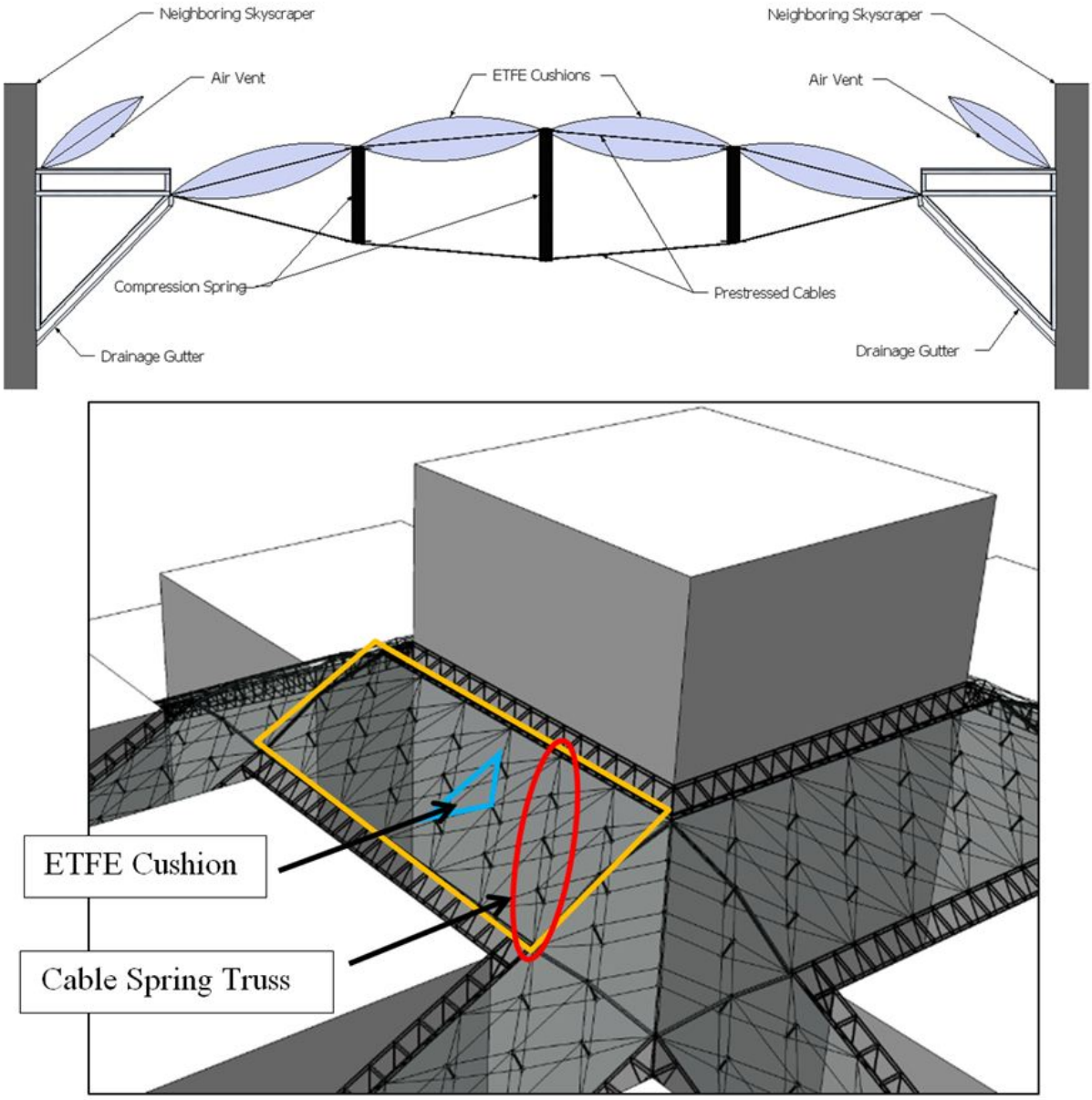

Figure 1-3: ETFE Envelope Between Buildings (Bessey, 2012)

CHAPTER 2. RELATED WORK

The following four sections review literature on the use of skybridges and atria in current building design, analysis models for connected tall buildings, and optimization methods for tall buildings. The highlighted buildings that incorporate the use of skybridges or atria suggest the popularity of their use and the importance of understanding their effect on structural behavior and design. The analysis and optimization models reviewed suggest that others have developed more simplified methods for analyzing and optimizing tall connected buildings but none of them are specific to hinge skybridges with atria envelope connections.

2.1 Skybridges

Buildings that have incorporated skybridges into their design are highlighted in the next few sections and are distinguished by the type of connection between the skybridge and the skyscraper. These connections include roller, rigid, and hinge. There are now over 50 tall buildings around the world that have incorporated skybridges (Wood 2013). These and the following examples further support the popularity and importance of skybridge implementation.

2.1.1 Roller-Connected Skybridges

One of the most prominent examples of a roller-connected skybridge is the Petronas Towers in Kuala Lumpur, Malaysia shown in Figure 2-1. Twin 88-story office towers are connected at 41st story with a skybridge. The main bridge is a two-level steel frame with large

beams and columns that connect to continuous girders. The girders are connected to the two towers with roller bearings, allowing the two towers to sway or twist independently of each other. The skybridge has an inverted V-shaped, two-hinged arch that supports the bridge midspan. The main bridge girders have a rotational pin directly over the arch allowing the bridge to rise and fall as the towers move closer or further apart (Abada 2004).

The Nina Towers in Hong Kong, China are two towers, one 80 stories and one 42 stories with a roller-connected skybridge at the 41st story shown in Figure 2-2 (CTBUH 2007). The lower tower was named after one of Hong Kong's largest privately owned companies, Nina Wang and the tallest tower after her husband, Teddy Wang. Together, both towers are referred to as the Nina Tower (Toronto 2009).

(a) Elevation View (b) Skybridge Frame

Figure 2-1: Petronas Towers (Abada 2004)

(a) Elevation View (CTBUH 2007) (b) Skybridge View (Toronto 2009)

Figure 2-2: Nina Towers

The Pinnacle@Duxton in Singapore is a seven-tower, 50-story, residential complex where each tower is connected to the adjacent towers at the 26th and 50th stories shown in Figure 2-3 (Ming et al. 2010). The skybridge at the 26th story is reserved for the use of residents only as a fire escape, jogging track, fitness center, outdoor gym, child's playground, community plaza, and 2 observation decks. The skybridge on the 50th story is open to public and residents. The structural design of the towers consisted of a reinforced concrete beam-column-slab rigid frame where all loads were transferred directly to the foundation; no transfer beams were used. The skybridges are made of steel 3-dimensional triangular trusses with concrete slabs on top.

Lengths vary with the longest at 48 meters and a width of 20 meters and depth of 3.9 meters. The truss is stable without lateral support and could be erected independently (Engineers 2010).

(a) Elevation View

(b) Skybridge Frame

Figure 2-3: Pinnacle@Duxton (Engineers 2010)

The Linked Hybrid in Beijing, China is an eight-tower 22-story complex connected with skybridges between each building shown in Figure 2-4. The skybridges serve as transportation between each tower but in addition, each skybridge has its own unique function such as housing a swimming pool, a fitness room, a cafe, a gallery, auditorium and a mini salon (Holl 2009). The bridges are steel trusses placed in special "friction pendulum" seismic isolators, allowing the bridges to slide vertically or horizontally relative to the other buildings (Nordenson 2010).

The Highlight Towers in Munich, Germany is a twin tower complex with towers of varying heights, joined by two steel skybridges at the 9th, 10th and 20th stories, which can be disconnected and attached to the tower wherever needed (Emporis 2012), as illustrated in Figure 2-5 (Architectism 2011).

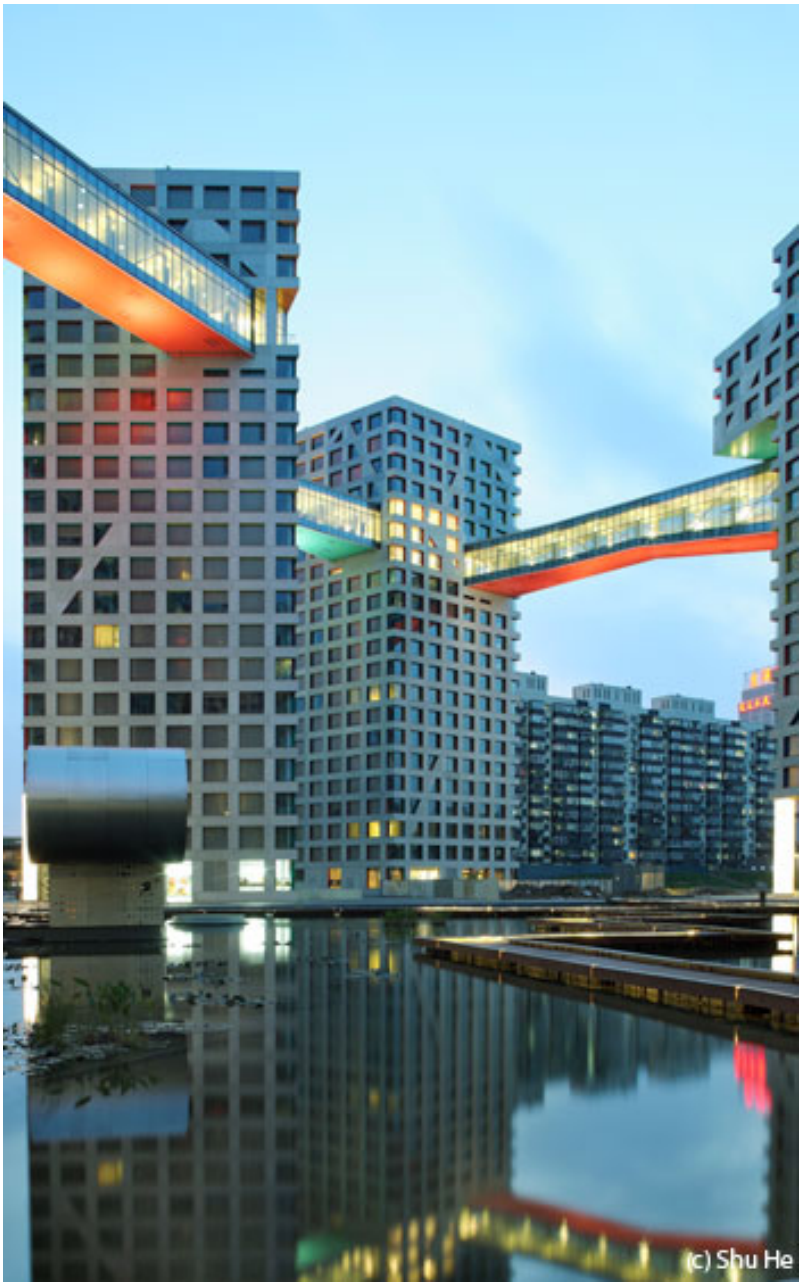

Figure 2-4: Linked Hybrid (Holl 2009)

The National Congress Complex of Brasilia in Brazil was the first modern building to have a bridge between two towers at a height above ground (Wood 2003) shown in Figure 2-6 (Zimbres 2006).

The Kajima Corporation Buildings in Tokyo, Japan was a two-tower building connected together with skybridges at three different levels shown in Figure 2-7 (CTBUH 2013).

The Bahrain World Trade Center is a two-tower 50-story complex in Manama, Bahrain shown in Figure 2-8. The two towers are linked with three skybridges that each hold a wind turbine, which are expected to supply 11-15 percent of the tower's total power consumption (Haklar 2009).

Sky Habitat is a two-tower apartment complex in Singapore 38-stories tall scheduled to be completed in 2016. The two towers are connected with skybridges at multiple levels where the skybridge at the top story has been designated as the "Swimmable Skybridge" and will be built on top of Sky Habitat (Haklar 2009). The swimming pool on the top story extends the length of the skybridge, from tower to tower, as illustrated in Figure 2-9.

Figure 2-5: Highlight Towers (Architectism 2011)

Figure 2-6: National Congress Complex of Brasilia (Zimbres 2006)

Figure 2-7: Kajima Corporation Buildings (CTBUH 2013)

(a) Elevation View (b) Skybridge View

Figure 2-8: Bahrain World Trade Center (Haklar 2009)

Figure 2-9: Sky Habitat Swimmable Skybridge (Haklar 2009)

Marina Bay Sands in Singapore is a three-tower 55-story hotel with a skybridge that connects all three towers at the top called Sands SkyPark. The skybridge houses the longest elevated swimming pool in the world at 191 meters above the ground and rooftop restaurants, club facilities, lush gardens, and a cantilevered observation deck, as illustrated in Figure 2-10. The skybridge has four movement joints beneath the main pools, allowing for separate displacement between each tower (Haklar 2009).

Figure 2-10: Marina Bay Sands Skybridge - SkyPark (Haklar 2009)

2.1.2 Rigid-Connected Skybridges

The Shanghai World Financial Center (SWFC) in Shanghai, China, and the Kingdom Centere in Riyadh, Saudi Arabia are shown in Figure 2-11 (Architect 2009) and Figure 2-13

(CTBUH 2011), respectively. They are both single skyscrapers but with skybridges at the top story. These skybridges do not actually connect separate towers but rather, two portions of the same building in a rigid connection. Both buildings have two of the tallest walkways in the world (Emporis 2008). Note that the skybridge is a deep truss structure connecting the sides of the top of the SWFC in Figure 2-12 (Lee 2013).

Figure 2-11: Shanghai World Financial Center (Architect 2009)

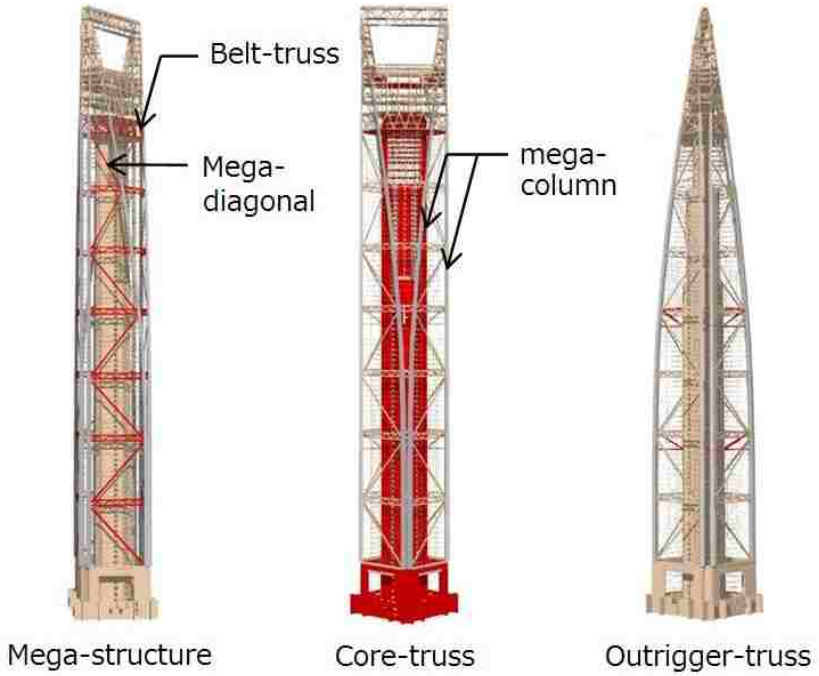

Figure 2-12: Shanghai WFC Structural System Elevation Views (Lee 2013)

Figure 2-13: Kingdom Centere (CTBUH 2011)

The Shanghai International Design Center in Shanghai, China, shown in Figure 2-14, is a two-tower connected building. The two towers are of different heights and are connected by a deep truss skybridge which links the two buildings together at multiple stories. The deep truss skybridge forces the buildings to act in unison under lateral loads (Lu 2009).

The Gate of the Orient in Suzhou, China, shown in Figure 2-15 (SkyscraperCity 2013), incorporates an arch that connects the top eight stories of the two towers, which provides transportation for the hotel and apartments on those stories (Luong and Kwok 2012).

Huaxi Tower in Huaxi, China is a three tower hotel and residential structure connected by skybridges at multiple levels shown in Figure 2-16 (Hartley-Parkinson 2011).

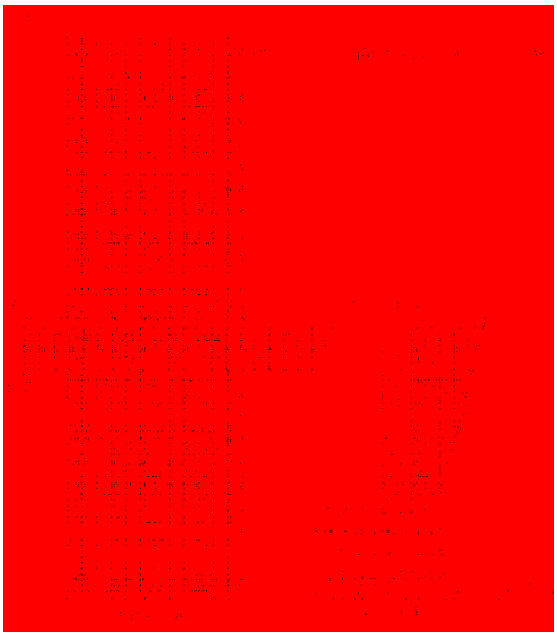

Figure 2-14: Shanghai International Design Center (Lu 2009)

Figure 2-15: Gate of the Orient (SkyscraperCity 2013)

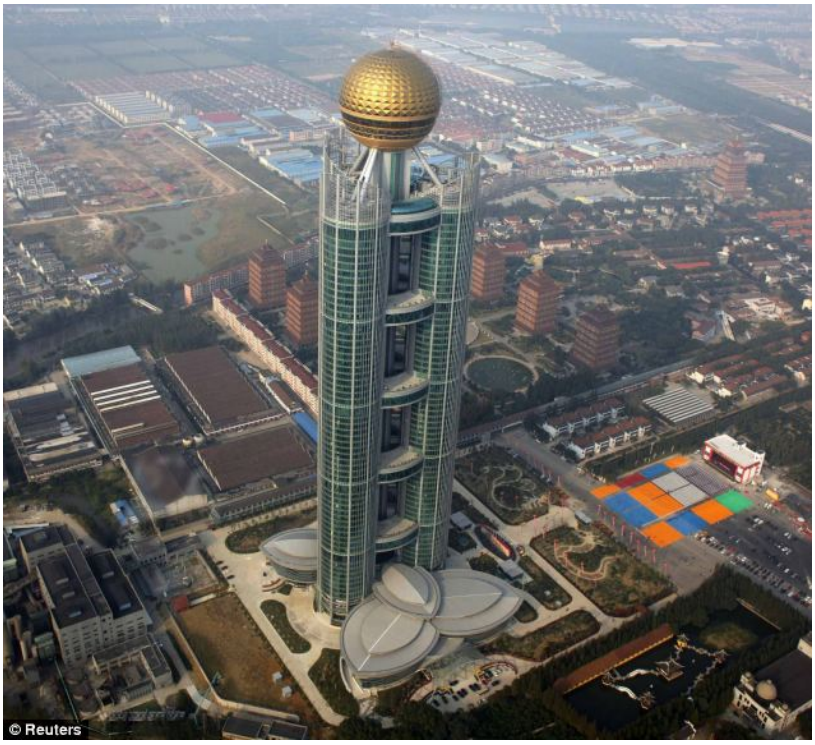

Figure 2-16: Huaxi Tower (Hartley-Parkinson 2011)

The China Central Television Headquarters (CCTV) in Beijing, China shown in Figure 2-17 is another example of connected tall buildings but its connecting "bridge" was designed much different than a typical bridge. It incorporated a combined system of a cantilevering overhang that connected the two towers with an external continuous diagrid tube system, where the diagonal braces visually express the pattern of forces within the structure (Luong and Kwok 2012).

Figure 2-17: China Central Television Headquarters (Luong and Kwok 2012)

The Arch, one of several buildings that make up the commercial and residential project Union Square in Hong Kong, is an 81-story tall residential skyscraper. It is made up of four separate towers called the Star, Sky, Sun and Moon towers. The Sun and Moon towers are

connected at the 69th story and above, which forms the arch below (Wikipedia 2013), as illustrated in Figure 2-18.

Figure 2-18: Union Square - The Arch (Wikipedia 2013)

The East Pacific Center in Shenzhen, China is a skyscraper complex comprised of four towers, 85, 72, 40 and 29 stories tall. The two tallest buildings are connected mid-height by a

rigid connected skybridge shown in the picture on the left of Figure 2-19 (SkyscraperPage 2013). The deep truss of the skybridge is shown in the picture on the right.

(a) Elevation View (b) Skybridge Frame

Figure 2-19: East Pacific Center (SkyscraperPage 2013)

2.1.3 Hinge-Connected Skybridges

Island Tower Sky Club in Fukuoka City, Japan is a three 42-story tower apartment building shown in Figure 2-20 (Wikipedia 2010). The building towers have three-fold rotational symmetry. The towers are connected at the 15th, 26th and 37th stories by truss skybridges. The lower part of the buildings are designed as one structural element with a continous foundation. Each of the three towers have a core wall at the center of the plan with perimeter columns and connecting beams. The trusses are connected to the towers by vibration control dampers which

decrease the overturning response to lateral loads. The skybridges are constructed of concrete slabs supported by steel trusses. Each tower was modeled as a lumped mass model with shear and bending springs in two horizontal directions. The skybridges were modeled to evaluate the effect of the dampers on the building (Nishimura 2011).

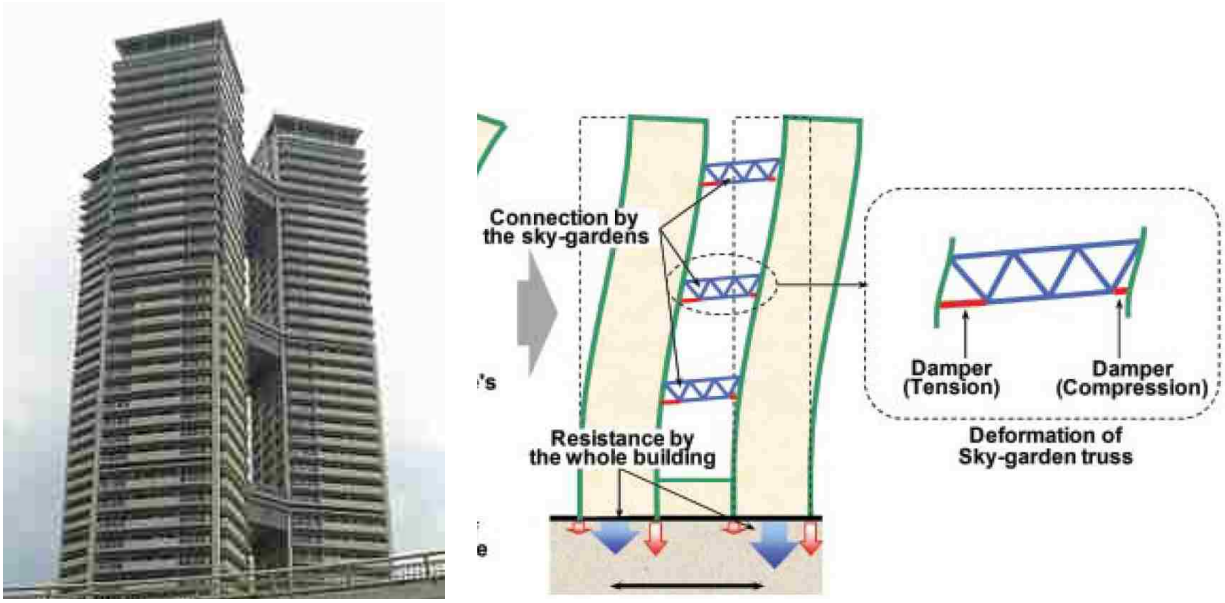

(a) Elevation View (Wikipedia 2010) (b) Skybridge Connections (Nishimura 2011)

Figure 2-20: Island Tower Sky Club

The Umeda Sky Building in Osaka, Japan shown in Figure 2-21 consists of two 40 story towers that are connected at the top story by an atrium platform with a large hole in the middle that serves as an observation deck. The construction of the towers was completed first, and then the deck which was assembled separately, was hoisted into place at the top of the buildings (WikiArquitectura 2010). Because of the long span, the skybridge behavior is closer to hinge-connected than to rigid-connected.

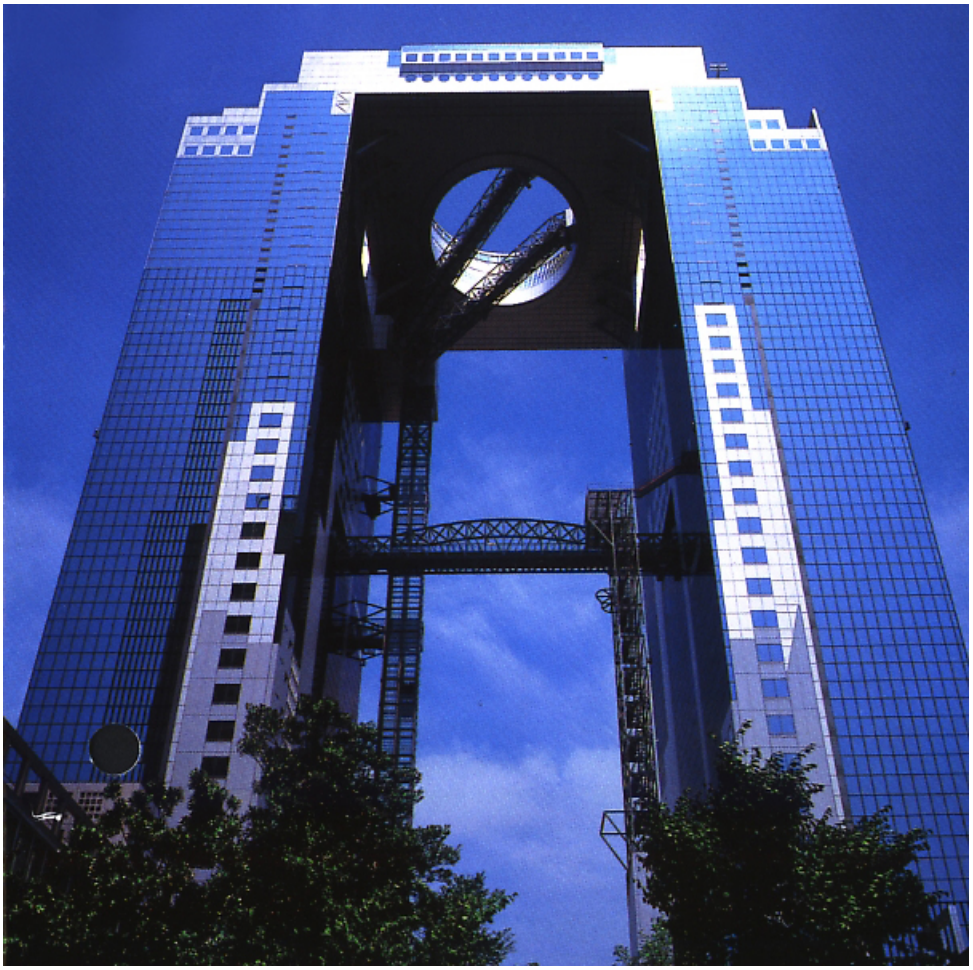

Figure 2-21: Umeda Sky Building (WikiArquitectura 2010)

Zhoushan Eastern Port Business Center, Zhoushan City, China is a two tower office building connected by a steel truss diaphragm at the top shown in Figure 2-22. The two reinforced concrete towers are connected by a steel truss (Zhou 2011). Again, the long span suggests hinge-connected behavior.

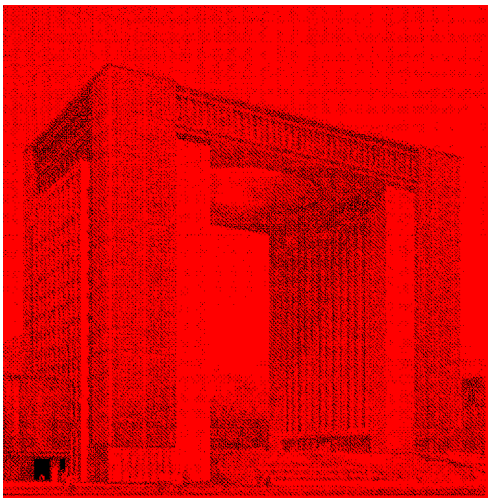

Figure 2-22: Zhoushan Eastern Port Business Center (Zhou 2011)

2.2 Atria Between Buildings

Buildings that have incorporated atria into their design are highlighted in this section. Most of these examples use glass atria envelopes, while some use lightweight ETFE atria envelopes. These examples further support the popularity and importance of atria implementation.

Tower Place in London, England has one of the largest glass atriums in Europe that links two office buildings together, as illustrated in Figure 2-23 (Speyer 2013).

The Network Rail Headquarters, in Milton Keynes, England is a new national center for networking office building, as illustrated in Figure 2-24. Long steel trusses form a large atrium that ties the four blocks of the office together. Each of the office blocks are separate, standalone

structures, linked together by the large central atrium. The atrium is made of steel trusses which support the glass roof. Most of the trusses are supported directly by the office blocks, where others are supported by steel columns (NSC 2011).

(a) Elevation View

(b) Aerial View

Figure 2-23: Tower Place (Speyer 2013)

(a) Aerial View

(b) Atrium Trusses

Figure 2-24: Network Rail Headquarters (NSC 2011)

Alcohol, Tobacco, Firearms and Explosives (ATF) Headquarters in Washington, DC is a highly secure, blast resistant facility, with two eight-story buildings and one six-story radial building, as illustrated in Figure 2-25 (Safdie 2008). The three buildings are connected at levels three through six by an atrium and bridges (Davis 2012).

(a) Elevation View (Davis 2012)

(b) Atrium View (Safdie 2008)

Figure 2-25: ATF Headquarters

City Creek Center in Salt Lake City, Utah is a mixed use project with several buildings incorporating retail, residential, office and parking, as illustrated in Figure 2-26. A retractable, barrel-vaulted roof spans one city block between buildings. Each section is 73 meters long and 18 meters wide. Each retractable roof portion is made of three pairs of glass-covered, arching panels, supported by a steel frame. When closed, the panels provide an air and water-tight seal to shield occupants from inclement weather (AISC 2013).

(a) Aerial View

(b) Atrium View

Figure 2-26: City Creek Center (AISC 2013)

The Parkview Green project in Beijing, China shown in Figure 2-27 has achieved a LEED platinum rating, the highest rating given by the U.S. Green Building Council (Xiaohua 2009). It consists of two 18-story and two 9-story buildings connected with skybridges. The buildings support an ETFE roof, and the sides of the quarter-pyramid are triple-glazed glass. The ETFE roof significantly reduces the gravity loads on the entire structure.

(a) Elevation View (ARUP 2008)

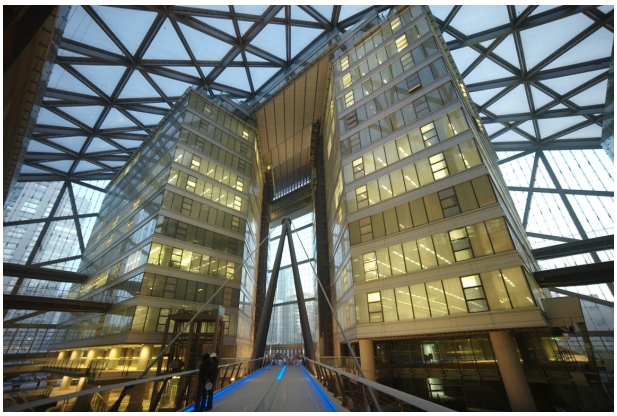

(b) ETFE Roof (OpenBuildings 2011)

Figure 2-27: Parkview Green

The National Geospatial Intelligence Agency located in Springfield, Virginia, is shown in Figure 2-28. The building is composed of two curved overlapping buildings around a central atrium making the overall shape of the building a lens. The atrium roof spans between buildings and is made of an ETFE fabric roof supported by arched steel tube members. A pedestrian bridge also spans between the two towers (AISC 2013).

(a) Aerial View

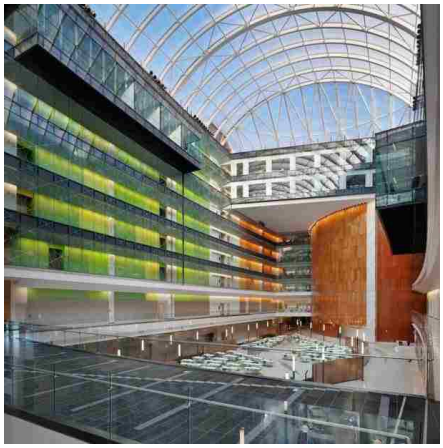

(b) ETFE Atrium

Figure 2-28: National Geospatial Intelligence Agency (AISC 2013)

The Radclyffe School in Oldham, England is an existing five building school complex built in 1975 shown in Figure 2-29. A steel and cable supported ETFE envelope was added to the buildings where they intersect in 2008. The ETFE atrium provides teachers and students with weather protected space for education and recreational purposes with maximum available light but minimal structural weight on the buildings, unlike glass (Architen 2008).

Failsworth School in Oldham, England, built in 1975, is similar to the Radclyffe School in that a cable supported ETFE envelope was added to span between two buildings in 2008, as illustrated in Figure 2-30 (Johnson 2008).

Trinity Walk Shopping Center in Wakefield, England is a partially enclosed shopping center shown in Figure 2-31. An ETFE roof with a supporting steel structure spans the shopping center street while providing natural light to shoppers below (Architen 2011).

Figure 2-29: Radclyffe School (Architen 2008)

Figure 2-30: Failsworth School (Johnson 2008)

Figure 2-31: Trinity Walk Shopping Center (Architen 2011)

The Avenues of Kuwait is the largest shopping mall in Kuwait, as illustrated in Figure 2-32, and the second largest in the Middle East after the Dubai Mall. An arched steel structure

supports the ETFE envelope that spans the pedestrian walkway between shopping buildings (Foiltec 2013).

While the previously reviewed buildings have incorporated atria between separate buildings using ETFE as the envelope material, none of the buildings are high-rise buildings. The work in this dissertation will further extend the effects of ETFE envelopes between skyscrapers. The University of Columbia has specifically considered atria that span voids between skyscrapers for the Columbia Building Intelligence Project. These atria will affect ventilation and drive down energy costs (Anderson 2011). A conceptual design for atria between skyscrapers is shown in Figure 2-33.

Figure 2-32: The Avenues of Kuwait (Foiltec 2013)

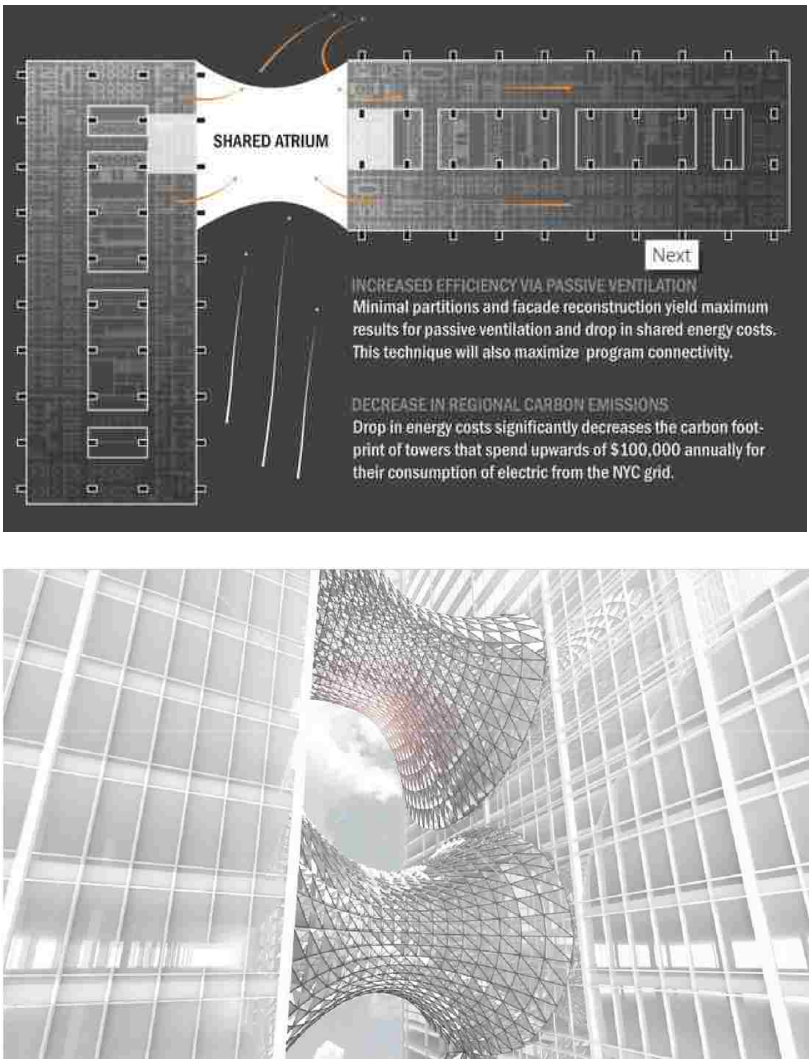

Figure 2-33: Columbia Building Intelligence Project (Anderson 2011)

2.3 Analysis Methods of Connected Tall Buildings

Approximate analysis methods for connected buildings can be broken up into continuum methods and discrete methods. Continuum methods model tall buildings as vertical cantilevers, and approximate displacements as continuous functions of vertical position using flexure/shear beam theory. Discrete methods construct stiffness or flexibility matrices for the system. The finite element method is an example of a discrete method. Lee (2013) explored these two

methods for single skyscrapers and found that there were problems with the continuum methods especially if the buildings incorporated outriggers. The continuum methods cannot reproduce points of contraflexure exhibited in the deflected shapes of tall buildings with outriggers. The work of Lee (2013) is extended in this dissertation to include multiple skyscrapers connected with skybridges and atria. This work goes beyond Lee's work to include calculation of the natural period by inverse iteration.

Most of the studies performed on connected tall buildings found that skybridges improved performance under lateral loading. Lim et al. (2011) developed a simplified analytical model for the structural coupling of generic twin buildings with a skybridge. The skybridge is a fixed-connected member between buildings. The structural coupling of the connected skyscrapers is modeled by introducing a six-degree-of-freedom model lumped at the skybridge level. The equations of motion of the reduced system are derived and under free vibration analysis, the natural frequencies and modal shapes are obtained for relative stiffness of the inter-building beam representing the skybridge. Lim et al. found that the calculated natural frequencies and modes of vibration depend on the skybridge stiffness. The empirical formulas developed can be used for preliminary design of twin buildings with structural coupling.

Lim (2007) studied the effects of structural coupling on the wind-induced response of twin tall buildings connected by a skybridge. Lim found that the adverse aerodynamic interference effects caused by close proximity of the buildings can be significantly reduced by the coupling. Neglecting such interactions may lead to excessively conservative estimates of the wind-induced response of the buildings. Lim stated "the aerodynamic performance of tall buildings has not been fully understood and no comprehensive analytical nor codified models have been developed to adequately address this topic. Accordingly, wind tunnel testing remains

the only reliable tool used in fundamental and applied studies of wind effects on tall buildings," (Lim 2007, p. 383). It was also found that the response at the top of the buildings was greatly affected by structural coupling; top story accelerations were largest when there was no structural coupling. Also, upwind buildings had larger response than downwind buildings. The largest response of the buildings was reduced by 30 percent by incorporating a skybridge. Overall, structural coupling should be taken into account in wind-resistant design of twin tall buildings.

Xie and Irwin (1998) studied structural coupling of connectd twin buildings under base aerodynamic loading and found that the structural coupling led to equal response of the buildings. Boggs and Hosoya (2001) studied a two-tower structure with a common podium, susceptible to coupled wind-induced motions. They measured aerodynamic forces and sampled wind pressures distributed on the building surfaces by using two force balances mounted inside two isolated models of tall buildings. The data accumulated was used to calculate wind-induced building response for structural coupling between the two buildings which can be extended to a larger number of connected tall buildings. Overall, they represent a significant improvement in treatment of aerodynamic loading and structural coupling effects, for twin and multiple buildings.

Nishimura (2011) studied the effect of dampers on three similar slender towers. The Island Tower Sky Club in Fukuoka City, Japan is a super high rise apartment block, previously shown in Figure 2-20. The towers are connected at three different levels by aerial garden trusses. The aerial gardens are connected to the towers by vibration control dampers to reduce the overturning effects of the towers caused by wind and earthquakes. The structure of each tower is provided with a core wall (super-flex-wall) that carries a large part of the seismic load. The validity of the control system implemented is confirmed by vibration tests conducted at the aerial

gardens. For large earthquakes, the structural analysis shows that the dampers can reduce the story drift displacement at upper stories by up to 40 percent. An elaborate control system combining base-isolation and connecting the buildings with skybridges reduces earthquake and wind-induced motion by 30 percent.

Yuan (2011) investigated the effect of connection location on dynamic characteristics of a connected three tower high rise building (The Shanghai International Design Center previously shown in Figure 2-14). The three towers have equal height of 25 stories (100 meters) and are connected between the 19th and 20th story. The three towers are constructed of a frame-shear wall structure, reinforced concrete core wall system and reinforced concrete external frame. Skybridges are rigidly connected to each of the towers. The layout and elevation of the structure is shown in Figure 2-34. Various finite element models were used to determine the effect of different connection locations between buildings. Results show that when the connection is located at the top level, maximum acceleration values are largest and when the connection is at the 18th and 19th levels, max acceleration was smallest. According to modal analysis, the natural periods and mode shapes of different models are obtained and results show that structural natural period and mode shape will be changed when the connection position is changed.

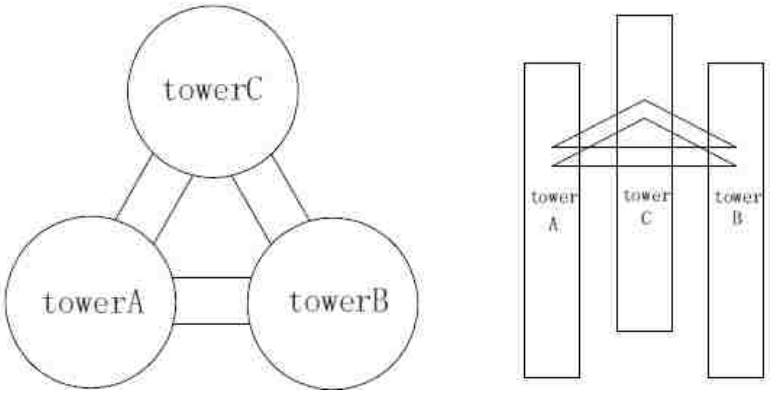

Figure 2-34: Layout and Elevation of Three-Tower Connected High-Rise Structure (Yuan 2011)

Zhou (2011) performed a shaking table model test of the Zhoushan Eastern Port Business Center which is a multi-tower office building, connected by a long-span corridor at its top (previously shown in Figure 2-22). The span of the corridor is 58 meters and is located 69.1 meters above ground which may induce severe vertical vibration during strong earthquakes. A round opening is included in the architectural design as previously shown in Figure 2-22. Experimental results were compared with a FEM and results show that despite structural complexity, the overall responses of the building meet the requirements of the Chinese design code and the torsion of the structure is not a concern. From experimental results, for lower intensity earthquakes, no damage was found at the connection of the truss to the towers but cracks were found in coupling beams at lower levels of the towers. For higher intensity earthquakes, existing cracks in the beams were extended in the tower and new cracks were found in the tower shear walls. Additionally, the connecting truss buckled. Conclusions from these tests found that the connecting truss and the rigid joints between the truss and towers worked well to keep the two towers deforming together under three earthquake levels but the steel truss members buckled. The stiffness reduction due to the existence of the round opening is obvious especially under the major earthquake level. Thus the strength and stiffness of the long-span truss should be improved due to the potentially large vertical acceleration under strong earthquakes.

Mu (2011) investigated the stress response for a high rise twin tower connected with trusses of changing stiffness. The towers are 544 meters tall with 136 stories. The tower consists of a frame core tube structure with eight stories strengthened by outriggers and belt shape trusses. Five trusses connect the two towers at varying heights. A plan view of the connected towers is shown in Figure 2-35. An FEM was used to analyze the building. The results from the

connected towers were compared with a single tower and results indicate that with connected trusses the twin tower connected structures have better performance (less story drift) and higher structural effectiveness. The axial forces in the trusses increase with increased depth of truss and increased height placement in the building. The moment in the truss increases as the truss is increased in height placement in the building.

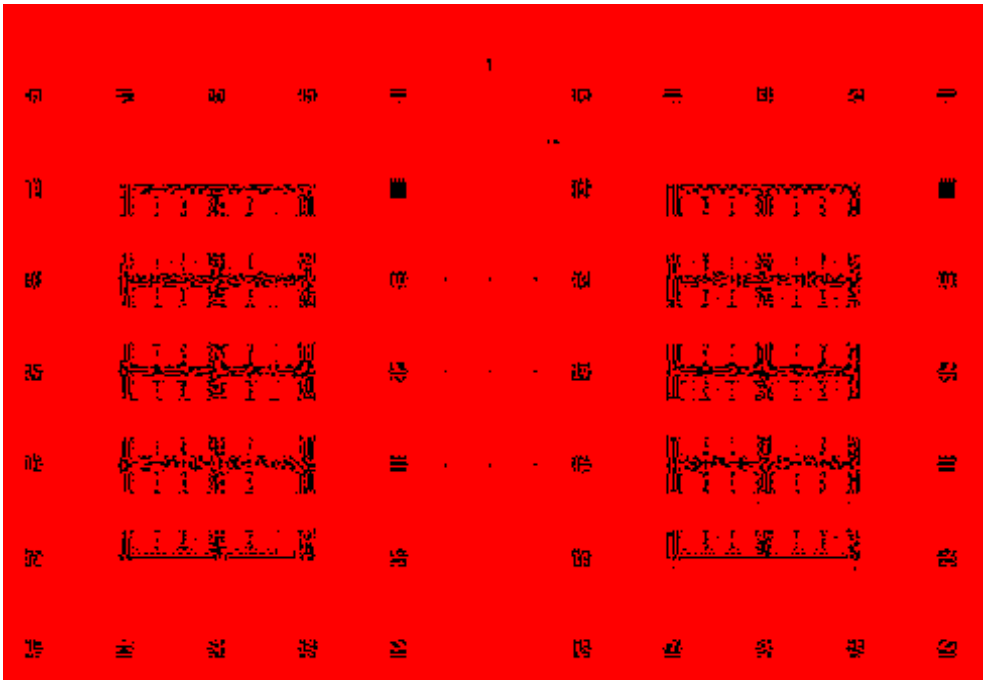

Figure 2-35: Plan View of Twin Tower Connected Building (Mu 2011)

A study was done by Bharti (2010) on the seismic response of two adjacent buildings of different heights (20 and 10 stories) using magnetorheological (MR) dampers. The study investigated whether MR dampers placed between the two buildings at varying heights reduced the seismic response in both buildings. The study found that the displacement was controlled significantly with the dampers, particularly with the shorter building but still notable with the taller building as well. In addition, the study found that there is no need to provide linkages at every story and significant displacement control is possible with fewer damper linkages. While a

skybridge acts more as a spring than a damper, it can also help reduce seismic response and are not required at every story to do so.

Patel (2010) describes the use of viscous dampers for seismic response control of similar adjacent structures. Four different earthquake ground motions were applied. Patel found that the viscous dampers can help reduce the response and the dampers further decrease response if they are not used at every story.

Luco (1998) studied the seismic response of tall buildings by modeling stiff external shear beams, flexible internal shear beams connected by links at various elevations as shown in Figure 2-36. Luco found that if the links were rigid, the seismic response of the overall system was reduced but the shear beams in the middle had to be more flexible. If the links were flexible, then both of the connected shear beams were required for overall stiffness.

Figure 2-36: Stiff External and Flexible Internal Shear Beams Connected at Various Elevations (Luco 1998)

2.4 Optimization Methods for Tall Buildings

Spence and Gioffrè (2011) developed an efficient Reliability-Based Design Optimization (RBDO) algorithm for the member size optimization of tall buildings subject to multiple load conditions. The procedure is based on the concept of decoupling the reliability analysis from the optimization loop, which allows the reliability analysis to be performed separately from the successive deterministic optimization loop, guaranteeing far greater efficiency than traditional approaches. A sequence of approximate explicit sub-problems in terms of the design variables around the current design points was developed and then solved using gradient-based algorithms without the need to perform any additional structural analyses due to the explicit nature of the sub-problem. The algorithm was tested on a full scale planar frame subject to wind loads. Convergence of the algorithm was steady and rapid and many of the constraints were controlling at the optimum design.

Liu et al. (2003) developed an effective method for determining the optimal placement of actuators in tall buildings under seismic loading by using a genetic algorithm. The non-linear and non-continuous nature of the problem made the genetic algorithm invaluable for optimal design. A 16-story tall building with rectangular shape was considered under 18 different earthquake records. Liu et al. found that mainly the design criteria and structural parameters (i.e., damping, mass, and stiffness) were the main influencing parameters for placement location of the actuators.

Chan and Wong (2008) used a genetic algorithm to explore optimal topologies of steel frameworks and to optimize sizes of members in the structure. A hybrid genetic algorithm and optimality criteria method was incorporated to bring a balance to exploration of global search algorithms and exploitation of efficient local search methods. This would then make the hybrid

method efficient for optimizing tall buildings with many structural elements. This method was tested using two 40-story steel frameworks and results show that the hybrid method generated superior designs compared to a pure genetic algorithm method.

Kundu et al. (2002) explored implementing a genetic algorithm to effectively design vibration control devices for two or more individually constructed buildings. The buildings are controlled by actuators installed in the connective sections between the buildings. The genetic algorithm is used to solve for optimal values of damping and stiffness constants that minimizes the performance index of the system. It was shown by simulation, that vibration without spillover instability of a twin tower-like structure is well controlled.

Another type of optimization technique called an Particle Swarm Optimization (PSO) algorithm was used by Liang and Liu (2009) which optimizes neural networks. "PSO's have been compared to genetic algorithms to efficiently search large search areas. The technique is used to simulate social behavior among individuals (particles) 'flying' through a multidimensional search space. Each particle represents a single intersection of all search dimensions. The particles evaluate their positions relevant to a goal (fitness) at each iteration, and particles in a local neighborhood share memories of their 'best' positions, and then use those memories to adjust their own velocities, and in turn subsequent positions," (Liang and Liu 2009, p. 182) The PSO was used to determine the optimum structure system of high-rising buildings. Results show that the accuracy and convergence velocity is much better than other gradient-based algorithms.

CHAPTER 3. SIMPLIFIED SKYSCRAPER SKYBRIDGE MODEL

The simplified skyscraper skybridge model (SSSM) is developed to analyze skyscrapers with roller-connected and hinge-connected skybridges. In this dissertation, it will be assumed that all skyscrapers consist of a square core with eight megacolumns periodically connected to the core by outriggers as shown in Figure 3-1. Core-megacolumn outrigger systems are one of the most effective methods in controlling the lateral drift in tall buildings (Smith and Salim 1981). Such systems provide unobstructed interior space between the core and megacolumns and unobstructed view to the outside between the megacolumns. The steps of the SSSM consist of: 1) determination of megacolumn areas, 2) construction of the stiffness matrix, 3) evaluation of volume, weight, mass, and period, 4) calculation of lateral force vectors, and 5) calculation of displacement and stress constraints.

The SSSM subdivides the skyscraper vertically into intervals, where i=1 is the top interval and increasing downward. It will be assumed that every interval consists of 10 stories for all skyscrapers in this dissertation, and that the story height is constant for all stories and all skyscrapers in the system. Outriggers and skybridges are located at the top of each interval. It will be assumed that the cross-sectional areas of the core and megacolumns remain constant in each interval, but may change from interval to interval. It will also be assumed that cores, megacolumns, outriggers, and skybridges have been transformed to equivalent all-concrete

sections by multiplying steel cross-sectional area by the ratio of steel elastic modulus to concrete elastic modulus.

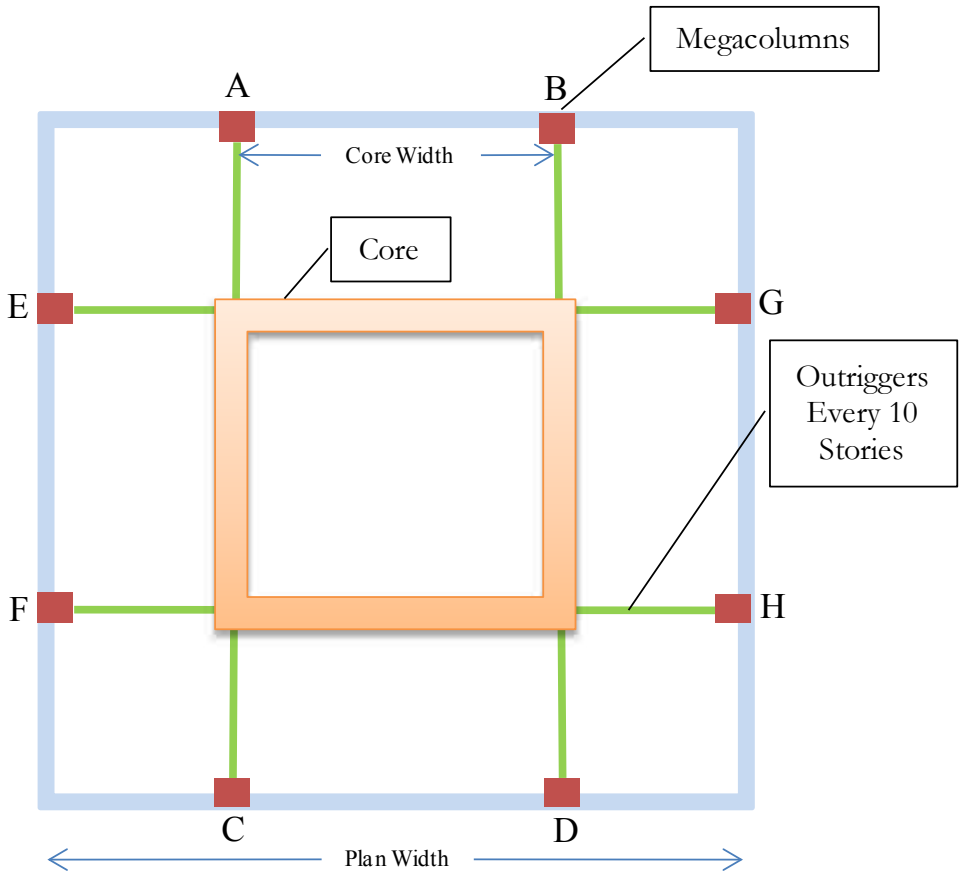

Figure 3-1: Plan View of All Skyscrapers

3.1 Determination of Megacolumn Areas

The first step in the SSSM is to determine the cross-sectional areas of the megacolumns for each skyscraper. The cross-sectional areas of the megacolumns are determined from the principle that the axial strain in the megacolumns must be the same axial strain in the core under gravity loads. If gravity load axial strains are not the same in the core and megacolumns, then unacceptably large differential vertical displacements may accumulate in the upper stories of the

skyscraper. Equating axial strains at the base of interval *i* leads to the formula for megacolumn area in terms of core area given in Equations 3.1-1, 3.1-2, and 3.1-3:

$$\varepsilon_i = \frac{F_i^{core} + \gamma h A_i^{core}}{E A_i^{core}} = \frac{F_i^{col} + \gamma h A_i^{col}}{E A_i^{col}} \Rightarrow A_i^{col} = A_i^{core} \frac{F_i^{col}}{F_i^{core}} \quad \textbf{(3.1-1)}$$

$$F_i^{core} = F_{i-1}^{core} + \gamma h A_{i-1}^{core} + n A_{trib}^{core} (D^{floor} + L^{floor}) + \frac{\gamma V_i^{out}}{2} \quad \textbf{(3.1-2)}$$

$$\begin{aligned} F_i^{col} &= F_{i-1}^{col} + h\gamma A_{i-1}^{col} + n A_{trib}^{col} \left(D^{floor} + L^{floor}\right) + 4 w^{plan} h D^{clad} + \frac{\gamma V_i^{Tcol}}{2} \\ &+ \gamma A_i^{bridge} n_i^{bridge} \frac{w^{spacing}}{2} + w^{bridge} n_i^{bridge} \frac{w^{spacing}}{2} \left(+ D^{bridge} + L^{bridge}\right) \end{aligned} \quad \textbf{(3.1-3)}$$

where,

ε_i = axial strain at bottom of interval *i*

F_i^{core} = axial force in core at base of interval *i* excluding interval *i* self weight

F_i^{col} = axial force in megacolumns at base of interval *i* excluding interval *i* self weight

A_i^{core} = cross-sectional area of the core in interval *i*

A_i^{col} = cross-sectional area of eight megacolumns in interval *i*

V_i^{out} = volume of all eight outrigger trusses at top of interval *i*

A_i^{bridge} = cross sectional area of skybridge in interval *i*

n_i^{bridge} = number of skybridges connected to skyscraper at interval *i*

and the following values have been assumed throughout the dissertation:

γ = concrete unit weight = 21.7kN/m^3 (0.138kip/ft^3)

E = concrete modulus of elasticity = 43.8MPa (914,782kip/ft^2)

n = number of stories per interval = 10

h = interval height = 37.5m (123ft)

w^{plan} = plan width = 50m (164ft)

w^{core} = core width = 25m (82ft)

$w^{spacing}$ = spacing between skyscrapers = 25m (82ft)

w^{bridge} = skybridge width = 12.5m (41ft)

$A_{trib}{}^{core}$ = core tributary area = $(37.5m)^2$ $((123ft)^2)$

$A_{trib}{}^{col}$ = tributary area for eight megacolumns = $(50m)^2$ - $(37.5m)^2$ $((164ft)^2-(123ft)^2)$

D^{floor} = floor dead load per area = 4.31kPa (90psf)

L^{floor} = floor live load per area = 2.39kPa (50psf)

D^{clad} = cladding load per area = 1.28kPa (26.7psf)

D^{bridge} = skybridge dead load per area = 4.31kPa (90psf)

L^{bridge} = skybridge live load per area = 2.87kPa (60psf)

3.2 Construction of the Stiffness Matrix

The second step in the SSSM is to construct a stiffness matrix for lateral load analysis of a single skyscraper or connected skyscrapers. The SSSM uses far fewer DOF's than is required for finite element analysis. For finite element analysis, there are six DOF's for each unsupported node (three translational and three rotational). This leads to thousands of DOF's for a single skyscraper, and hundreds of thousands of DOF's for many connected skyscrapers. The SSSM is based on only three dominant DOF's at the top of each interval: 1) horizontal displacement, 2) rotation of the core, and 3) vertical megacolumn displacement. The horizontal core displacement at the top of an interval represents the horizontal displacement of both the core and megacolumns because it is assumed that the floor diaphragm was axially rigid. Assuming lateral loads are exerted from left to right in Figure 3-1 and that plan width is twice the core width, the vertical

megacolumn displacement is equal to: 1) the vertical displacement of megacolumns E and F, 2) the negative of the vertical displacements of megacolumns G and H, 3) twice the vertical displacement of megacolumns A and C, and 4) the negative of twice the vertical displacement of megacolumns B and D. With only three DOF's for each 10-story interval, the total number of DOF's in a 70-story skyscraper is 21, and the total number of DOF's in a 100 connected 70-story skyscraper system is 1050 (only 50 skyscrapers need be analyzed if symmetry is exploited).

A simplified model for a 30-story skyscraper (three intervals) is shown in Figure 3-2. Note that in each interval, one member represents the core (thick blue line), one member represents all eight megacolumns (thin vertical green line), and one member represents all eight outriggers at each interval (thin orange lines). The nine dominant DOF's have been numbered and are represented by blue arrows showing positive directions in Figure 3-2. The 9x9 structure stiffness matrix is given in Table 3-1. The element in row *i* and column *j* represents the force at DOF *i* due to a unit displacement at DOF *j*. The elements in the stiffness matrix in Table 3-1 are in terms of the stiffness's of the members shown in Figure 3-2.

The axial stiffness of all eight megacolumns in interval *i* is given by Equation 3.2-1. The reason for the factor 5/8 is due to the fact that megacolumns A,B,C,D in Figure 3-1 contribute only 25 percent of their axial stiffness to the DOF while megacolumns E,F,G,H contribute 100 percent of their axial stiffness to the DOF.

$$C_i = \frac{5}{8}\left(\frac{EA_i^{col}}{h}\right) \qquad \textbf{(3.2-1)}$$

The flexural stiffness of the core and megacolumns in interval *i* is given by Equation 3.2-2. The first term is the modulus of elasticity multiplied by the moment of inertia of the core. The

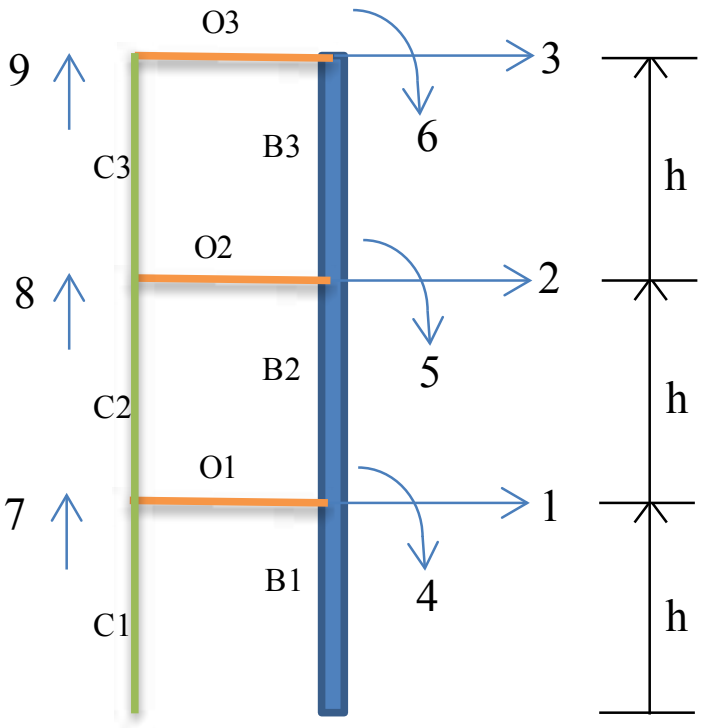

Figure 3-2: DOF's and Members of a Single Skyscraper

Table 3-1: Single Skyscraper Structure Stiffness Matrix

	DOF 1	DOF 2	DOF 3	DOF 4	DOF 5	DOF 6	DOF 7	DOF 8	DOF 9
DOF 1	$\frac{12B_1}{h^3}+\frac{12B_2}{h^3}$	$\frac{-12B_2}{h^3}$	0	$\frac{6B_2}{h^2}-\frac{6B_1}{h^2}$	$\frac{6B_2}{h^2}$	0	0	0	0
DOF 2	$\frac{-12B_2}{h^3}$	$\frac{12B_2}{h^3}+\frac{12B_3}{h^3}$	$\frac{-12\cdot B_3}{h^3}$	$\frac{-6B_2}{h^2}$	$\frac{6B_3}{h^2}-\frac{6B_2}{h^2}$	$\frac{6B_3}{h^2}$	0	0	0
DOF 3	0	$\frac{-12\cdot B_3}{h^3}$	$\frac{12B_3}{h^3}$	0	$\frac{-6B_3}{h^2}$	$\frac{-6B_3}{h^2}$	0	0	0
DOF 4	$\frac{6B_2}{h^2}-\frac{6B_1}{h^2}$	$\frac{-6B_2}{h^2}$	0	$\frac{4B_1}{h}+\frac{4B_2}{h}+O_1\cdot d^2$	$\frac{2B_2}{h}$	0	$-O_1\cdot d$	0	0
DOF 5	$\frac{6B_2}{h^2}$	$\frac{6B_3}{h^2}-\frac{6B_2}{h^2}$	$\frac{-6B_3}{h^2}$	$\frac{2B_2}{h}$	$\frac{4B_2}{h}+\frac{4B_3}{h}+O_2\cdot d^2$	$\frac{2B_3}{h}$	0	$-O_2\cdot d$	0
DOF 6	0	$\frac{6B_3}{h^2}$	$\frac{-6B_3}{h^2}$	0	$\frac{2B_3}{h}$	$\frac{4B_3}{h}+O_3\cdot d^2$	0	0	$-O_3\cdot d$
DOF 7	0	0	0	$-O_1\cdot d$	0	0	$O_1+C_1+C_2$	$-C_2$	0
DOF 8	0	0	0	0	$-O_2\cdot d$	0	$-C_2$	$O_2+C_2+C_3$	$-C_3$
DOF 9	0	0	0	0	0	$-O_3\cdot d$	0	$-C_3$	O_3+C_3

second term is the modulus of elasticity multiplied by the sum of the local moments of inertia of the solid square megacolumns. Usually, the first term is much greater than the second term.

$$B_i = \frac{EA_i^{core}\left(w^{core}\right)^2}{6} + \frac{E\left(A_i^{col}\right)^2}{96} \qquad \textbf{(3.2-2)}$$

In this dissertation, it is assumed that each of the outrigger trusses consists of two members as shown in Figure 3-3. Let L^{out} be the length of one of those members and S^{out} be the sine of the angle from the horizontal to one of those members. The shear stiffness of all eight outrigger trusses in interval i is given by Equation 3.2-3. Figure 3-3 helps to explain the coupling created by the outriggers between the core rotation DOF and the megacolumn vertical displacement DOF. The top part of Figure 3-3 shows a positive unit megacolumn vertical displacement but no core rotation. Such a displacement requires a positive vertical force O_i at the megacolumn and a negative moment dO_i at the core where the distance d is half the plan width. The bottom part of Figure 3-3 shows a positive unit core rotation but no megacolumn vertical displacement. Such a rotation requires a negative vertical force of dO_i at the megacolumn and a positive moment of d^2O_i at the core. These forces and moments appear in Table 3-1.

$$O_i = \frac{5}{8}\left(EV_i^{out}\right)\left(\frac{S^{out}}{L^{out}}\right)^2 \qquad \textbf{(3.2-3)}$$

A simplified model for two 30-story skyscrapers connected with skybridges is shown in Figure 3-4. Since there are multiple skyscrapers there are not only more DOF's but skybridges now couple the horizontal DOF's of the system. The DOF's are numbered as shown in Figure 3-4. Numbering DOF's in this fashion enables the structure stiffness matrix to be partitioned,

which eventually simplifies and reduces computation. The structure stiffness matrix is given in Table 3-2.

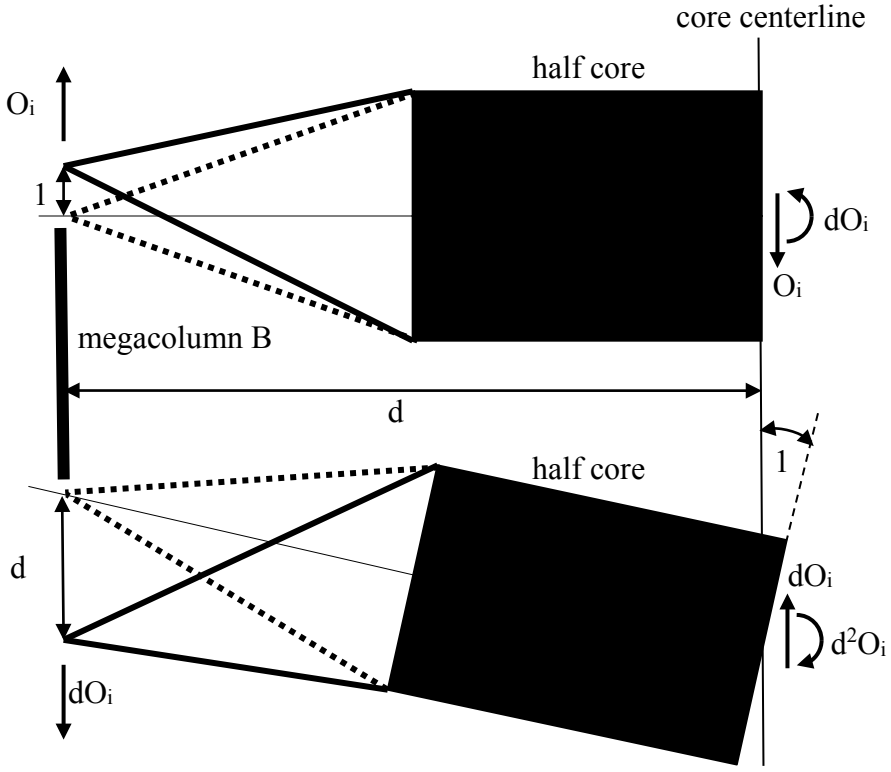

Figure 3-3. Stiffness of Two-Member Outrigger Truss

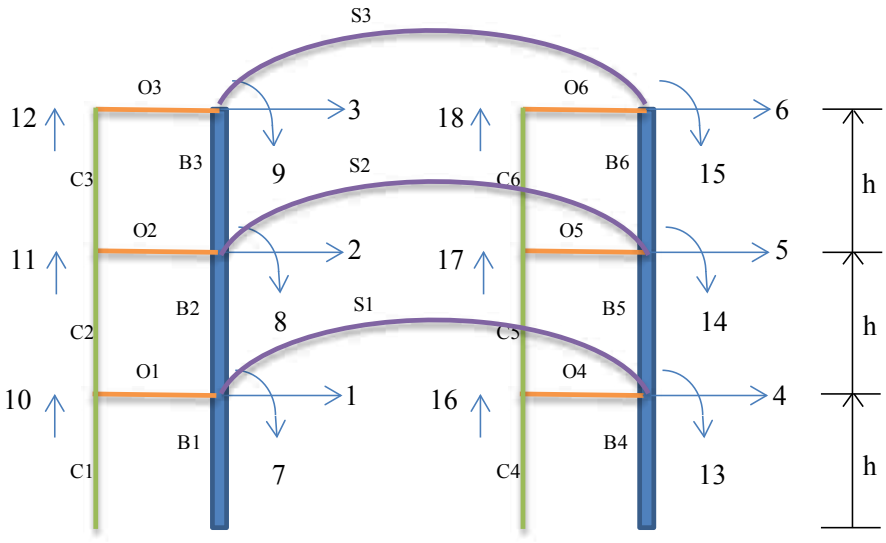

Figure 3-4. Simplified DOF's of Two Skyscrapers Connected with Skybridges

Table 3-2: Two Skyscraper Structure Stiffness Matrix

DOF 1	$\frac{}{h^3}+\frac{}{h^3}+S_1$	$\frac{}{h^3}$	0	$-S_1$	0	0	$\frac{}{h^2}-\frac{}{h^2}$	$\frac{}{h^2}$	0	0	0	0	$\frac{}{h^2}-\frac{}{h^2}$	$\frac{}{h^2}$	0	0	0
DOF 2	$\frac{-12B_2}{h^3}$	$\frac{12B_2}{h^3}+\frac{12B_3}{h^3}+S_2$	$\frac{-12\cdot B_3}{h^3}$	0	$-S_2$	0	$\frac{-6B_2}{h^2}$	$\frac{6B_3}{h^2}-\frac{6B_2}{h^2}$	$\frac{6B_3}{h^2}$	0	0	0	$\frac{-6B_5}{h^2}$	$\frac{6B_6}{h^2}-\frac{6B_5}{h^2}$	$\frac{6B_6}{h^2}$	0	0
DOF 3	0	$\frac{-12B_3}{h^3}$	$\frac{12B_3}{h^3}+S_3$	0	0	$-S_3$	0	$\frac{-6B_3}{h^2}$	$\frac{-6B_3}{h^2}$	0	0	0	0	$\frac{-6B_6}{h^2}$	$\frac{-6B_6}{h^2}$	0	0
DOF 4	$-S_1$	0	0	$\frac{12B_4}{h^3}+\frac{12B_5}{h^3}+S_1$	$\frac{-12B_5}{h^3}$	0	0	0	0	0	0	0	0	0	0	0	0
DOF 5	0	$-S_2$	0	$\frac{-12B_5}{h^3}$	$\frac{12B_5}{h^3}+\frac{12B_6}{h^3}+S_2$	$\frac{-12B_6}{h^3}$	0	0	0	0	0	0	0	0	0	0	0
DOF 6	0	0	$-S_3$	0	$\frac{-12B_6}{h^3}$	$\frac{12B_6}{h^3}+S_3$	0	0	0	0	0	0	0	0	0	0	0
DOF 7	$\frac{6B_2}{h^2}-\frac{6B_1}{h^2}$	$\frac{-6B_2}{h^2}$	0	0	0	0	$\frac{4B_1}{h}+\frac{4B_2}{h}+O_1\cdot d^2$	$\frac{2B_2}{h}$	0	$-O_1\cdot d$	0	0	0	0	0	0	0
DOF 8	$\frac{6B_2}{h^2}$	$\frac{6B_3}{h^2}-\frac{6B_2}{h^2}$	$\frac{-6B_3}{h^2}$	0	0	0	$\frac{2B_2}{h}$	$\frac{4B_2}{h}+\frac{4B_3}{h}+O_2\cdot d^2$	$\frac{2B_3}{h}$	0	$-O_2\cdot d$	0	0	0	0	0	0
DOF 9	0	$\frac{6B_3}{h^2}$	$\frac{-6B_3}{h^2}$	0	0	0	0	$\frac{2B_3}{h}$	$\frac{4B_3}{h}+O_3\cdot d^2$	0	0	$-O_3\cdot d$	0	0	0	0	0
DOF 10	0	0	0	0	0	0	$-O_1\cdot d$	0	0	$C_1+C_2+O_1$	$-C_2$	0	0	0	0	0	0
DOF 11	0	0	0	0	0	0	0	$-O_2\cdot d$	0	$-C_2$	$C_2+C_3+O_2$	$-C_3$	0	0	0	0	0
DOF 12	0	0	0	0	0	0	0	0	$-O_3\cdot d$	0	$-C_3$	C_3+O_3	0	0	0	0	0
DOF 13	$\frac{6B_5}{h^2}-\frac{6B_4}{h^2}$	$\frac{-6B_5}{h^2}$	0	0	0	0	0	0	0	0	0	0	$\frac{4B_4}{h}+\frac{4B_5}{h}+O_4\cdot d^2$	$\frac{2B_5}{h}$	0	$-O_4\cdot d$	0
DOF 14	$\frac{6B_5}{h^2}$	$\frac{6B_6}{h^2}-\frac{6B_5}{h^2}$	$\frac{-6B_6}{h^2}$	0	0	0	0	0	0	0	0	0	$\frac{2B_5}{h}$	$\frac{4B_5}{h}+\frac{4B_6}{h}+O_5\cdot d^2$	$\frac{2B_6}{h}$	0	$-O_5\cdot$
DOF 15	0	$\frac{6B_6}{h^2}$	$\frac{-6B_6}{h^2}$	0	0	0	0	0	0	0	0	0	0	$\frac{2B_6}{h}$	$\frac{4B_6}{h}+O_6\cdot d^2$	0	0
DOF 16	0	0	0	0	0	0	0	0	0	0	0	0	$-O_4\cdot d$	0	0	$C_4+C_5+O_4$	$-C5$
DOF 17	0	0	0	0	0	0	0	0	0	0	0	0	0	$-O_5\cdot d$	0	$-C_5$	C_5+C_6
DOF 18	0	0	0	0	0	0	0	0	0	0	0	0	0	0	$-O_6\cdot d$	0	$-C_6$

The length of the skybridges is equal to the spacing between skyscrapers. For skybridges parallel to the lateral loading, the skybridge stiffness is axial as given by Equation 3.2-4. For skybridges perpendicular to the lateral loading, the skybridge area is assumed to be concentrated at both sides of the skybridge width, and the skybridge stiffness is flexural as given by Equation 3.2-5.

$$S_i = \frac{EA_i^{bridge}}{w^{spacing}} \tag{3.2-4}$$

$$S_i = \frac{12E}{\left(w^{spacing}\right)^3}\left(A_i^{bridge}\left(\frac{w^{bridge}}{2}\right)^2\right) \tag{3.2-5}$$

Partitioning and condensation of the structure stiffness matrix saves computation time and storage. The structure stiffness matrix for a single 30-story skyscraper can be partitioned as shown in Table 3-3. Note that the upper left partition K_{HH} corresponds to the horizontal displacement DOF's, and the bottom right partition K_{VV} corresponds to the rotational and vertical displacement DOF's. The partition K_{HV} represents the coupling between the horizontal DOF's and the rotational/vertical DOF's. There are three reasons the stiffness matrix is partitioned in this way. First, it was assumed that the only applied forces were at the horizontal DOF's. Second, mass was associated only with the horizontal DOF's. This will come into play when the natural period of the system is computed. Third, the only coupling of DOF's between skyscrapers was coupling between the horizontal DOF's – the rotational/vertical DOF's were not coupled between skyscrapers connected with skybridges.

Table 3-3: Partitioned Structure Stiffness Matrix for a Single Skyscraper

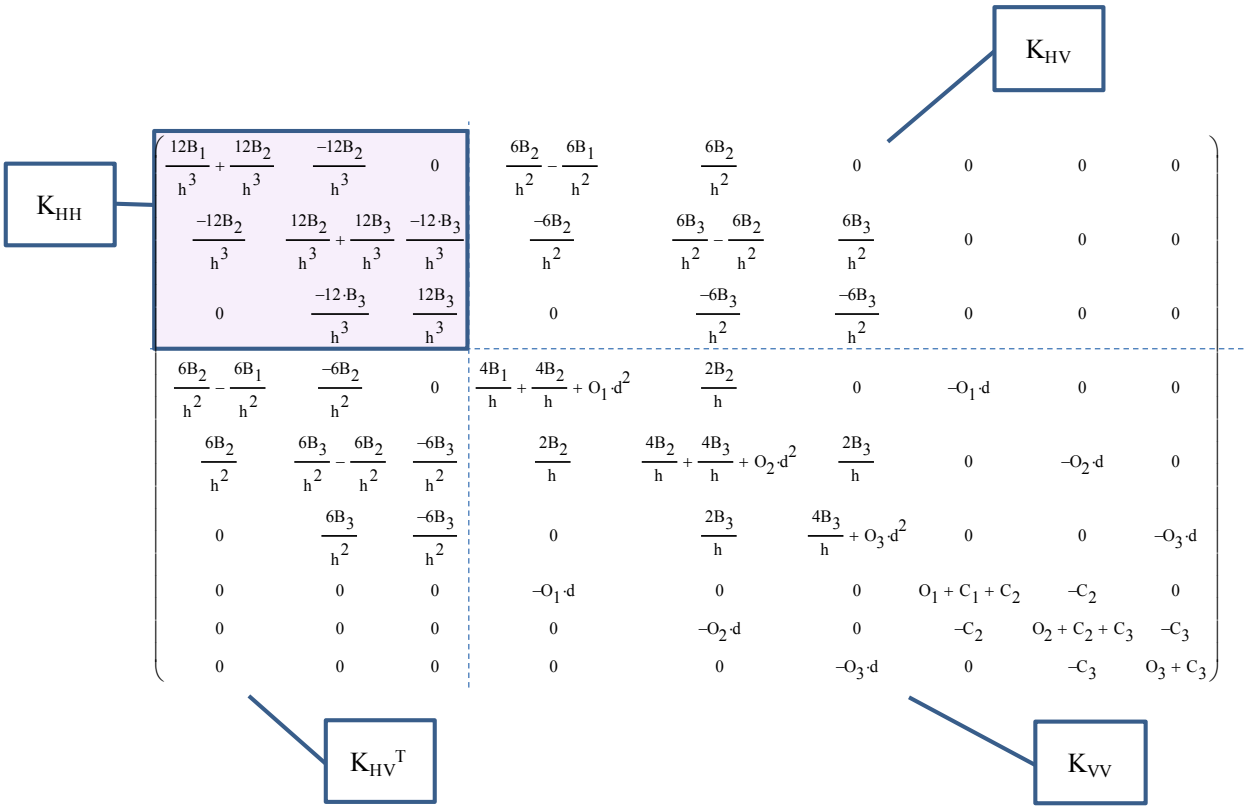

The fact that the only applied forces are at the horizontal DOF's allows the structure stiffness matrix to be condensed. Equation 3.2-6 gives the partitioned equations where F_H are the applied forces at the horizontal DOF's, U_H are the displacements at the horizontal DOF's, and U_V are the displacements at the rotational/vertical DOF's.

$$\begin{bmatrix} K_{HH} & K_{HV} \\ K_{HV}^T & K_{VV} \end{bmatrix} \begin{bmatrix} U_H \\ U_V \end{bmatrix} = \begin{bmatrix} F_H \\ 0 \end{bmatrix} \tag{3.2-6}$$

From the bottom partitioned equation:

$$U_V = -K_{VV}^{-1} K_{HV}^T U_H \tag{3.2-7}$$

Substitute into top partitioned equation:

$$\left(K_{HH} - K_{HV}K_{VV}^{-1}K_{HV}^{T}\right)U_H = F_H \tag{3.2-8}$$

The condensed stiffness matrix is given by Equation 3.2-9:

$$K_{cond} = K_{HH} - K_{HV}K_{VV}^{-1}K_{HV}^{T} \tag{3.2-9}$$

When multiple skyscrapers are involved, the entire structure stiffness matrix such as the one in Table 3-2 for two skyscrapers is never actually assembled. This is because the rotational/vertical DOF's are uncoupled between skyscrapers, and it is wasteful to store and multiply by all the zeros in the matrix that represent this uncoupling. The entire K_{HH} matrix is assembled, and then the K_{HV} and K_{VV} matrices are assembled separately for each skyscraper. Accordingly, the condensed structure stiffness matrix is given by Equation 3.2-10. An example of this entire matrix for a six-skyscraper connected system is shown in Table 3-4, where *NA* indicates matrices not assembled.

$$K = K_{HH} - \sum_{skyscrapers} K_{HV}K_{VV}^{-1}K_{HV}^{T} \tag{3.2-10}$$

Table 3-4: Condensed Stiffness Matrix for a Six-Skyscraper Connected System

K_{HH}	K_{HV1}	K_{HV2}	K_{HV3}	K_{HV4}	K_{HV5}	K_{HV6}
K_{HVT1}	K_{VV1}	NA	NA	NA	NA	NA
K_{HVT2}	NA	K_{VV2}	NA	NA	NA	NA
K_{HVT3}	NA	NA	K_{VV3}	NA	NA	NA
K_{HVT4}	NA	NA	NA	K_{VV4}	NA	NA
K_{HVT5}	NA	NA	NA	NA	K_{VV5}	NA
K_{HVT6}	NA	NA	NA	NA	NA	K_{VV6}

For a system of N_S skyscrapers each with N_I intervals, the number of floating point operators (FLOPS) required to triangularize the entire uncondensed stiffness matrix is given by Equation 3.2-11:

$$\frac{1}{6}\left(3N_S N_I\right)^3 = 4.5N_S^3 N_I^3 \tag{3.2-11}$$

The number of FLOPS required to triangularize the condensed stiffness matrix is given by Equation 3.2-12:

$$\frac{1}{6}\left(N_S N_I\right)^3 = 0.1667N_S^3 N_I^3 \tag{3.2-12}$$

The number of FLOPS required for the matrix triple products in Equation 3.2-10 is given by Equation 3.2-13:

$$N_S N_I^3\left(2N_S^2 + 4N_S + 1.333\right) \tag{3.2-13}$$

Comparing Equation 3.2-11 to the sum of Equations 3.2-12 and 3.2-13, the condensation approach has the same number of FLOPS as the non-condensation approach for two skyscrapers, and has half as many FLOPS for 50 or more skyscrapers.

The number of bytes required to store the double-precision elements of the uncondensed stiffness matrix is given by Equation 3.2-14:

$$8\left(3N_S N_I\right)^2 = 72N_S^2 N_I^2 \tag{3.2-14}$$

The number of bytes required to store the double-precision elements of the condensed stiffness matrix in Table 3-4 is given by Equation 3.2-15:

$$8\left(\left(N_S N_I\right)^2 + N_S\left(N_S N_I\right)\left(2N_I\right) + N_S\left(2N_I\right)^2\right) = 24N_S^2 N_I^2 + 32N_S N_I^2 \qquad \textbf{(3.2-15)}$$

Comparing Equation 3.2-14 to Equation 3.2-15, the condensation approach uses half as many bytes as the non-condensation approach for three skyscrapers, and one-third as many bytes for 50 or more skyscrapers.

3.3 Evaluation of Volume, Weight, Mass and Period

The volume of concrete of all structural elements at interval *i* of a particular skyscraper is given by Equation 3.3-1:

$$V_i = hA_i^{core} + hA_i^{col} + V_i^{out} + A_i^{bridge} n_i^{bridge} \frac{w^{spacing}}{2} \qquad \textbf{(3.3-1)}$$

The optimization objective is the minimization of the total volume of structural material, which is the sum of V_i over the intervals and over the skyscrapers in the system.

The dead weight at interval *i* is obtained from the structural volume at interval *i* in Equation 3.3-2:

$$W_i = \gamma V_i + \left(w^{plan}\right)^2 D^{floor} + 4w^{plan} hD^{clad} + w^{bridge} n_i^{bridge} \frac{w^{spacing}}{2} D^{bridge} \qquad \textbf{(3.3-2)}$$

As stated previously in Section 3.2, mass is associated only with the horizontal DOF's at each interval of each skyscraper. This fact implies that the condensed mass matrix for the

system, M_{cond}, is a diagonal matrix where the value of the diagonal element in the *ith* row and *jth* column is simply the dead weight of the interval *i* associated with DOF *j*, divided by *g* = acceleration of gravity = 9.81m/s^2.

The fundamental natural period of the system of skyscrapers is determined by the well-known process of inverse iteration. This process is based on the orthogonality of mode shape vectors and the Rayleigh quotient. The steps of inverse iteration are as follows:

1) Initialize v_0 to be a vector of one's for k=0

2) Iterate $v_k = K_{cond}^{-1} M_{cond} v_{k-1}$

3) Normalize vector v_k by dividing by $\sqrt{v_k^T M_{cond} v_k}$

4) Evaluate the period $T_k = \dfrac{2\pi}{\sqrt{v_k^T K_{cond} v_k}}$

5) Stop if $T_k - T_{k-1}$ is relatively small, otherwise go to Step 2 and iterate again

In Step 2, the condensed stiffness matrix is not inverted, but rather backsubstitution is performed with the triangularized condensed stiffness matrix.

3.4 Calculation of Lateral Force Vectors

As stated previously in Section 3.2, the only applied forces are at the horizontal DOF's. This implies that the condensed force vector consists of forces at the horizontal DOF's due to seismic and wind loading.

3.4.1 Seismic Forces

The seismic force at the horizontal DOF associated with interval *i* of a particular skyscraper is calculated according to Equation 3.4-1:

$$F_i^{seismic} = \frac{W_i (H_i)^2}{\sum_k \left(W_k (H_k)^2\right)} \frac{S_a}{R} \sum_k W_k \qquad \textbf{(3.4-1)}$$

where,

H_i = height of interval i above ground (m)

S_a = spectral response acceleration

R = ductility factor (6 for Special Reinforced Concrete Shear Walls)

The value of S_a is calculated from natural period of the system of skyscrapers determined in Section 3.3. Based on ASCE (2010), S_a can be calculated using Equations 3.4-2 to 3.4-6:

$$T_0 = \frac{0.2 S_{D1}}{S_{DS}} \qquad T_s = \frac{S_{D1}}{S_{DS}} \qquad \textbf{(3.4-2)}$$

For $T < T_0$: $$S_a = S_{DS}\left(0.4 + 0.6\frac{T}{T_0}\right) \qquad \textbf{(3.4-3)}$$

For $T_0 < T \le T_s$: $$S_a = S_{DS} \qquad \textbf{(3.4-4)}$$

For $T_s < T \le T_L$: $$S_a = \frac{S_{D1}}{T} \qquad \textbf{(3.4-5)}$$

For $T_L < T$: $$S_a = \frac{S_{D1} T_L}{T^2} \qquad \textbf{(3.4-6)}$$

where,

T = natural period of system of skyscrapers (seconds)

T_L = long-period transition period (seconds)

S_{D1} = design spectral response acceleration parameter at period of one second

S_{DS} = design spectral response acceleration parameter at short

The parameters S_{D1}, S_{DS}, and T_L are dependent upon the location of the building, type of building, and soil type at that location. The values in Table 3-5 were used for the two seismic sites considered in this dissertation.

Table 3-5: Low and High-Seismic Site Parameters

	Low-Seismic	High-Seismic
S_{DS}	0.34	0.75
S_{D1}	0.54	1.10
T_L	12	12

3.4.2 Wind Forces

The lateral wind pressure p^{wind} in psf at a given height H above ground is based on ASCE (2010) and is given by Equation 3.4-7.

$$p^{wind} = 0.00256 K_{zt} K_d I V^2 \left(2.01 \left(\frac{H}{H_g} \right)^{\frac{2}{\alpha}} \right) \left(G_f C_{ext} - C_{\text{int}} \right) \quad \textbf{(3.4-7)}$$

where,

K_{zt} = topographic factor (1.0)

K_d = wind directionality factor (0.85)

I = importance factor based on Occupancy Category II (1.0)

V = design wind speed in miles per hour (150mph)

H_g = exposure reference height (700ft for obstructed, 1200ft for unobstructed)

α = exposure exponent (11.5 for obstructed, 7 for unobstructed)

G_f = gust effect factor (0.8509 for obstructed, 0.8089 for unobstructed)

C_{ext} = external pressure coefficient (0.8)

C_{int} = internal pressure coefficient (0.18)

As shown in Figure 3-5 for a system of equal-height skyscrapers, the exposure of the skyscrapers on the windward side of the system is considered to be unobstructed (blue boxes). The remaining non-windward skyscrapers have zero wind pressure if the system is enclosed in an envelope (green boxes). If the system is not enclosed in an envelope, the exposure of the remaining non-windward skyscrapers is considered to be obstructed (red boxes). For a system of unequal-height skyscrapers, a skyscraper may experience unobstructed wind pressure above the height of the skyscraper immediately in front, and obstructed (no envelope case) or zero (envelope case) wind pressure below the height of the skyscraper immediately in front.

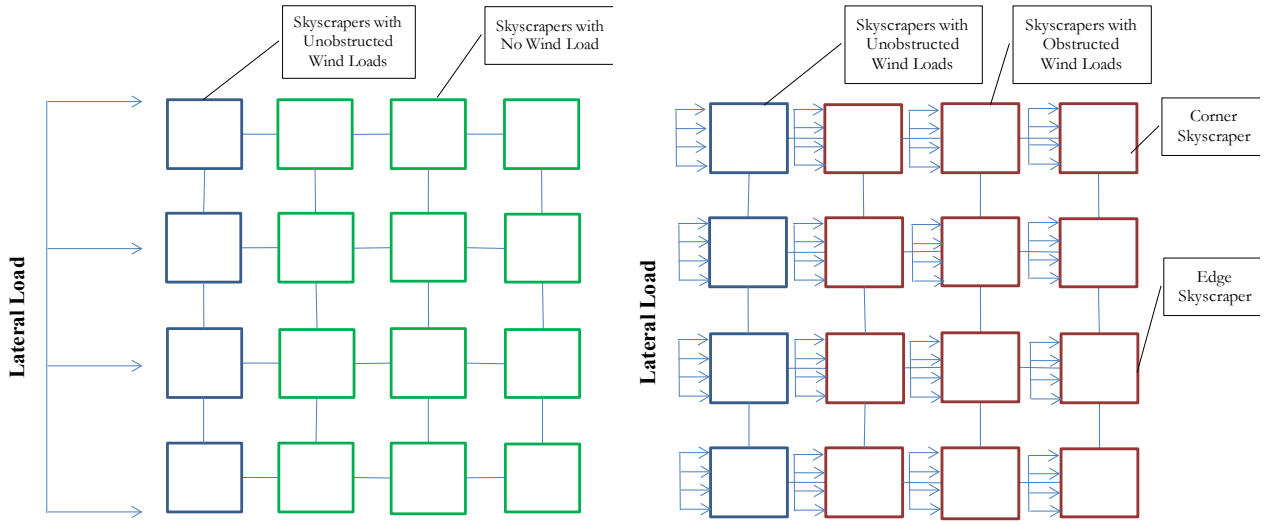

(a) With Envelope (b) Without Envelope

Figure 3-5: Wind Loads

The wind pressure is obtained from Equation 3.4-7 for every story in every skyscraper. The wind force at the top of a particular interval is obtained by summing over the five stories

above and the five stories below the product of: wind pressure, story height = $h/10$, and w_{trib}^{wind} = wind tributary width given by Equations 3.4-8 to 3.4-10:

no envelope: $$w_{trib}^{wind} = w^{plan} \quad \textbf{(3.4-8)}$$

corner skyscraper with envelope: $$w_{trib}^{wind} = w^{plan} + \frac{w^{spacing}}{2} \quad \textbf{(3.4-9)}$$

edge skyscraper with envelope: $$w_{trib}^{wind} = w^{plan} + w^{spacing} \quad \textbf{(3.4-10)}$$

3.5 Calculation of Displacement and Stress Constraints

Horizontal displacements at the DOF's are calculated by performing backsubstitution with the triangularized condensed stiffness matrix and the condensed force vector. Vertical and rotational displacements at the DOF's are calculated separately for each skyscraper from Equation 3.2-7. Let Δ_i^H, Δ_i^V, and θ_i be the horizontal, vertical, and rotational displacements at the top of interval i, where intervals are numbered from top to bottom. These displacements are calculated separately for wind and seismic loading. The drift for interval i is calculated according to Equation 3.5-1. This drift is constrained to be less than 1/360 for wind loading (IBC 2006), and less than 1/50 for seismic loading (ASCE 2010).

$$D_i = \frac{\left|\Delta_i^H - \Delta_{i+1}^H\right|}{h} \quad \textbf{(3.5-1)}$$

Stress constraints are evaluated in the core, megacolumns, outriggers, and skybridges in every interval of every skyscraper. Stress is constrained to be less than the assumed allowable value of 48,000 kPa for concrete. Stress is calculated as the sum of gravity load stress and lateral load stress. Gravity load stress at the bottom of interval i is the same for the core and

megacolumns as shown in Equation 3.5-2. Lateral load stress in the core and megacolumns is given by Equations 3.5-3 and 3.5-4, respectively:

$$\sigma_i^{core\_grav} = \sigma_i^{col\_grav} = \frac{F_i^{core}}{A_i^{core}} + \gamma h = \frac{F_i^{col}}{A_i^{col}} + \gamma h \tag{3.5-2}$$

$$\sigma_i^{core\_lat} = \frac{Ew^{core}}{2} \max\left(\left| \frac{6\left(\Delta_i^H - \Delta_{i+1}^H\right)}{h^2} - \frac{2\theta_i + 4\theta_{i+1}}{h} \right|, \left| \frac{6\left(\Delta_i^H - \Delta_{i+1}^H\right)}{h^2} - \frac{4\theta_i + 2\theta_{i+1}}{h} \right| \right) \tag{3.5-3}$$

$$\sigma_i^{col\_lat} = \frac{E\left(\Delta_i^V - \Delta_{i+1}^V\right)}{h} \tag{3.5-4}$$

The gravity load stress in the two-member outrigger trusses is given by Equation 3.5-5. The lateral load stress at the top interval is given by Equation 3.5-6, and at all other intervals by Equation 3.5-7.

$$\sigma_i^{out\_grav} = \left(S^{out}\right)^2 \sigma_i^{col\_grav} \tag{3.5-5}$$

$$\sigma_i^{out\_lat} = \frac{ES^{out}}{L^{out}} \left[\theta_i \frac{w^{plan}}{2} - \Delta_i^V \right] \tag{3.5-6}$$

$$\sigma_i^{out\_lat} = \frac{ES^{out}}{L^{out}} \left[\left(\theta_i + \left(\frac{S^{out} L^{out}}{h} \right) \left(\theta_{i-1} - \theta_i\right) \right) \frac{w^{plan}}{2} - \Delta_i^V \right] \tag{3.5-7}$$

Assuming the skybridges have a depth of d^{bridge} = 2m, and assuming the skybridge area is concentrated at the top and bottom of the depth, the gravity skybridge stress at the center of the span is given by Equation 3.5-8:

$$\sigma_i^{bridge\_grav} = \frac{(D^{bridge} + L^{bridge})\left(w^{spacing}\right)^2}{4d^{bridge}A_i^{bridge}} \quad \textbf{(3.5-8)}$$

Let Δ_i^{bridge} be difference in horizontal displacement at the two ends of a skybridge under lateral loading. The lateral skybridge stress is given by Equation 3.5-9:

$$\sigma_i^{bridge\_lat} = \frac{E\Delta_i^{bridge}}{w^{spacing}} \quad \textbf{(3.5-9)}$$

Skybridge buckling is also constrained under lateral loading. The ratio of skybridge axial force to the critical buckling force of a simple column is given by Equation 3.5-10. For safety's sake, this ratio is constrained to be less than one-half.

$$r^{bridge\_buck} = \frac{E\Delta_i^{bridge}A_i^{bridge}/w^{spacing}}{\pi^2 EA_i^{bridge}\left(d^{bridge}/2\right)^2/\left(w^{spacing}\right)^2} = \frac{4\Delta_i^{bridge}w^{spacing}}{\pi^2\left(d^{bridge}\right)^2} \quad \textbf{(3.5-10)}$$

CHAPTER 4. COMPARISON OF SSSM TO FEM

A finite element program developed by Balling (1991) for analyzing space frames was used for comparison. The skyscraper model developed for this program will be described in Section 4.1, and the accuracy and efficiency will be compared with the SSSM in Sections 4.2 and 4.3, respectively.

4.1 Finite Element Model (FEM)

Figure 4-1 shows the elevation view and Figure 4-2 shows the plan view of the FEM at the top of a particular interval of a particular skyscraper. Note that there are three core nodes located at the center of the core at three different levels, eight megacolumn nodes located at the centers of the megacolumns, eight outrigger nodes located where outriggers attach to the core at two different levels, and four skybridge nodes located where the skybridges attach to the skyscraper. There are seven different element types: 1) core elements connecting vertically between core nodes, 2) megacolumn elements connecting vertically between megacolumn nodes, 3) outrigger elements connecting from outrigger nodes to megacolumn nodes, 4) core link elements connecting horizontally from core nodes to outrigger nodes, 5) floor link elements connecting horizontally from core nodes to megacolumn nodes, 6) perimeter link elements connecting horizontally between megacolumn nodes and skybridge nodes, and 7) skybridge elements connecting horizontally between the skybridge nodes of adjacent skyscrapers. For all elements, shear deformation is neglected, and Poisson's ratio is assumed to be equal to 0.25.

For core and megacolumn elements, the values of modulus of elasticity, cross-sectional area, strong moment of inertia, and weak moment of inertia are set equal to the values used in the SSSM. The value of the torsion constant is arbitrarily set to a large value of $1000m^4$. It was verified that this value did not impact the results due to the symmetry of the skyscrapers and loads, and the axial rigidity of the floor diaphragms. End connections are modeled as rigid-connected.

For outrigger elements, the values of moment of inertia and torsion constant are set equal to zero since these elements have only axial stiffness. The values of cross-sectional area and modulus of elasticity are set equal to the values used in the SSSM. End connections are modeled as hinge-connected.

Core link elements extend from the center of the core to the core perimeter where outriggers are attached. Core link elements are modeled as flexurally, torsionally, and axially rigid by setting the value of modulus of elasticity to $10^{12}KPa$, moment of inertia to $1000m^4$, torsion constant to $1000m^4$, and cross-sectional area to $1000m^2$. End connections are modeled as rigid-connected.

For floor link elements, the values of moment of inertia and torsion constant are set equal to zero since these elements have only axial stiffness. Floor link elements are modeled as axially rigid by setting the value of modulus of elasticity to $10^{12}KPa$ and cross-sectional area to $1000m^2$. End connections are modeled as hinge-connected.

Perimeter link elements are modeled as torsionally, axially, and flexurally rigid by setting the value of modulus of elasticity to $10^{12}KPa$, torsion constant to $1000m^4$, moment of inertia to $1000m^4$, and cross-sectional area to $1000m^2$. These elements are hinge-connected to megacolumn nodes and rigid connected to skybridge nodes.

For skybridge elements, the values of modulus of elasticity, cross-sectional area, strong moment of inertia, and weak moment of inertia are set equal to the values used in the SSSM. The value of the torsion constant is arbitrarily set to zero. End connections are modeled as hinge-connected about the horizontal axis and rigid-connected about the vertical axis.

Gravity point loads representing dead, live, and cladding loads are applied at each core node and megacolumn node. Lateral wind point loads are applied at core nodes. Gravity dead and live distributed loads are applied to skybridge elements. The magnitudes of gravity and lateral wind loads were obtained from the SSSM as explained in Sections 3.3 and 3.4, respectively. Lateral seismic loads were not considered in this comparison.

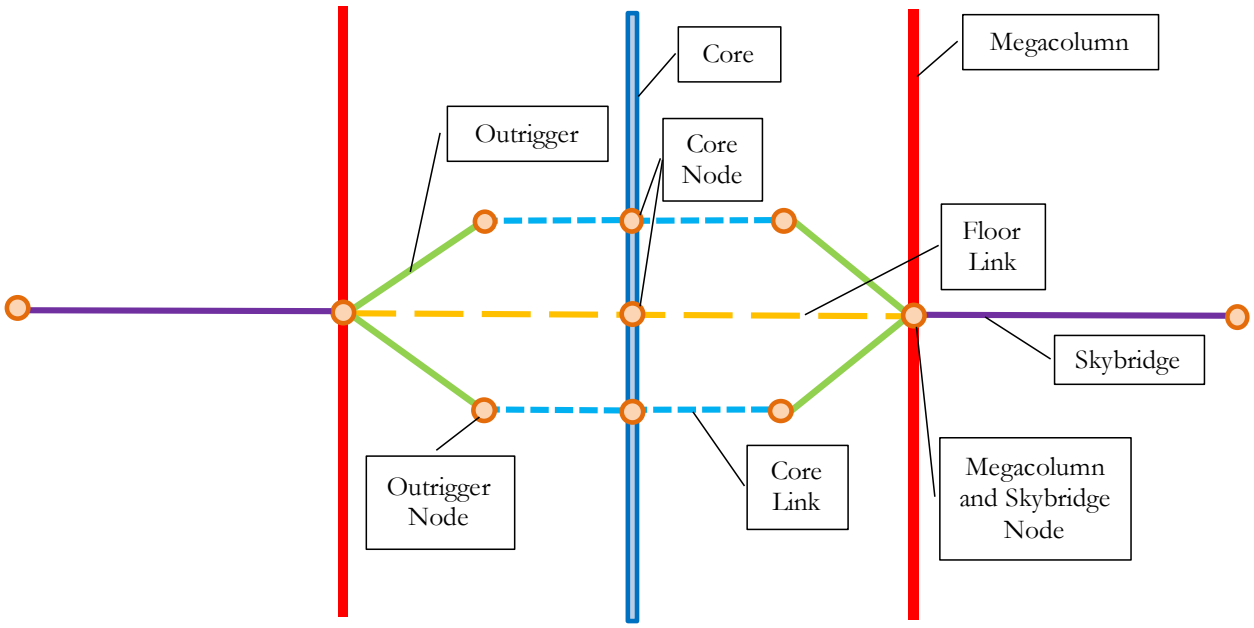

Figure 4-1: Elevation View of Particular Skyscraper Interval

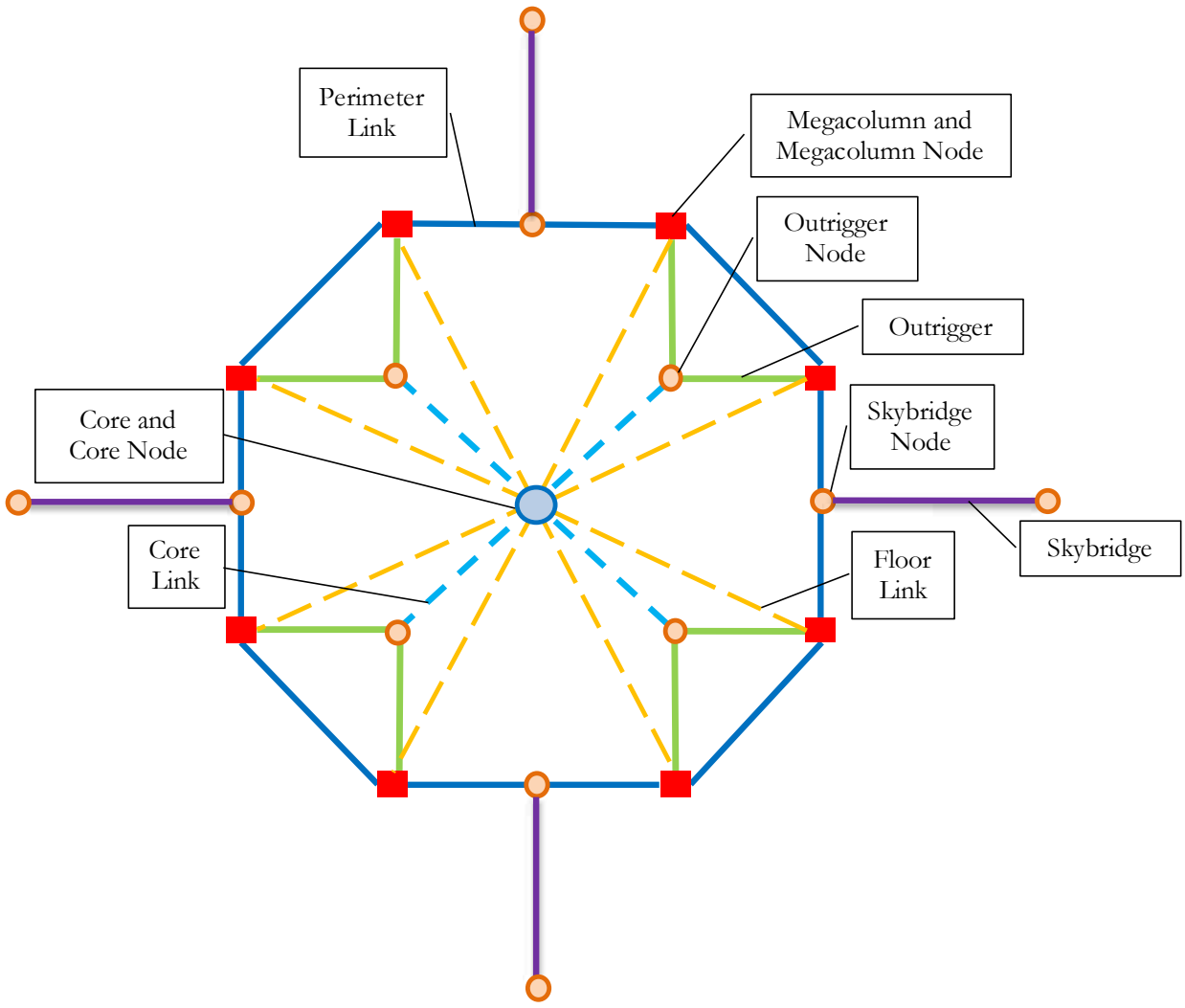

Figure 4-2: Plan View of Particular Skyscraper Interval

4.2 Accuracy Comparison

Results from the SSSM and the FEM model are compared in this section for the three types of skyscraper systems: 1) single 40-story skyscraper, 2) four 40-story skyscrapers with 16 skybridges, and 3) sixteen 40-story skyscrapers with 96 skybridges. Ratios of FEM to SSSM values were calculated for every interval of every skyscraper for: 1) horizontal displacement at the core node at the top of the interval, 2) interval drift defined as the difference in horizontal core displacement between top and bottom of the interval divided by the interval height,

3) rotation at the core node at the top of the interval, 4) maximum vertical displacement over the eight megacolumn nodes at the top of the interval, 5) stress in the core element at the bottom of the interval, 6) maximum stress over the eight megacolumn elements in the interval, and 7) maximum stress in the 16 outrigger elements at the top of the interval. Rather than report these ratios for every interval and every skyscraper, the max, and min over the intervals and skyscrapers is reported in the tables in this section. Ratios of FEM to SSSM values were calculated for stress and buckling of every skybridge oriented parallel to the lateral loading. The max and min over all these parallel skybridges is reported in the tables in this section. Stresses in skybridges oriented perpendicular to the lateral loading were relatively small and are not reported. The average absolute value of the error between FEM and SSSM for every interval and skyscraper or skybridge is also reported in the tables. The horizontal core displacement are plotted for the FEM and SSSM for every skyscraper in the system.

4.2.1 Single Skyscraper

Table 4-1 shows the FEM to SSSM ratios for displacement in a single 10-story skyscraper. Note that the maximum difference is 3 percent. Table 4-2 shows the FEM to SSSM ratios for stress. Note that the maximum difference is 5 percent for the core, 1 percent for megacolumns, and 10 percent for outriggers. Figure 4-3 shows the close agreement between SSSM and FEM displacements.

Table 4-1: FEM to SSSM Ratios for Single Skyscraper Displacements

	Core Horizontal	Core Drift	Core Rotation	Megacolumn Vertical
Max Ratio	1.00	1.00	1.03	1.01
Min Ratio	0.98	0.98	0.98	1.00
Average Error	0.011	0.014	0.037	0.003

Table 4-2: FEM to SSSM Ratios for Single Skyscraper Stresses

	Core	Megacolumn	Outrigger
Max Ratio	1.00	1.01	0.95
Min Ratio	0.95	1.00	0.90
Average Error	0.037	0.005	0.069

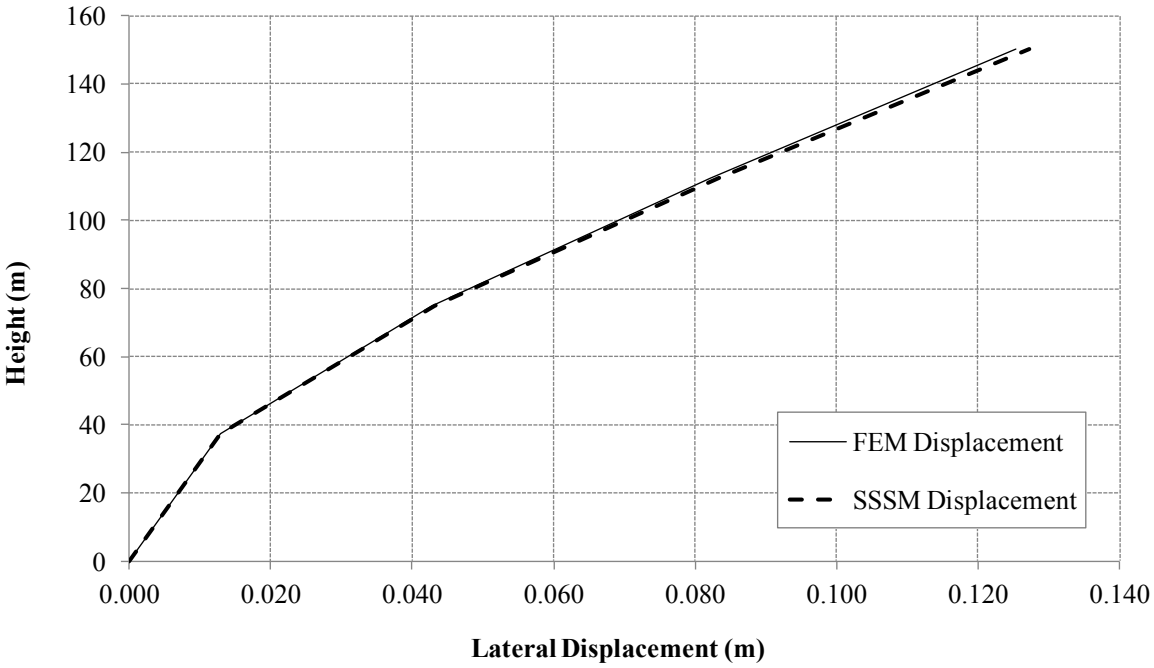

Figure 4-3: FEM and SSSM Lateral Wind Displacement for Single Skyscraper

4.2.2 Four-Skyscraper System

The four-skyscraper system consists of four 40-story skyscrapers connected with skybridges at each interval (16 total skybridges). It was assumed that the spaces between buildings were enclosed with an envelope so that lateral loads were applied only to the two windward skyscrapers. A plan view of this configuration is shown in Figure 4-4.

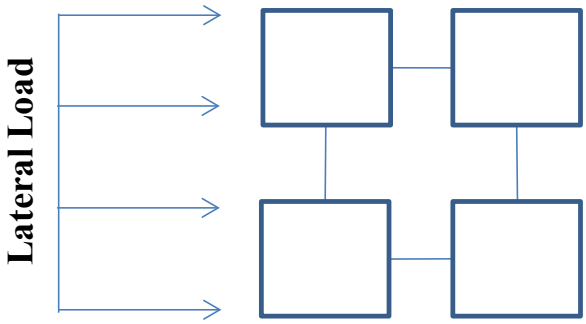

Figure 4-4: Plan View of Four-Skyscraper System

Table 4-3 shows the FEM to SSSM ratios for displacement in a four-skyscraper hinge-connected system. Note that the maximum difference is 3 percent. Table 4-4 shows the FEM to SSSM ratios for stress. Note that the maximum difference is 4 percent for the core, 5 percent for megacolumns, and 8 percent for outriggers. Table 4-5 shows the FEM to SSSM ratios for skybridge stress and buckling. Note that the maximum difference is 3 percent. Figure 4-5 shows the close agreement between SSSM and FEM displacements. Multiple lines indicate individual skyscrapers in the 4-skyscraper hinge-connected system (some of the skyscrapers overlap and have the same displacement).

Table 4-3: FEM to SSSM Ratios for Four-Skyscraper System Displacements

	Core Horizontal	Core Drift	Core Rotation	Megacolumn Vertical
Max Ratio	1.01	1.01	1.03	1.00
Min Ratio	0.99	0.99	0.99	1.00
Average Error	0.006	0.008	0.013	0.002

Table 4-4: FEM to SSSM Ratios for Four-Skyscraper System Stresses

	Core	Megacolumn	Outrigger
Max Ratio	1.01	1.05	1.08
Min Ratio	0.96	1.01	0.92
Average Error	0.025	0.036	0.057

Table 4-5: FEM to SSSM Ratios for Four-Skyscraper Skybridges

	Stress	Buckling
Max Ratio	1.01	1.03
Min Ratio	1.00	1.00
Average Error	0.006	0.019

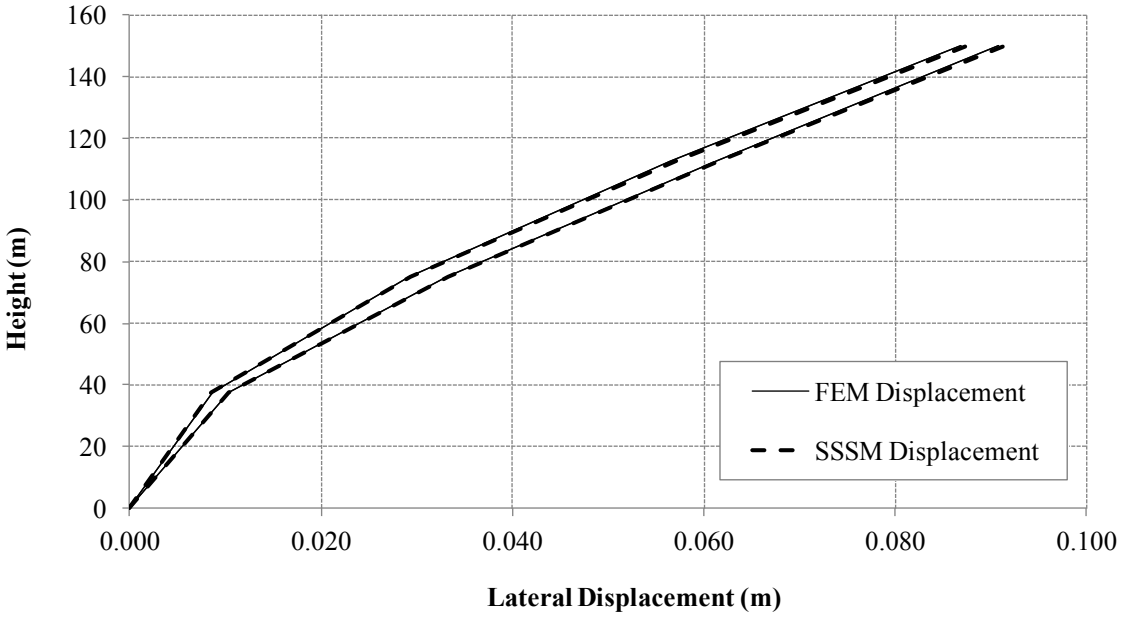

Figure 4-5: FEM and SSSM Lateral Wind Displacement for Four-Skyscraper System

4.2.3 16-Skyscraper System

The 16-skyscraper system consists of sixteen 40-story skyscrapers connected with skybridges at each interval (96 total skybridges). It was assumed that the spaces between buildings were enclosed with an envelope so that lateral loads were applied only to the four windward skyscrapers. A plan view of this configuration is shown in Figure 4-6. Symmetry was exploited therefore only skyscrapers above the dashed line were modeled.

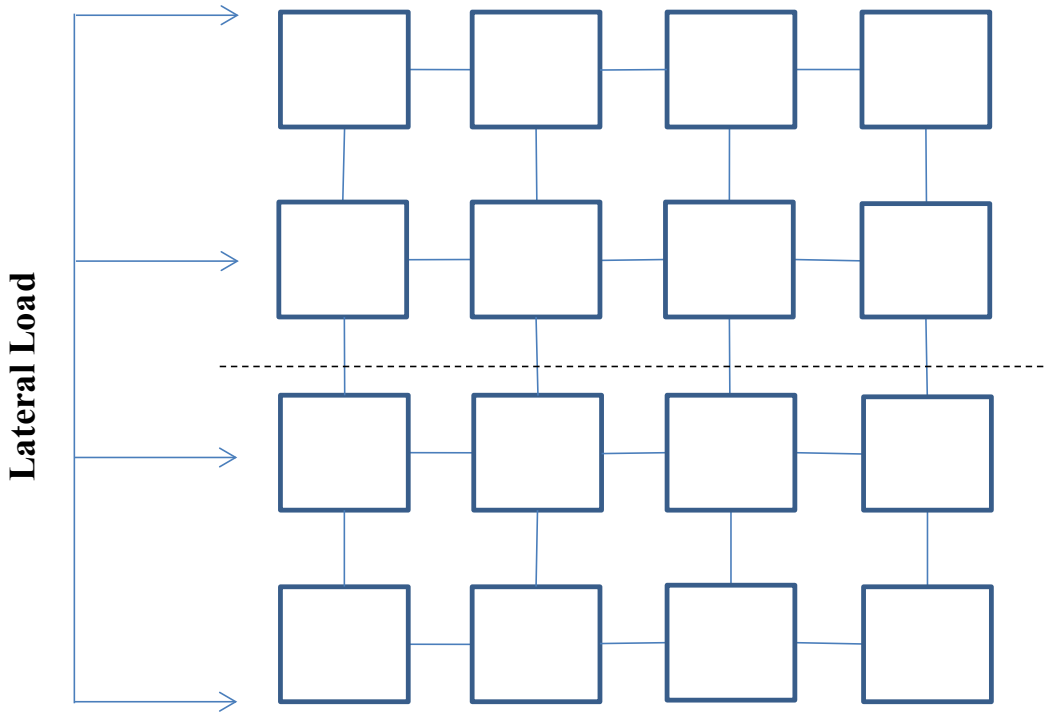

Figure 4-6: Plan View of 16-Skyscraper System

Table 4-6 shows the FEM to SSSM ratios for displacement in a 16-skyscraper hinge-connected system. Note that the maximum difference is 2 percent. Table 4-7 shows the FEM to SSSM ratios for stress. Note that the maximum difference is 2 percent for the core, 5 percent for megacolumns, and 17 percent for outriggers. Table 4-8 shows the FEM to SSSM ratios for skybridge stress and buckling. Note that the maximum difference is 6 percent. Figure 4-7 shows the close agreement between SSSM and FEM displacements.

Table 4-6: FEM to SSSM Ratios for 16-Skyscraper System Displacements

	Core Horizontal	Core Drift	Core Rotation	Megacolumn Vertical
Max Ratio	1.01	1.01	1.02	1.01
Min Ratio	0.99	0.99	0.98	0.99
Average Error	0.004	0.005	0.008	0.005

Table 4-7: FEM to SSSM Ratios for 16-Skyscraper System Stresses

	Core	Megacolumn	Outrigger
Max Ratio	1.02	1.05	1.17
Min Ratio	0.98	1.03	0.85
Average Error	0.013	0.043	0.087

Table 4-8: FEM to SSSM Ratios for 16-Skyscraper System Skybridges

	Stress	Buckling
Max Ratio	1.01	1.06
Min Ratio	1.00	0.99
Average Error	0.004	0.019

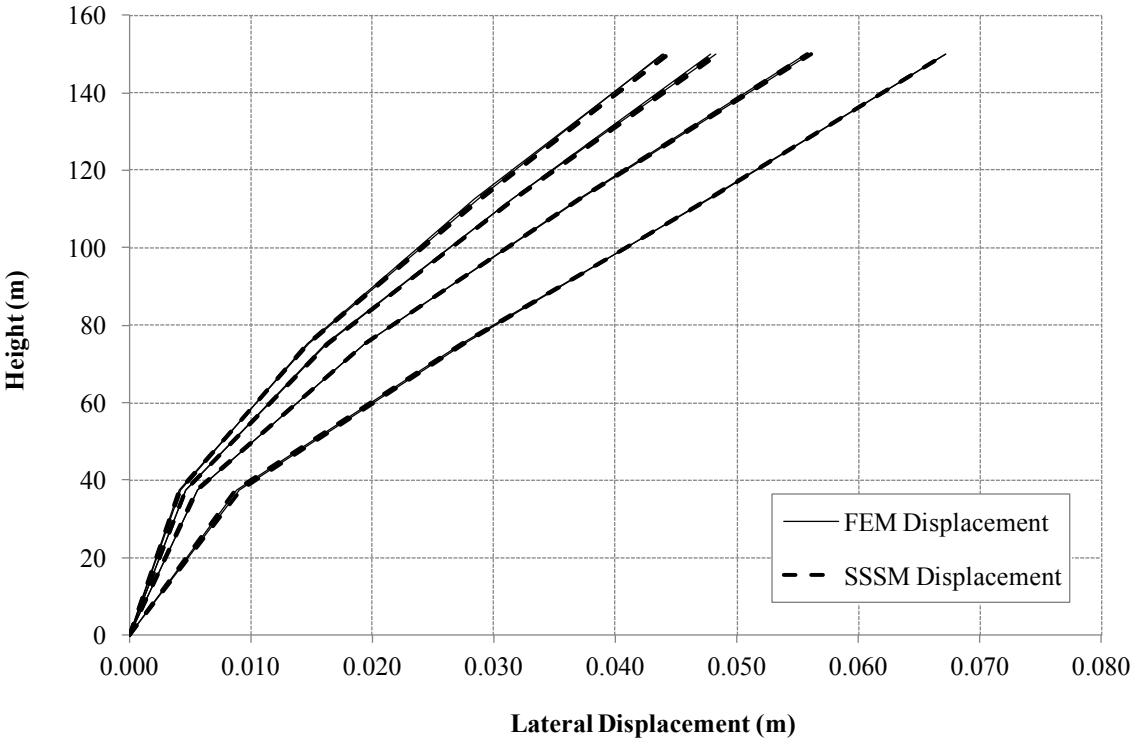

Figure 4-7: FEM and SSSM Lateral Wind Displacement for 16-Skyscraper System

4.3 Efficiency Comparison

One motivation for creating the SSSM was to significantly reduce the amount of computer memory and computation time required for analysis. The amount of computer memory is dominated by the size of the system stiffness matrix that must be stored. For the FEM, the number of elements in the system stiffness matrix is the square of the number of DOF's. The number of DOF's is equal to six times the number of nodes minus the number of supports. These data are given in Table 4-9. It should be noted that symmetry was exploited in the 16-skyscraper system but not in the four-skyscraper system. The number of bytes to store the stiffness matrix is eight times the number of elements in the matrix since each element is a double-precision number. For the SSSM, the number of bytes to store the condensed stiffness matrix is given by Equation 3.2-15, which uses the data given in Table 4-10, where N_S = number of skyscrapers and N_I = number of intervals. Note the dramatic difference in DOF's between the two models; the SSSM reduces the DOF's by a factor of 41. The computation time is dominated by the number of FLOPS required to triangularize the system stiffness matrix. For the FEM, this is equal to 1/6 times the cube of the number of DOF's. For the SSSM, this is equal to the sum of Equations 3.2-12 and 3.2-13. The efficiency comparison between the FEM and SSSM is shown in Table 4-11. The difference is quite dramatic, where the SSSM reduces FLOPS by a factor of 115,403, and bytes by a factor of 4,323. Indeed, it is not feasible to use the FEM to optimize large systems of skyscrapers.

Table 4-9: FEM Efficiency Parameters

System Type	Nodes	Supports	DOF's
Single Skyscraper	91	54	492
4-Skyscraper System	364	216	1,968
16-Skyscraper System	728	432	3,936

Table 4-10: SSSM Efficiency Parameters

System Type	N_S	N_I	DOF's
Single Skyscraper	1	4	12
4-Skyscraper System	4	4	48
16-Skyscraper System	8	4	96

Table 4-11: Efficiency Comparison Between FEM and SSSM

System Type	Analysis Model	Speed (FLOPS)	Memory (Bytes)
Single Skyscraper	FEM	19,849,248	1,936,512
	SSSM	480	896
4-Skyscraper System	FEM	1,270,351,872	30,984,192
	SSSM	13,312	8,192
16-Skyscraper System	FEM	10,162,814,976	123,936,768
	SSSM	88,064	28,672

CHAPTER 5. OPTIMIZATION PROBLEMS

Four skyscraper systems were optimized in this research: 1) 16-skyscraper box, 2) 64-skyscraper box, 3) 25-skyscraper pyramid, and 4) 100-skyscraper pyramid. Box systems represent skyscrapers of equal height and pyramid systems represent skyscrapers of varying heights. Each skyscraper system was optimized for two sites: 1) high-wind and high-seismic, and 2) high-wind and low-seismic. Separate optimizations were performed with and without envelope spanning between skyscrapers. Separate optimizations were performed with hinge-connected skybridges, with roller-connected skybridges, and without skybridges altogether. Thus there were 4x2x2x3 = 48 optimization problems that were solved in this research. Table 5-1 summarizes these different problems. In this and later tables, SB = skybridge, HWHS = high-wind high-seismic site, HWLS = high-wind low-seismic site, and Env = atria envelope.

Optimization problems are generally formulated to find the values of design variables that minimize an objective function and satisfy constraints. The remainder of this chapter will identify the design variables and constraints in each optimization problem. For all optimization problems, the objective was to minimize the total volume of concrete in core, megacolumns, outriggers, and skybridges.

Table 5-1: Skyscraper System Optimization Cases

HWLS Site	No SB	Roller SB	Pinned SB
25 Pyramid	No Env With Env	No Env With Env	No Env With Env
100 Pyramid	No Env With Env	No Env With Env	No Env With Env
16 Box	No Env With Env	No Env With Env	No Env With Env
64 Box	No Env With Env	No Env With Env	No Env With Env
HWHS Site	No SB	Roller SB	Pinned SB
25 Pyramid	No Env With Env	No Env With Env	No Env With Env
100 Pyramid	No Env With Env	No Env With Env	No Env With Env
16 Box	No Env With Env	No Env With Env	No Env With Env
64 Box	No Env With Env	No Env With Env	No Env With Env

5.1 16-Skyscraper Box

A 3-dimensional and elevation view of the 16-skyscraper box is shown in Figure 5-1 and Figure 5-2, respectively. All skyscrapers are 40 stories (4-Interval Skyscraper) tall. Skybridges at each interval are shown in orange. There are 12 exterior and four interior skyscrapers. The plan width for all of the skyscrapers in this dissertation is 50m, core width is 25m, spacing between skyscrapers is 25m and the interval height is 37.5m.

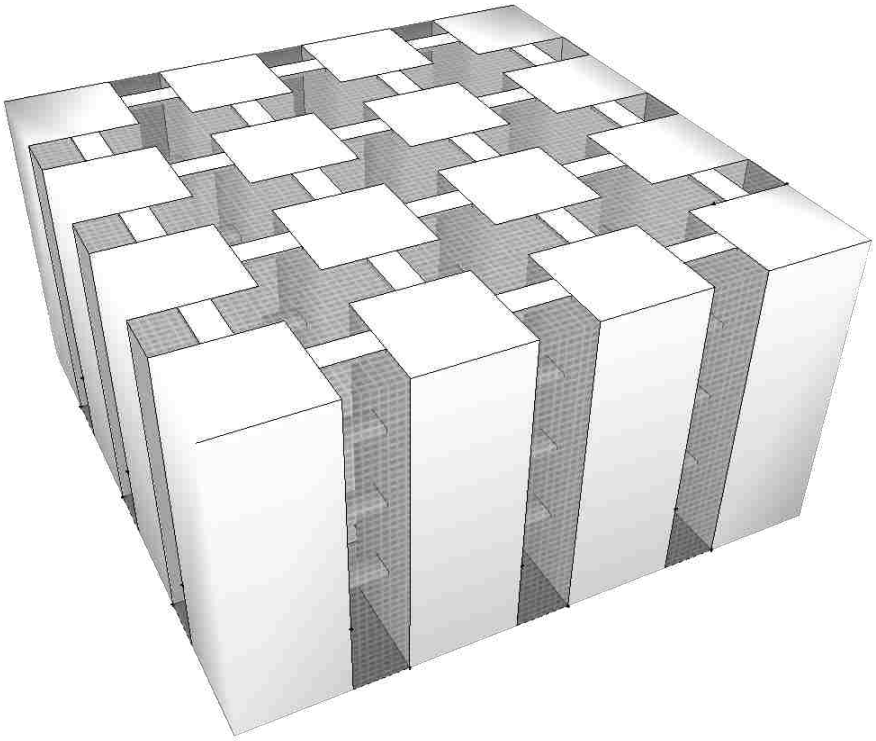

Figure 5-1: 16-Skyscraper Box 3-D View

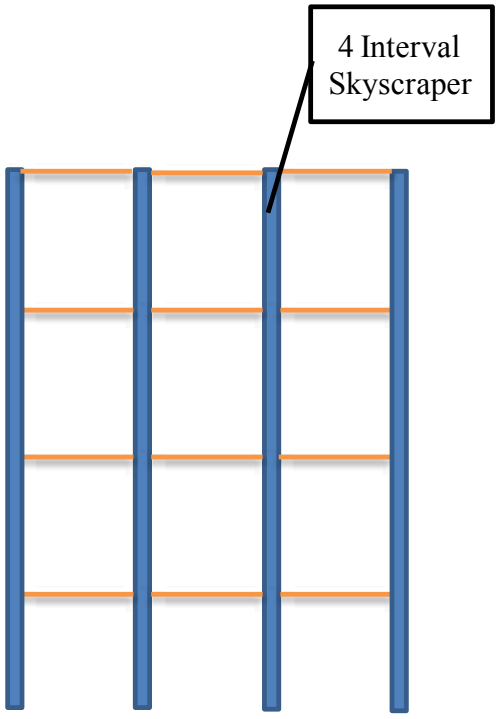

Figure 5-2: 16-Skyscraper Box Elevation View

Wind base shears in kN applied to each skyscraper in the system are shown with envelope and without envelope in Figure 5-3 and Figure 5-4, respectively. Summing these base shears gives a total lateral wind load of 122,963 kN with envelope and 287,810 kN without envelope. The ratio of these two values is 0.43.

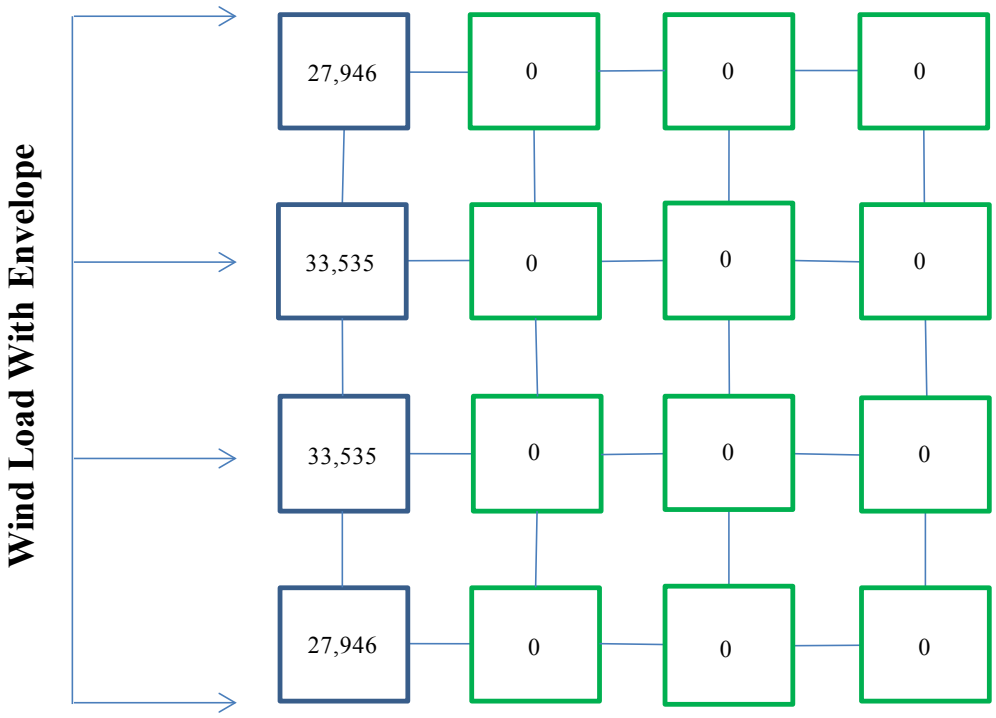

Figure 5-3: Total Lateral Wind Loads for 16-Skyscraper Box With Envelope

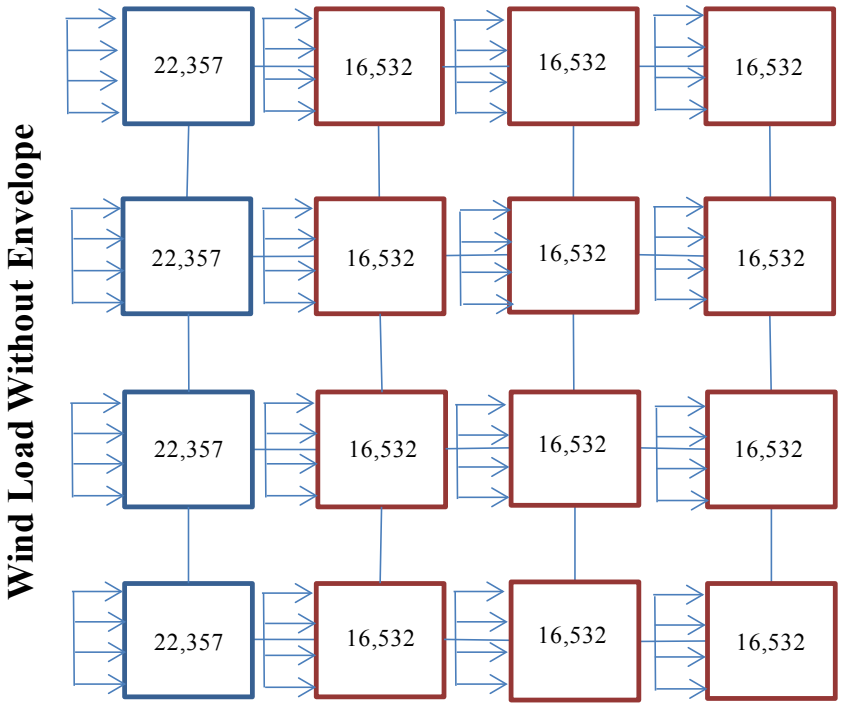

Figure 5-4: Total Lateral Wind Loads for 16-Skyscraper Box Without Envelope

Since the lateral load can act in any of four directions (north, south, east, west), the skyscrapers were grouped into three classes, and the skybridges were grouped into four classes per interval as shown in Figure 5-5. It is assumed that all skyscrapers or skybridges in a class must have the same size since lateral loading could be applied from any direction. For optimization problems with hinge-connected skybridges, design variables include the core thickness and outrigger volume for each interval for each skyscraper class and the skybridge area for each interval for each skybridge class for a total of 4x3x2+4x4 = 40 design variables. Note that there are no design variables for megacolumns because megacolumn area is determined from core area in the SSSM. In order to insure that core thickness increased from top to bottom of the skyscraper, the design variable at the top interval is the core thickness, while the design variables for lower intervals are the increments in core thickness. The minimum and maximum bounds for core thickness increments were 0.1m and 0.5m, respectively. The min and max

bounds for outrigger volume were $0m^3$ and $50m^3$, respectively. The min and max bounds for skybridge area were $0m^2$ and $0.5m^2$, respectively. These same min and max bounds were used for all optimization problems.

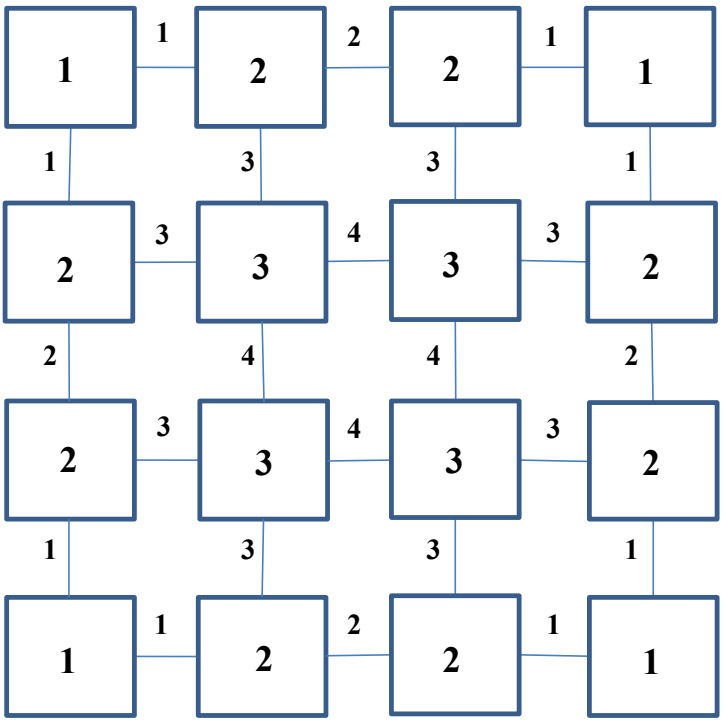

Figure 5-5: 16-Skyscraper Box Connected System Class Numbers

For optimization problems with roller-connected skybridges, the cross-sectional area of all skybridges is equal to Equation 5.1-1, which is based on the flexural stress under gravity load only at the center of the skybridge. Substituting the values for the constants from Chapter 3 into Equation 3.5-8, the area of all roller-connected skybridges is fixed at 0.1515 m^2.

$$A^{bridge} = \frac{D^{bridge} + L^{bridge}}{\frac{4d^{bridge}\sigma^{allow}}{\left(w^{spacing}\right)^2} - \gamma} \qquad \textbf{(5.1-1)}$$

Since skyscrapers displace independently when there are no skybridges, and when there are roller-connected skybridges, the optimization problems in these cases can be decomposed into a series of single-skyscraper optimization subproblems -- one skyscraper from each class. For each of these single-skyscraper optimization subproblems, there are eight design variables (core thickness and outrigger volume at each interval).

Lateral drift was constrained against allowable values in each interval for wind and for seismic loading for a total of eight constraints in all optimization problems and subproblems. For multi-skyscraper optimization problems with hinge-connected skybridges, core stress, megacolumn stress, and outrigger stress were constrained against allowable stress in every interval in each of eight skyscrapers (exploiting symmetry) for wind loading and seismic loading for a total of 192 constraints, and stress and buckling were constrained in every interval in each of six skybridges parallel to lateral loading (exploiting symmetry) for a total of 48 constraints. For single-skyscraper optimization subproblems, core stress, megacolumn stress, and outrigger stress were constrained against allowable stress in every interval for wind loading and seismic loading for a total of 24 constraints.

5.2 64-Skyscraper Box

A 3-D and elevation view of the 64-skyscraper box is shown in Figure 5-6 and Figure 5-7, respectively. All skyscrapers are 70 stories (7-Interval Skyscraper). They are connected at each interval with skybridges shown in orange. There are 28 exterior and 36 interior skyscrapers.

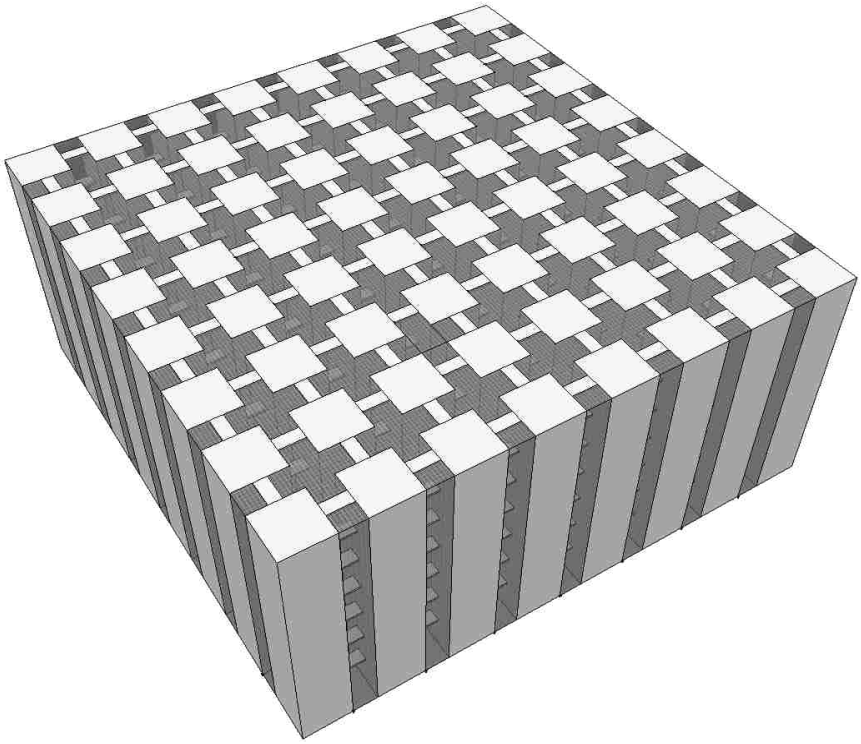

Figure 5-6: 64-Skyscraper Box 3-D View

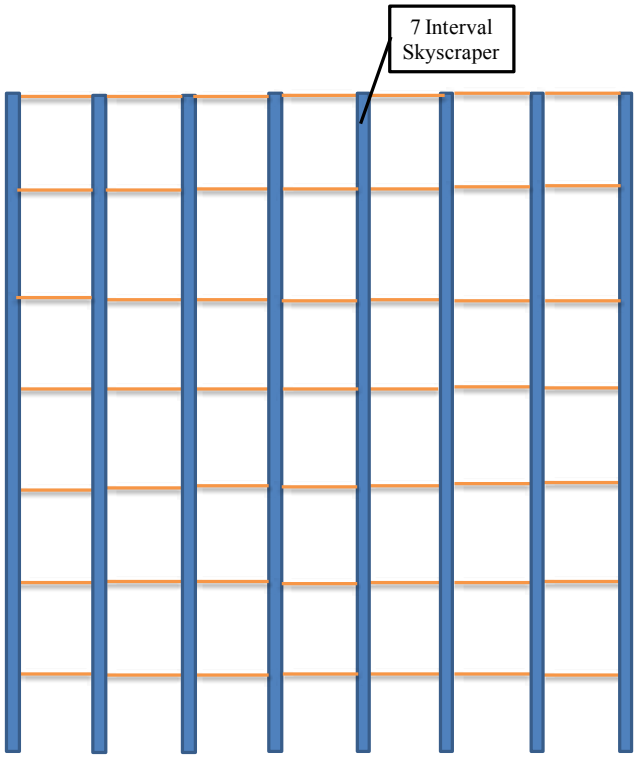

Figure 5-7: 64-Skyscraper Box Elevation View

Wind base shears in kN for the 64-skyscraper box are shown in Figure 5-8 and Figure 5-9 for with and without envelope, respectively. Summing these base shears gives a total lateral wind load of 517,864 kN with envelope and 2,328,338 kN without envelope. The ratio of these two values is 0.22.

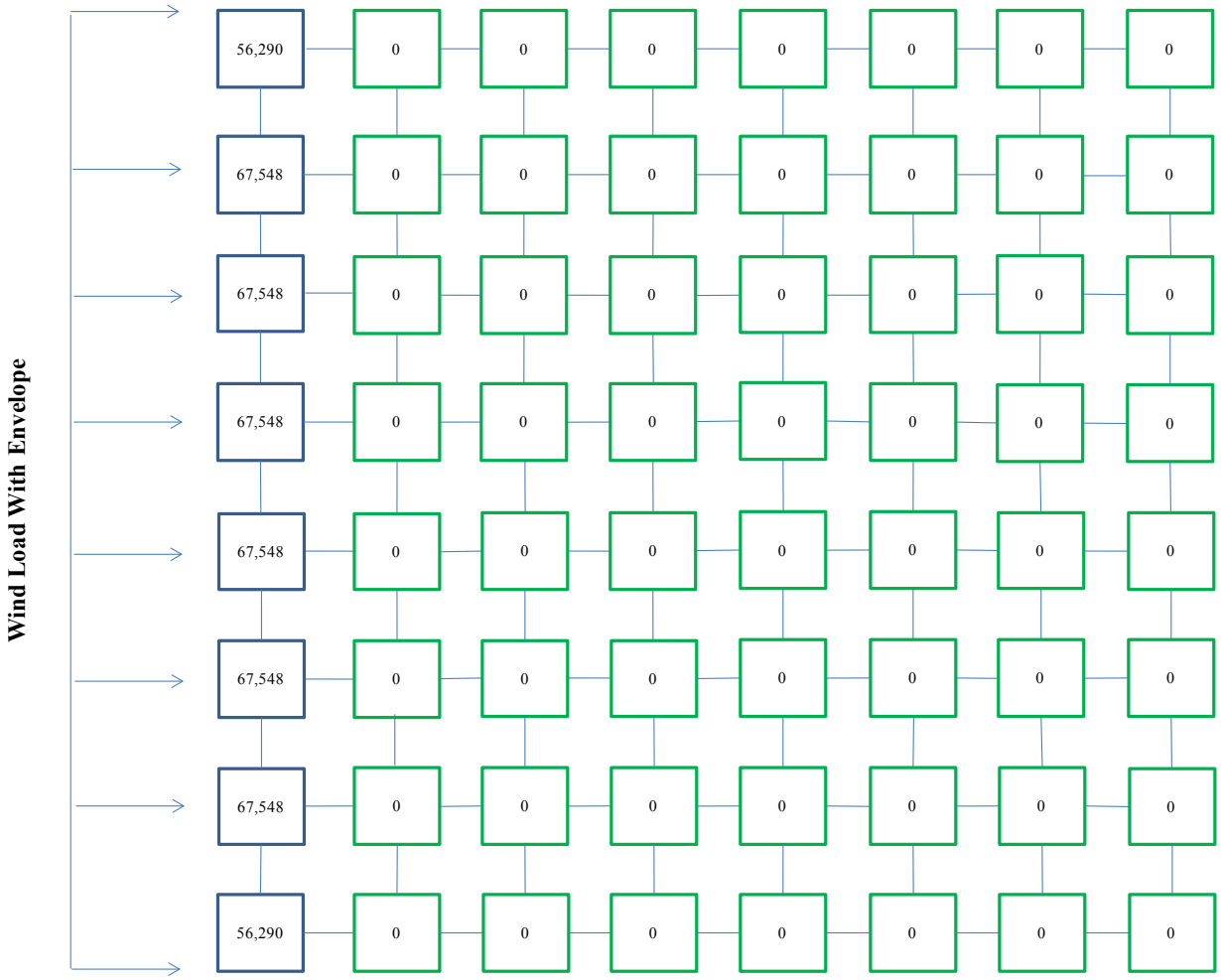

Figure 5-8: Total Lateral Wind Loads for 64-Skyscraper Box With Envelope

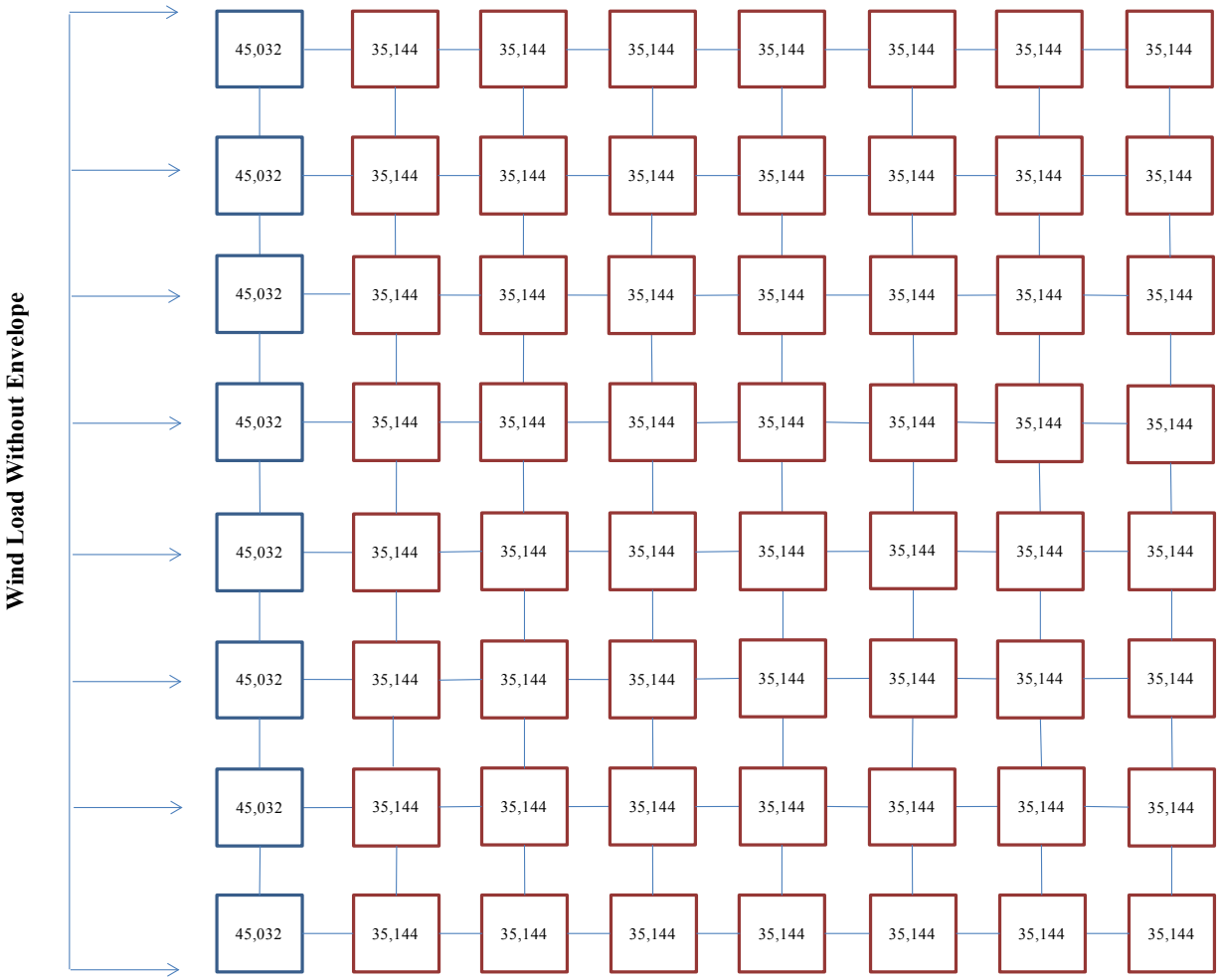

Figure 5-9: Total Lateral Wind Loads for 64-Skyscraper Box Without Envelope

Skyscraper and skybridge class numbers are shown in Figure 5-10. For optimization problems with hinge-connected skybridges, design variables include a total of 7x5x2+7x8 = 126. For optimization problems with no skybridges and with roller-connected skybridges, the total number of design variables for each single-skyscraper optimization subproblem is 14 (core thickness and outrigger volume at each interval). The skybridge cross-sectional area for roller-connected skybridges is $0.1515 m^2$.

The number of constraints for optimization problems with hinge-connected skybridges is 1344 (for each skyscraper, interval, and loading). There are a total of 112 skybridge constraints

(for each skybridge, interval, and loading). For single-skyscraper optimization subproblems there are 42 total constraints. All of these numbers assume symmetry is exploited.

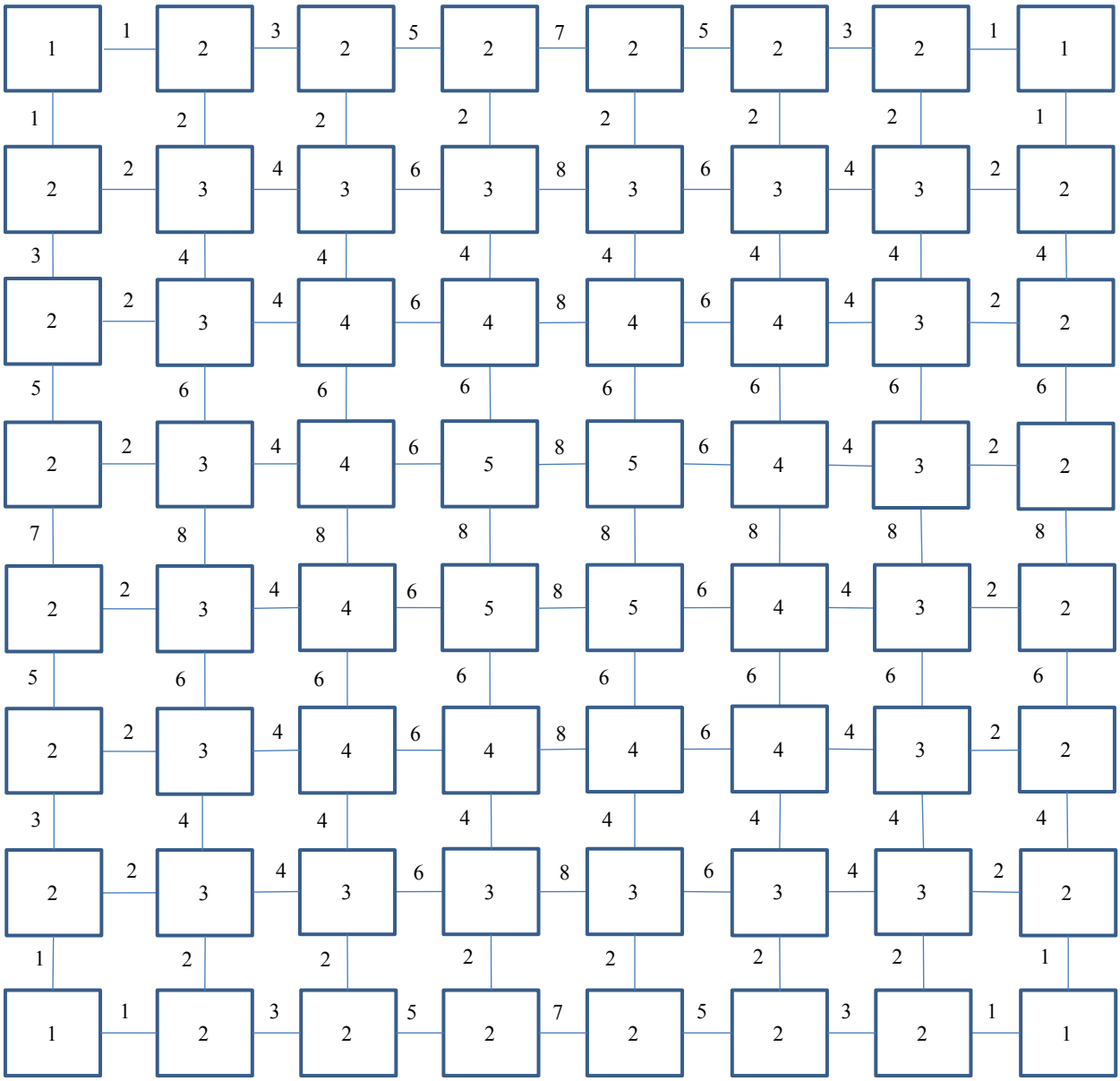

Figure 5-10: 64-Skyscraper Box Class Numbers

5.3 25-Skyscraper Pyramid

A 3-D and elevation view of the 25-skyscraper pyramid is shown in Figure 5-11 and Figure 5-12, respectively. Skyscrapers vary in height and are 20 stories (2-Interval Skyscrapers), 30 stories (3-Interval Skyscrapers) or 40 stories (4-Interval Skyscrapers). There are sixteen 2-interval, eight 3-interval, and one 4-interval skyscrapers.

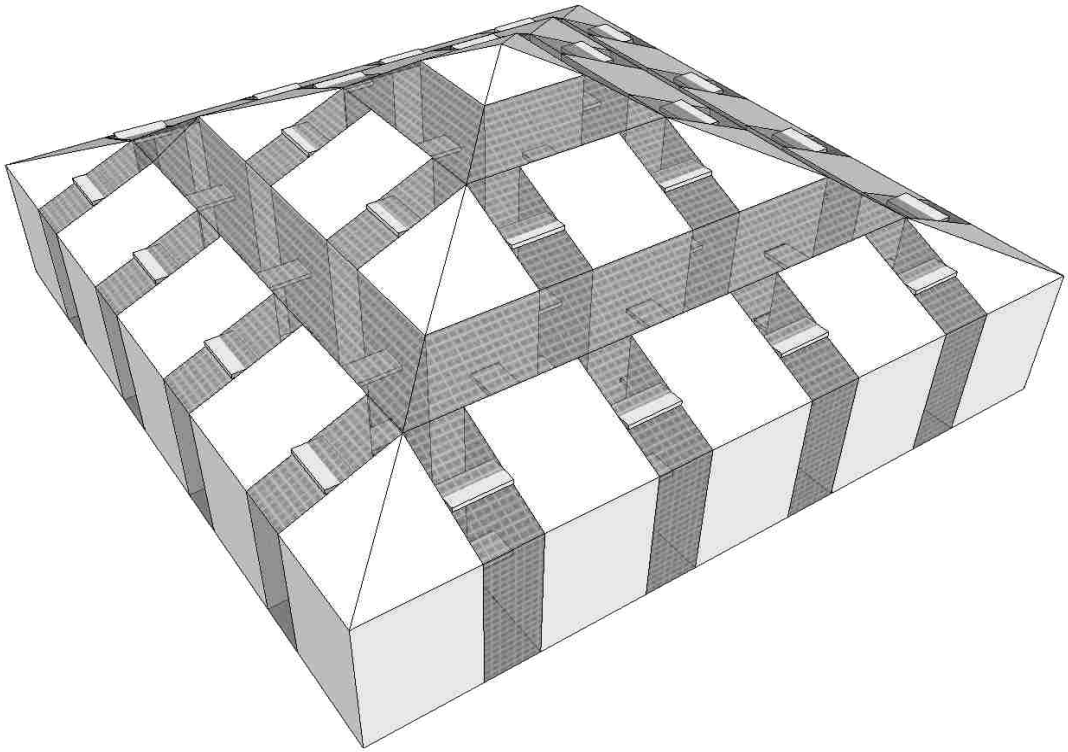

Figure 5-11: 25-Skyscraper Pyramid 3-D View

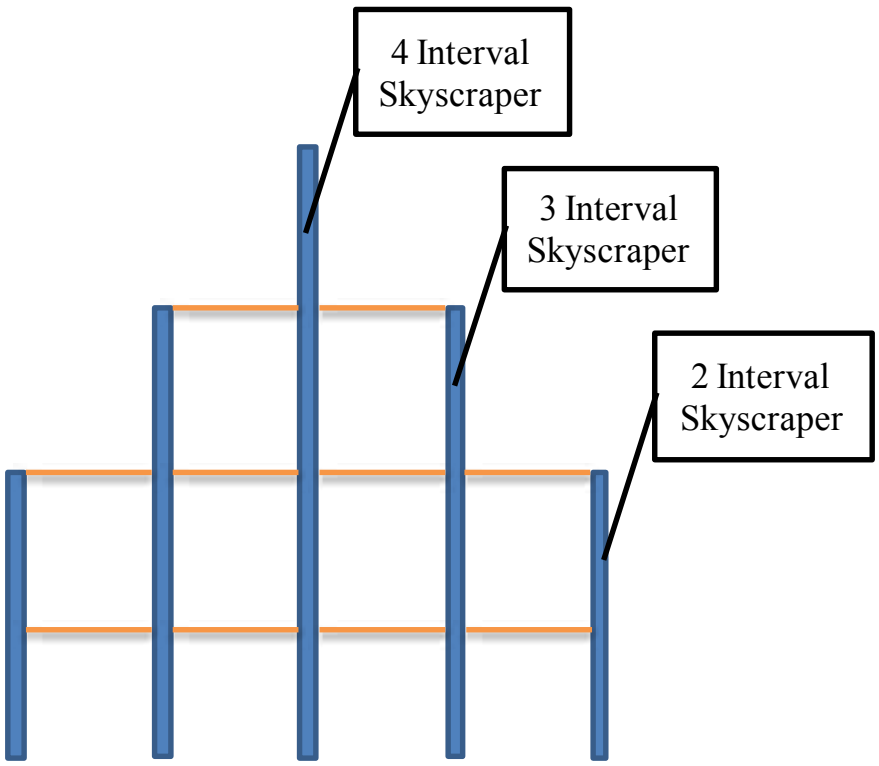

Figure 5-12: 25-Skyscraper Pyramid Elevation View

Wind base shears in kN for the 25-skyscraper pyramid are shown in Figure 5-13 and Figure 5-14 for with and without envelope, respectively. Summing these base shears gives a total lateral wind load of 68,518 kN with envelope and 218,877 kN without envelope. The ratio of these two values is 0.31.

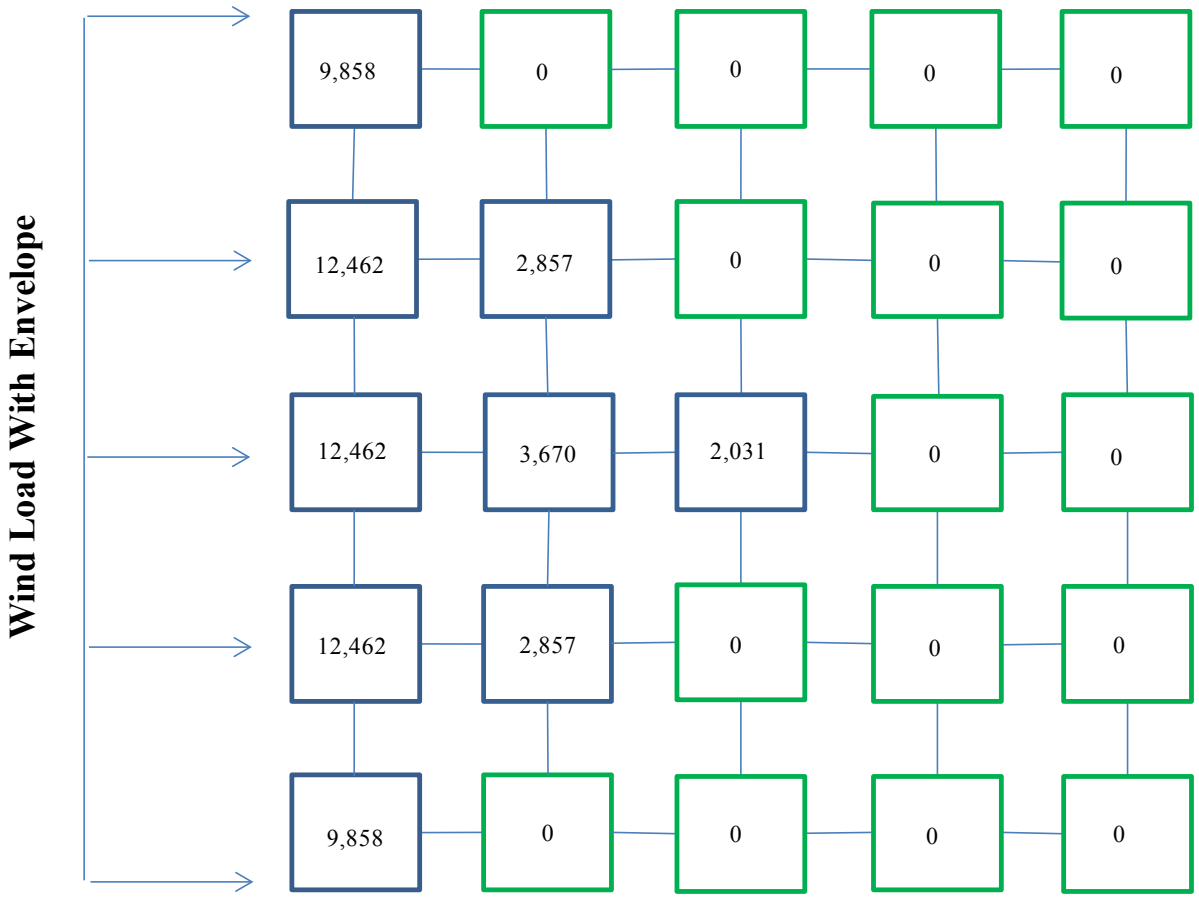

Figure 5-13: Total Lateral Wind Loads for 25-Skyscraper Pyramid With Envelope

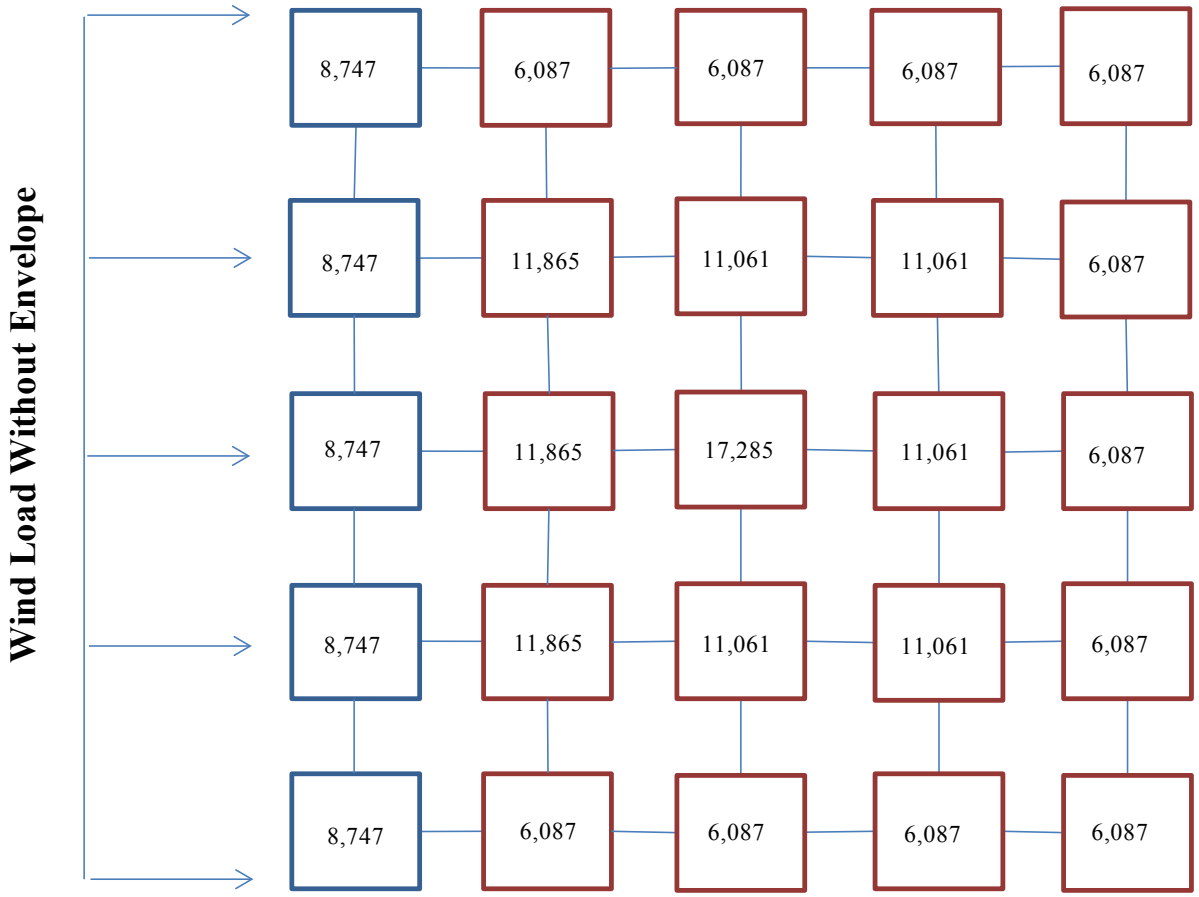

Figure 5-14: Total Lateral Wind Loads for 25-Skyscraper Pyramid Without Envelope

Skyscraper and skybridge class numbers are shown in Figure 5-15 and Figure 5-10. For optimization problems with hinge-connected skybridges, there are a total of 46 design variables. For optimization problems with no skybridges and with roller-connected skybridges, the total number of design variables for two, three and four interval single-skyscraper optimization subproblems is four, six, and eight. The skybridge cross-sectional area for roller-connected skybridges is $0.1515 m^2$.

The number of constraints for optimization problems with hinge-connected skybridges is 222. There are a total of 28 skybridge constraints. For single-skyscraper optimization

subproblems there are 12, 18, and 24 constraints for two, three, and four interval skyscrapers. All of these numbers assume symmetry is exploited.

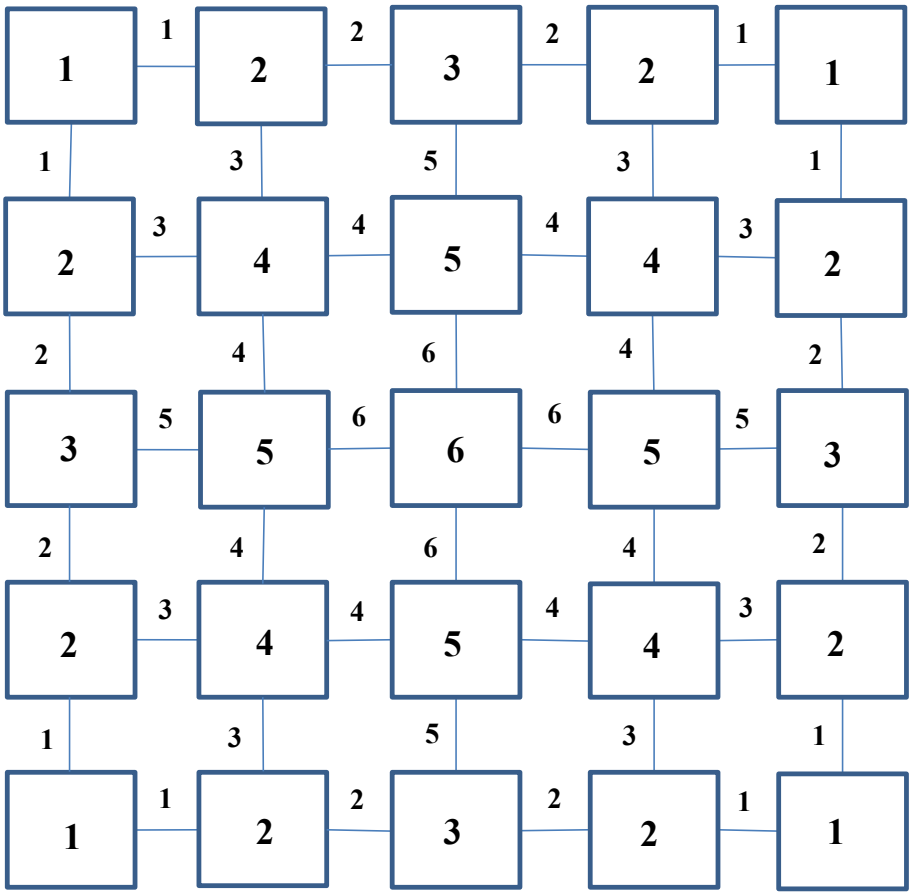

Figure 5-15: 25-Skyscraper Pyramid Class Numbers

5.4 100-Skyscraper Pyramid

A 3-D and elevation view of the 100-skyscraper pyramid is shown in Figure 5-16 and Figure 5-17, respectively. Skyscrapers vary in height and are 30 stories (3-Interval Skyscrapers), 40 stories (4-Interval Skyscrapers), 50 stories (5-Intervals Skyscrapers), 60 stories (6-Interval Skyscrapers), or 70 stories (7-Interval Skyscrapers). There are (36) 3-interval, (28) 4-interval, (20) 5-interval, (12) 6-interval, and four 7-interval skyscrapers.

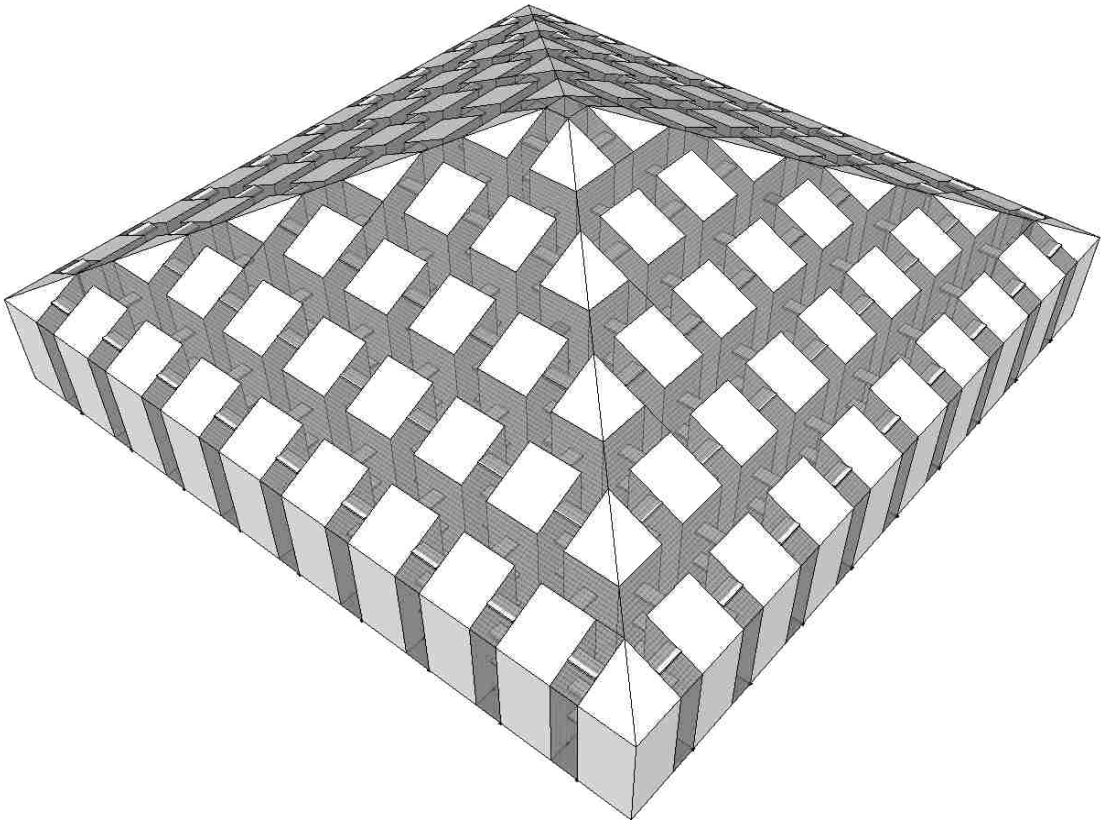

Figure 5-16: 100-Skyscraper Pyramid 3-D View

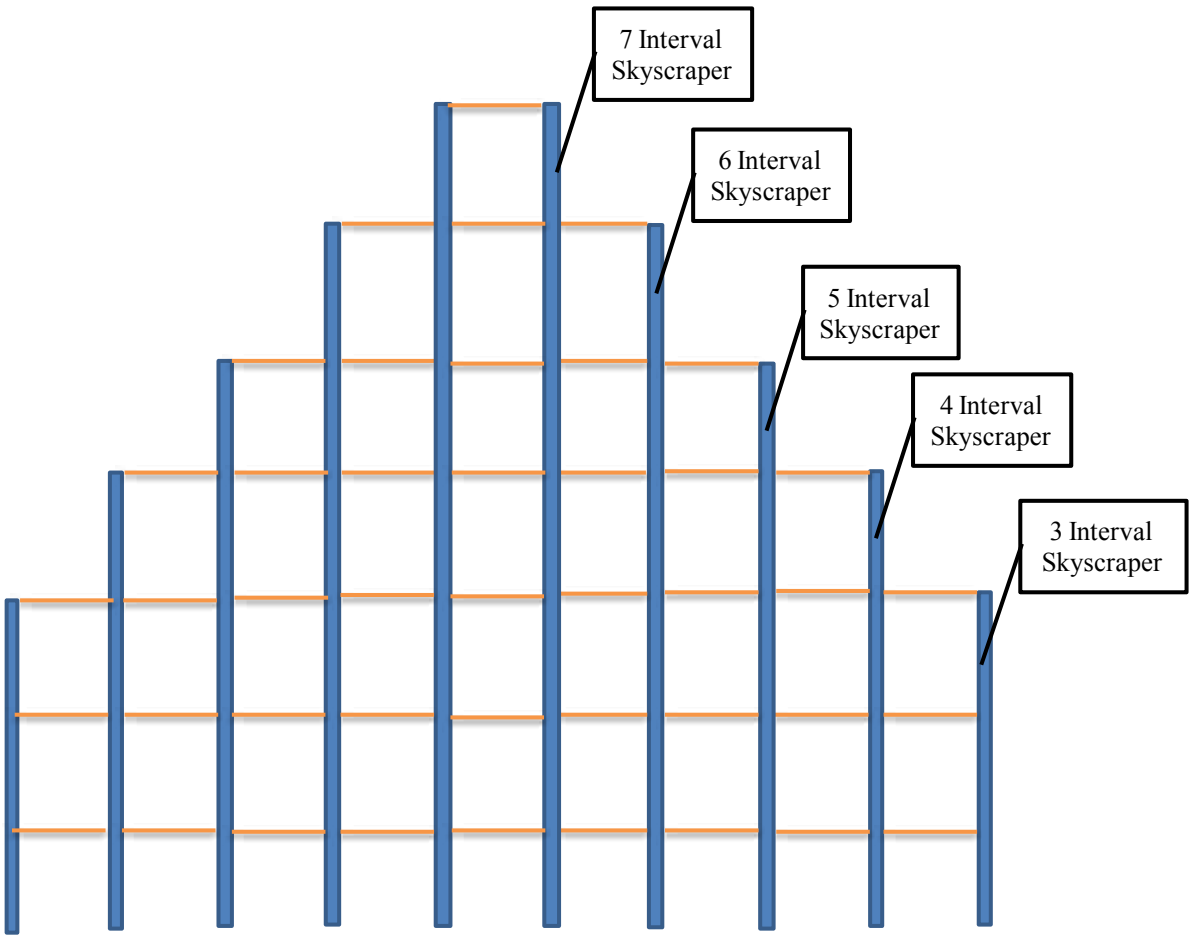

Figure 5-17: 100-Skyscraper Pyramid Elevation View

Wind base shears in kN for the 100-skyscraper pyramid are shown in Figure 5-18 and Figure 5-19 for with and without envelope, respectively. Summing these base shears gives a total lateral wind load of 284,696 kN with envelope and 1,850,411 kN without envelope. The ratio of these two values is 0.15.

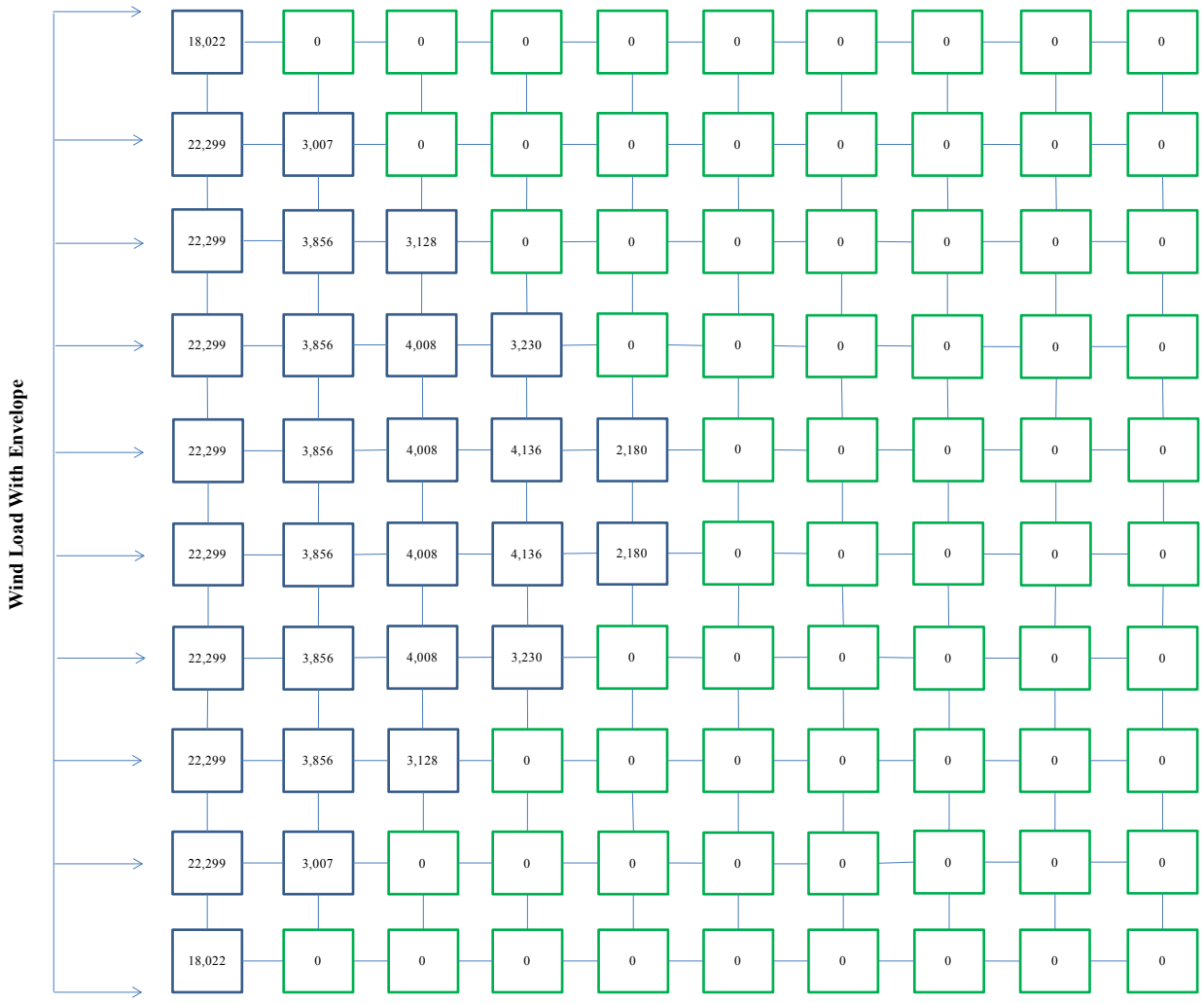

Figure 5-18: Total Lateral Wind Loads for 100-Skyscraper Pyramid With Envelope

Figure 5-19: Total Lateral Wind Loads for 100-Skyscraper Pyramid Without Envelope

Skyscraper and skybridge class numbers are shown in Figure 5-20. For optimization problems with hinge-connected skybridges, there is a total of 135 design variables. For optimization problems with no skybridges and with roller-connected skybridges, the total number of design variables for three, four, five, six and seven interval single-skyscraper optimization subproblems is six, eight, ten, 12, and 14. The skybridge cross-sectional area for roller-connected skybridges is $0.1515 m^2$.

The number of constraints for optimization problems with hinge-connected skybridges is 1260. There are a total of 98 skybridge constraints. For single-skyscraper optimization subproblems there are 18, 24, 30, 36, and 42 constraints for three, four, five, six, and seven interval skyscrapers. All of these numbers assume symmetry is exploited.

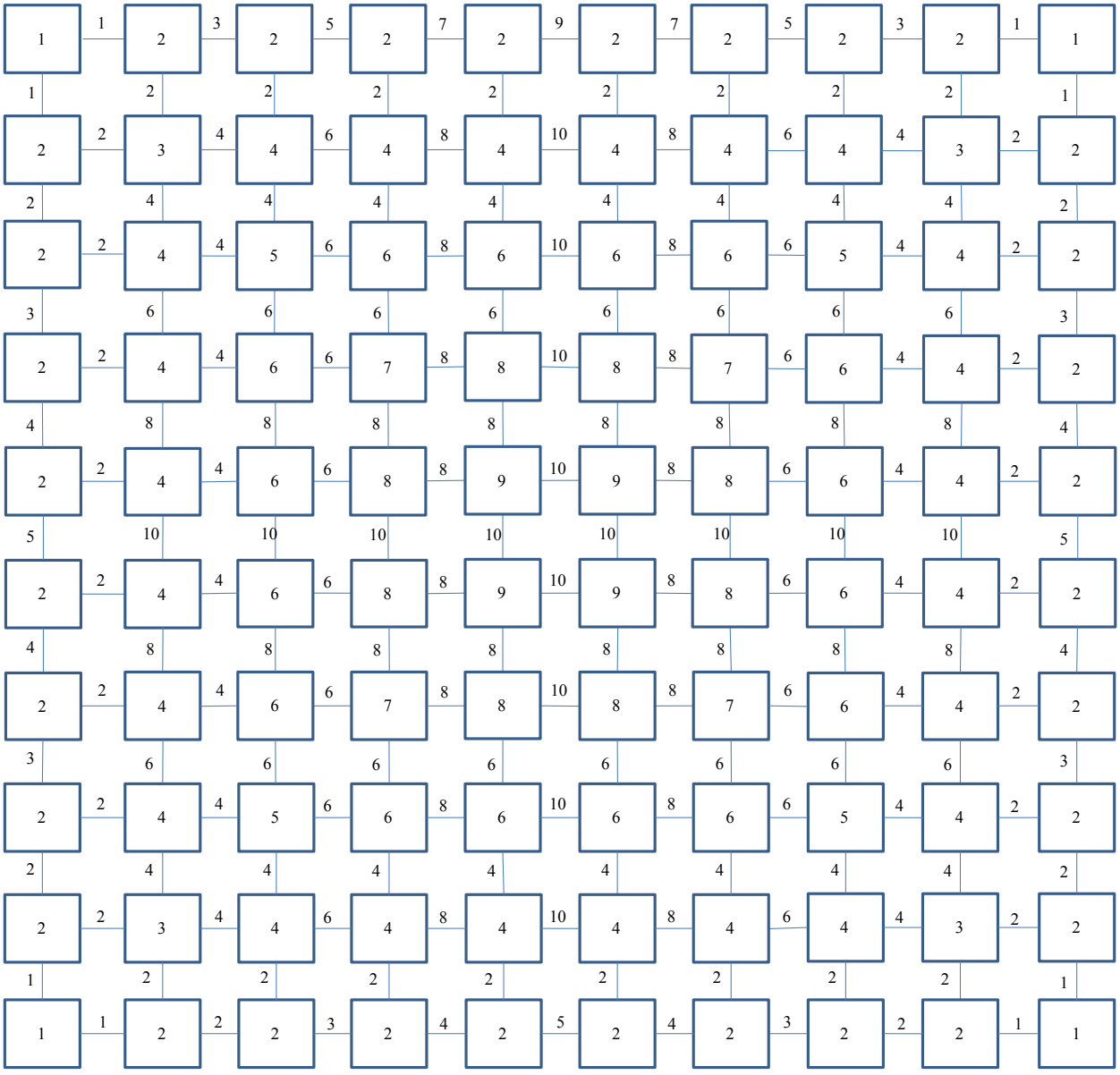

Figure 5-20: 100-Skyscraper Pyramid Class Numbers

CHAPTER 6. OPTIMIZATION STRATEGY

The optimization problems were solved with a strategy involving gradient-based algorithms and genetic algorithms. The two gradient-based algorithms used for optimization were Sequential Quadratic Programming (SQP) and Generalized Reduced Gradient (GRG) found in the software package, OptdesX 2.0.4, developed by Parkinson and Balling (2002). The genetic algorithm program that was used was a program developed by Balling (1991).

SQP converges to the optimum design by simultaneously improving the objective and tightening feasibility of the constraints. Only the optimal design is guaranteed to be feasible; intermediate designs may be infeasible (Parkinson 2010). GRG requires more function evaluations than SQP, but has the desirable property that it stays feasible once a feasible point is found. If the optimization process is stopped before the optimum is reached, a better design than the starting design is guaranteed. Both SQP and GRG are restricted to optimization problems with continuous design variables, relatively few design variables, differentiable objective and constraint functions, a single local optimum, and a single objective. Gradients in these algorithms are typically calculated by finite difference approximation.

According to Parkinson (2010) and Mettler et al. (1988), a genetic algorithm is a search algorithm based on natural selection, population and evolutionary operators that mimic survival of the fittest, including selection, crossover (reproduction), and mutation. The genetic algorithm for this research used: 1) 500 generations with a generation size of 500, 2) tournament selection with a tournament size of 5, 3) uniform crossover with a crossover probability of 1.0, and 4)

uniform mutation with a mutation probability of 0.1. Genetic algorithms are much simpler than gradient-based algorithms, but they generally require more executions of the analysis program than gradient-based algorithms. Genetic algorithms are effective at optimizing problems with discrete design variables, problems with many design variables, problems with multiple objectives, and problems with non-differentiable objective and constraint functions.

The strategy for solving multi-skyscraper optimization problems for systems with hinge-connected skybridges was to perform in series: 1) multiple executions of the SQP algorithm, 2) multiple executions of the GRG algorithm, and 3) multiple executions of the genetic algorithm. The starting design for SQP was a conservative design where the value of each design variable was near the maximum bound given in Chapter 5. The starting design for each execution was the final design from the preceding execution. Executions of an algorithm terminated when the maximum change in the optimum objective function was less than 0.001 percent. The SQP algorithm was executed first because of its efficiency. The GRG algorithm was executed secondly because of its property of guaranteeing feasibility. The genetic algorithm was executed third because of its ability to make further progress, especially on large problems. Table 6-1 shows the percent improvement in the objective function of the final GRG design over the starting design and the genetic algorithm design over the final GRG algorithm design. Bold values indicate the greatest improvement. Note that the most dramatic improvement was for the 100-skyscraper pyramid.

The strategy for solving single-skyscraper optimization problems for systems with no skybridges or roller-connected skybridges was to perform a single execution of the GRG algorithm. Additional executions of the GRG or SQP algorithm did not change the design. Neither did additional executions of the genetic algorithm.

Table 6-1: Gradient-Based VS. Genetic Algorithm Improvement

HWLS Site		Hinge Skybridge	
		Gradient	Genetic
16 Box	No Env	11.89%	2.54%
	With Env	11.43%	0.74%
64 Box	No Env	8.68%	4.29%
	With Env	7.81%	5.23%
25 Pyramid	No Env	18.56%	0.00%
	With Env	18.57%	0.00%
100 Pyramid	No Env	16.06%	34.08%
	With Env	**21.44%**	**52.44%**
Average		14.31%	12.41%
HWHS Site		Hinge Skybridge	
		Gradient	Genetic
16 Box	No Env	12.61%	3.80%
	With Env	12.89%	5.67%
64 Box	No Env	8.56%	2.34%
	With Env	8.46%	4.36%
25 Pyramid	No Env	19.14%	1.20%
	With Env	**20.77%**	9.06%
100 Pyramid	No Env	17.40%	**37.48%**
	With Env	14.22%	23.61%
Average		14.25%	10.94%

The genetic algorithm used in the research performed much better with discrete-valued design variables than with continuous-valued design variables. The optimization problem was discretized in the following fashion. Let O_i be the optimum value of continuous design variable i from the final execution of the GRG algorithm. It was assumed that the discrete design variables in the genetic algorithm were integer values ranging from 0 to 100. Let D_i the value of discrete design variable i. The corresponding continuous value C_i is given by Equation 6-1:

$$C_i = \frac{O_i D_i}{50} \tag{6-1}$$

Note that discrete values of 0, 50, and 100 correspond to continuous values of 0, O_i, and $2O_i$, respectively. The mapping of discrete to continuous design variables changes with each

execution. The first design in the starting generation of the genetic algorithm was a design with all discrete design variable values equal to 50 (i.e., best design from GRG algorithm). The other designs in the starting generation were generated randomly. The genetic algorithm employed "elitism" where every generation of children designs created by selection, crossover, and mutation had to compete with the generation of parent designs for survival to the next generation. Elitism guarantees that the final design in the genetic algorithm will be equal or better than the final design in the GRG algorithm. After executing the genetic algorithm for the first time, the optimum value of D_i was converted to C_i by Equation 6-1 which became the value of O_i for the next execution of the genetic algorithm.

The number of gradient-based algorithm executions (GRG or SQP), the number of genetic algorithm executions, and the total execution time for optimization is given in Table 6-2. Executions were performed on an HP Envy dv7 PC computer with 12.0 GB RAM and clock speed of 2.40 GHz. For each case, the max was taken over four optimization problems (i.e., with envelope, without envelope, HWHS site, HWLS site). For problems with roller-connected skybridges or no skybridges, a single execution of the GRG algorithm was performed for each of the single-skyscraper optimization subproblems. Recall that the number of subproblems is equal to the number of skyscraper classes, which is the value shown in Table 6-2 under max GRG/SQP executions.

Table 6-2: Execution Time for Connected Systems

	Skybridge Type	Max GRG/SQP Executions	Max Genetic Executions	Total Execution Time (minutes)
16 Box	Hinge SB	1	4	12.33
	Roller SB	3	0	0.10
	No SB	3	0	0.10
64 Box	Hinge SB	3	6	1444
	Roller SB	5	0	0.17
	No SB	5	0	0.17
25 Pyramid	Hinge SB	2	6	30.17
	Roller SB	6	0	0.20
	No SB	6	0	0.20
100 Pyramid	Hinge SB	4	8	1447
	Roller SB	9	0	0.30
	No SB	9	0	0.30

CHAPTER 7. OPTIMIZATION RESULTS

The following eight subsections present optimization results for each of the four skyscraper systems at each of the two sites. Data are presented in the same fashion in each subsection in the following order:

1) a table of optimum volume values of components (core, megacolumns, outriggers, skybridges)
2) a table of optimum skyscraper or system natural periods
3) a table of controlling constraint percentages and maximum drift vs. allowable ratios
4) graphs of lateral wind displacement vs. height for each skyscraper
5) graphs of combined core and megacolumn area vs. height for each skyscraper class
6) graphs of outrigger volume vs. height for each skyscraper class
7) graphs of total skybridge area vs. height

In the tables, skyscrapers are grouped into exterior (perimeter) skyscrapers and interior skyscrapers for box systems, and into 2-interval skyscrapers, 3-interval skyscrapers, 4-interval skyscrapers, etc. for pyramid systems. In the graphs, data for no skybridge cases are not shown since they are essentially the same as for the roller skybridge cases.

7.1 16-Skyscraper Box - HWLS Site

From Table 7-1, the overall lightest design is the hinge system with envelope. This design has 4.4 percent less volume than the roller system with envelope. The envelope leads to lower

volume for the hinge system, but leads to higher volume for the roller and no skybridge systems. The volumes of the exterior and interior skyscrapers are essentially the same for the hinge system with envelope, but the volumes of the exterior skyscrapers are notably more than the volumes of the interior skyscrapers for the roller system with envelope. In addition, the hinge system with envelope has larger skybridges than the roller system with envelope. This indicates that the primary difference between the roller system with envelope and the hinge system with envelope is that material is reallocated from the exterior skyscrapers to the skybridges, resulting in a lighter design. The optimal designs of hinge and roller systems without envelope are essentially the same. All of these trends are confirmed from the graphs in Figure 7-2, Figure 7-4, and Figure 7-3. Volume of cores, megacolumns, and outriggers decrease with height although the decrease is somewhat erratic for outriggers of the hinge system without envelope. This behavior is similar for the other optimized cases. It is interesting that the largest skybridges in the hinge system with envelope are located in the next-to-bottom interval, while the smallest skybridges are located in the bottom interval. This may be a result of the fact that lateral loads increase with height while skyscraper stiffness decreases with height.

From Table 7-2, the natural periods of systems with envelope indicate that the exterior skyscrapers are stiffer than the interior skyscrapers for the roller system, while the stiffness of the hinge system falls somewhere in between. Note that the natural periods of all systems and skyscrapers are about the same for systems without envelope. The same trend is shown in the lateral displacement graphs of Figure 7-1. For systems with envelope, the displacements of interior skyscrapers in the roller system are near zero while displacements of exterior skyscrapers are more than double the displacements of skyscrapers in the hinge system. This behavior is

similar for the other optimized cases. For systems without envelope, lateral displacements are about the same for all skyscrapers in hinge and roller systems.

Table 7-3 shows that the seismic stress controls the outrigger designs, minimum thickness of the core controls the core and megacolumn design, and wind stress controls the skybridge design for the hinge case. Note that wind drift does not control the design for the 16 box system.

Table 7-1: 16-Skyscraper Box, HWLS, Optimum Volume Values

Volumes (m^3)	# Sky-scrapers	With Envelope			No Envelope		
		Hinge Skybridge	Roller Skybridge	No Skybridge	Hinge Skybridge	Roller Skybridge	No Skybridge
Exterior Skyscraper Core Vol	12	1,521	1,600	1,602	1,549	1,562	1,562
Exterior Skyscraper Column Vol		1,389	1,460	1,409	1,413	1,425	1,374
Exterior Skyscraper Outrigger Vol		22	76	74	51	52	52
Interior Skyscraper Core Vol	4	1,514	1,516	1,516	1,535	1,535	1,537
Interior Skyscraper Column Vol		1,408	1,408	1,334	1,426	1,426	1,352
Interior Skyscraper Outrigger Vol		18	18	15	50	44	40
Total Skybridge Vol	--	608	364	--	378	364	--
Total System Vol	--	47,550	49,755	48,468	48,584	48,852	47,580

Table 7-2: 16-Skyscraper Box, HWLS Site, Optimum Periods

Period(s)	With Envelope			No Envelope		
	Hinge Skybridge	Roller Skybridge	No Skybridge	Hinge Skybridge	Roller Skybridge	No Skybridge
Exterior Skyscraper Period	--	2.861-3.003	2.852-2.998	--	3.134-3.168	3.124
Interior Skyscraper Period	--	3.770	3.780	--	3.243	3.242
System Period	3.632	--	--	3.152	--	--

Table 7-3: 16-Skyscraper Box, HWLS Site, Controlling Constraints

Controlling Constraint	With Envelope			No Envelope		
	Hinge Skybridge	Roller Skybridge	No Skybridge	Hinge Skybridge	Roller Skybridge	No Skybridge
Wind Stress Controls Core/Columns	17%	17%	25%	25%	25%	25%
Seismic Stress Controls Core/Columns	8%	8%	0%	0%	0%	0%
Min Thickness Controls Core/Columns	75%	75%	75%	75%	75%	75%
Nothing Controls Core/Columns	0%	0%	0%	0%	0%	0%
Wind Stress Controls Outriggers	0%	50%	50%	0%	33%	17%
Seismic Stress Controls Outriggers	58%	25%	25%	0%	0%	0%
Outriggers Deleted	0%	8%	0%	0%	8%	17%
Nothing Controls Outriggers	42%	17%	25%	100%	58%	67%
Wind Stress Controls Skybridges	69%	0%	0%	81%	0%	0%
Seismic Stress Controls Skybridges	0%	0%	0%	0%	0%	0%
Gravity Stress Controls Skybridges	0%	100%	0%	19%	100%	0%
Nothing Controls Skybridges	31%	0%	0%	0%	0%	0%
Max Wind Drift / Allowable	0.211	0.492	0.500	0.337	0.406	0.401
Max Seismic Drift / Allowable	0.050	0.052	0.051	0.045	0.046	0.046

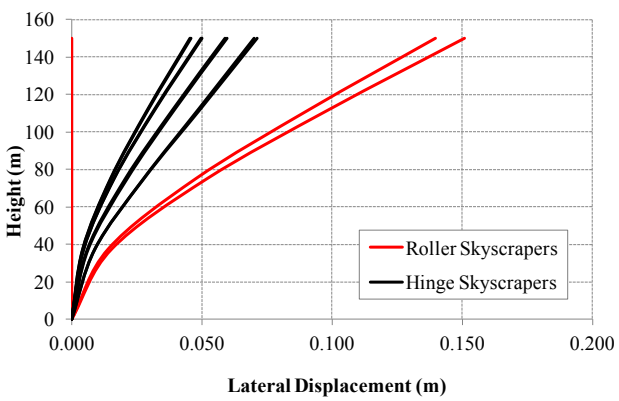

(a) With Envelope

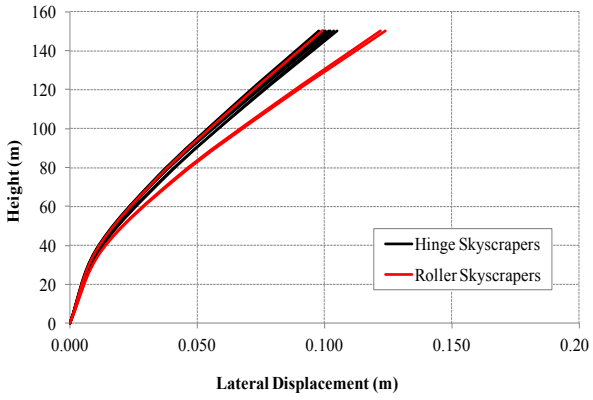

(b) No Envelope

Figure 7-1: 16-Skyscraper Box, HWLS Site, Wind Displacement

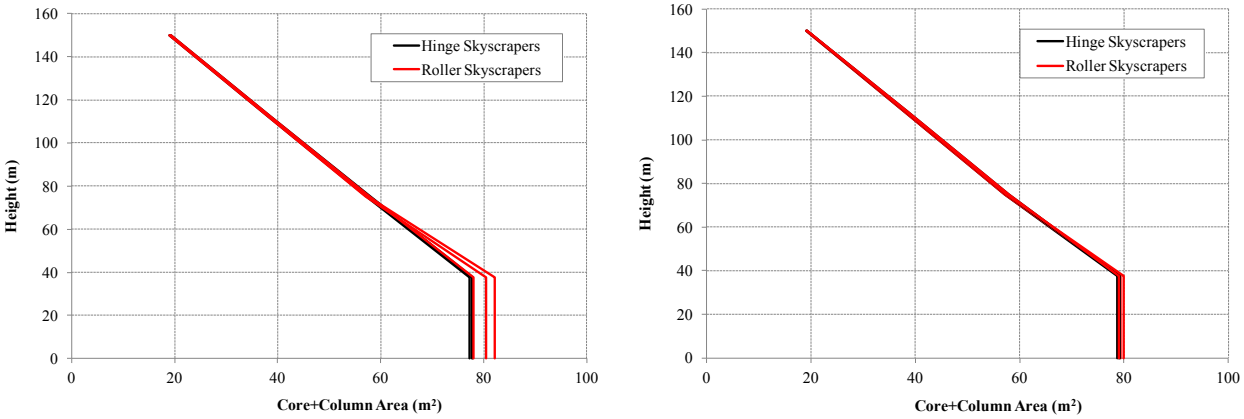

(a) With Envelope (b) No Envelope

Figure 7-2: 16-Skyscraper Box, HWLS Site, Combined Core and Column Area

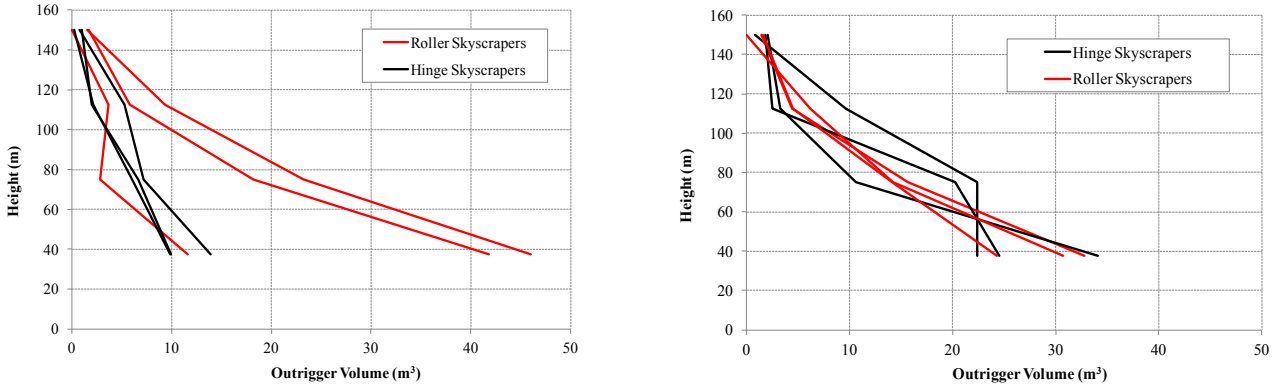

(a) With Envelope (b) No Envelope

Figure 7-3: 16-Skyscraper Box, HWLS Site, Outrigger Volumes

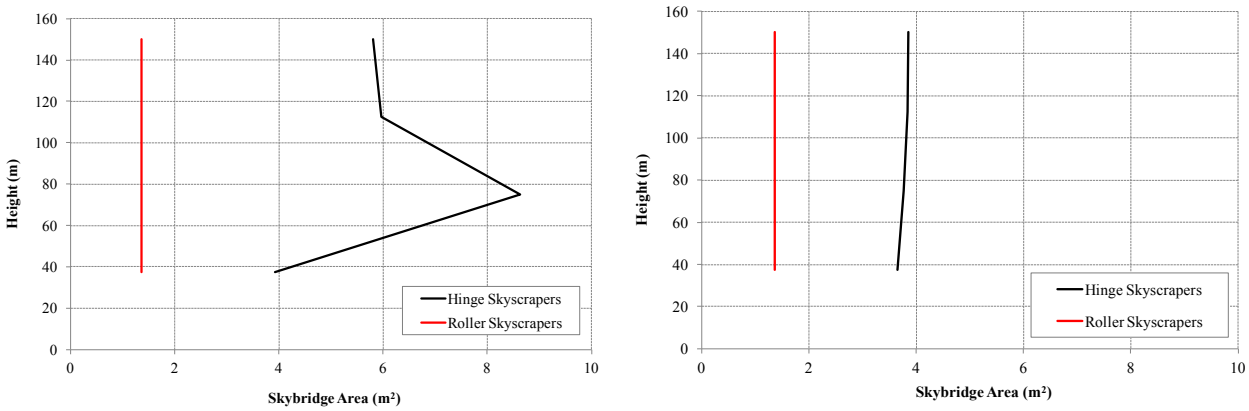

(a) With Envelope (b) No Envelope

Figure 7-4: 16-Skyscraper Box, HWLS Site, Total Skybridge Areas

7.2 16-Skyscraper Box - HWHS Site

From Table 7-4, the overall lightest design is the system without skybridges or envelope. However, the hinge system without envelope has more volume by only 2.9 percent and has essentially the same volume as the roller system with and without envelope. Exterior and interior skyscraper volumes are all very similar, and from Table 7-5, the natural periods of individual skyscrapers are all very similar, indicating that high seismicity controls the design for all skybridge cases with or without envelope. The high-seismic site prevents the re-distribution of volume from exterior skyscrapers to skybridges, thus making all cases similar in design.

Similar to results shown for the 16-skyscraper box HWLS case, volume of cores, megacolumns, and outriggers decrease with height, as illustrated in Figure 7-6 and Figure 7-7. Figure 7-8 shows that the skybridge volume is also smallest at the bottom interval and largest at the top.

Controlling constraints for the 16 box system at the high seismic site are similar to those at the low seismic site. Table 7-4 shows that the seismic stress controls the outrigger designs,

minimum thickness of the core controls the core and megacolumn design, and wind stress solely controls the skybridge design for the hinge case.

Table 7-4: 16-Skyscraper Box, HWHS Site, Optimum Volume Values

Volumes (m^3)	# Sky-scrapers	With Envelope			No Envelope		
		Hinge Skybridge	Roller Skybridge	No Skybridge	Hinge Skybridge	Roller Skybridge	No Skybridge
Exterior Skyscraper Core Vol	12	1,598	1,605	1,604	1,602	1,599	1,600
Exterior Skyscraper Column Vol		1,459	1,465	1,411	1,462	1,459	1,408
Exterior Skyscraper Outrigger Vol		90	87	87	82	87	80
Interior Skyscraper Core Vol	4	1,599	1,599	1,600	1,605	1,599	1,600
Interior Skyscraper Column Vol		1,487	1,486	1,408	1,491	1,486	1,408
Interior Skyscraper Outrigger Vol		85	88	80	78	88	71
Total Skybridge Vol	--	495	364	--	361	364	--
Total System Vol	--	50,945	50,936	49,586	50,818	50,786	49,367

Table 7-5: 16-Skyscraper Box, HWLS Site, Optimum Periods

Building Periods	With Envelope			No Envelope		
	Hinge Skybridge	Roller Skybridge	No Skybridge	Hinge Skybridge	Roller Skybridge	No Skybridge
Exterior Skyscraper Period	--	2.697-2.709	2.69-2.718	--	2.709-2.711	2.718
Interior Skyscraper Period	--	2.709	2.718	--	2.709	2.847
System Period	2.705	--	--	2.710	--	--

Table 7-6: 16-Skyscraper Box, HWHS Site, Controlling Constraints

Controlling Constraint	With Envelope			No Envelope		
	Hinge Skybridge	Roller Skybridge	No Skybridge	Hinge Skybridge	Roller Skybridge	No Skybridge
Wind Stress Controls Core/Columns	0%	8%	8%	0%	0%	0%
Seismic Stress Controls Core/Columns	25%	17%	17%	25%	25%	25%
Min Thickness Controls Core/Columns	75%	75%	75%	75%	75%	75%
Nothing Controls Core/Columns	0%	0%	0%	0%	0%	0%
Wind Stress Controls Outriggers	0%	0%	0%	0%	0%	0%
Seismic Stress Controls Outriggers	67%	75%	75%	75%	75%	75%
Outriggers Deleted	0%	0%	0%	0%	0%	17%
Nothing Controls Outriggers	33%	25%	25%	25%	25%	8%
Wind Stress Controls Skybridges	100%	0%	0%	56%	0%	0%
Seismic Stress Controls Skybridges	0%	0%	0%	0%	0%	0%
Gravity Stress Controls Skybridges	0%	100%	0%	44%	100%	0%
Nothing Controls Skybridges	0%	0%	0%	0%	0%	0%
Max Wind Drift / Allowable	0.130	0.412	0.419	0.235	0.278	0.283
Max Seismic Drift / Allowable	0.082	0.082	0.082	0.082	0.082	0.082

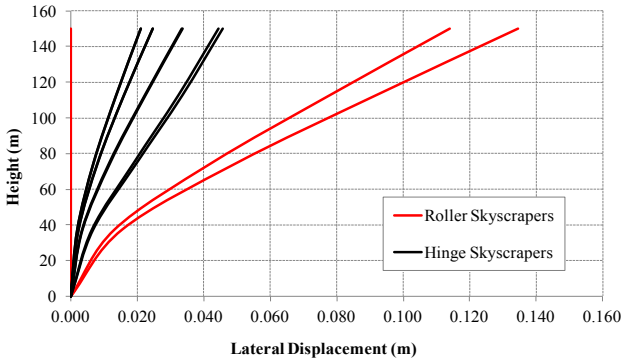

(a) With Envelope

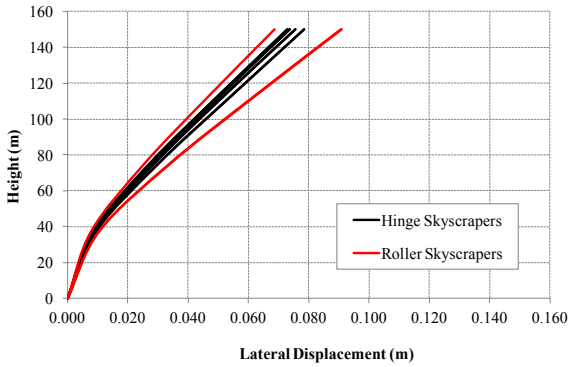

(b) No Envelope

Figure 7-5: 16-Skyscraper Box, HWHS Site, Wind Displacements

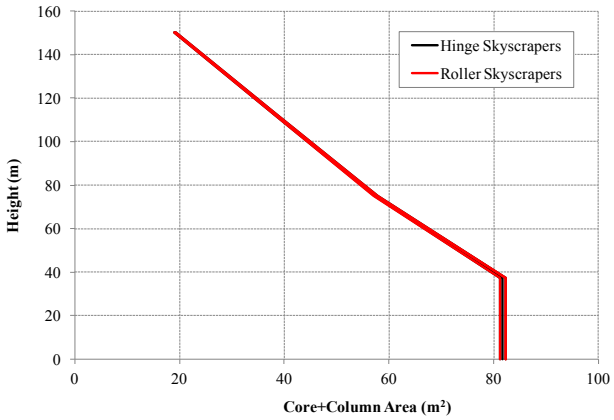

(a) With Envelope

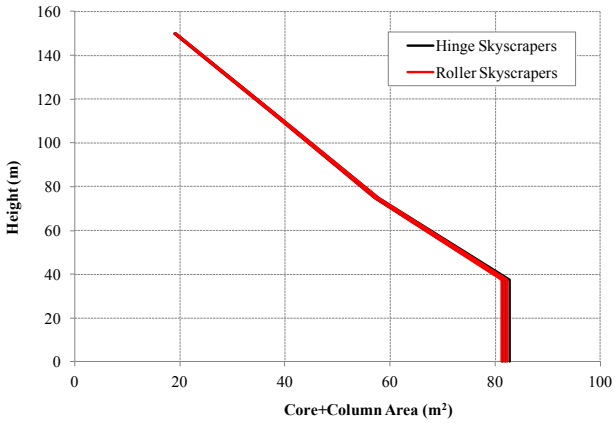

(b) No Envelope

Figure 7-6: 16-Skyscraper Box, HWHS Site, Combined Core and Column Areas

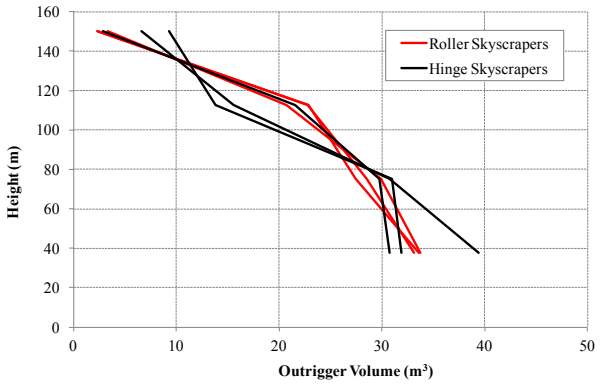

(a) With Envelope

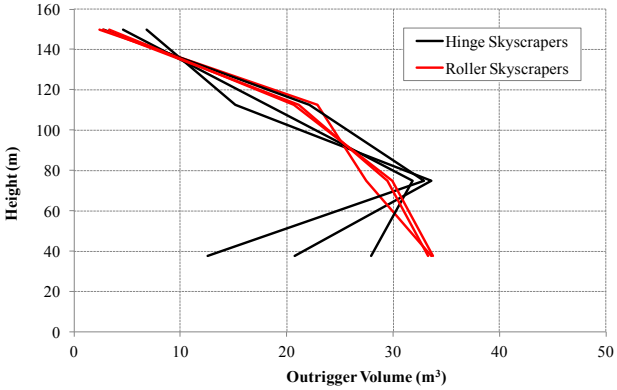

(b) No Envelope

Figure 7-7: 16-Skyscraper Box, HWHS Site, Outrigger Volumes

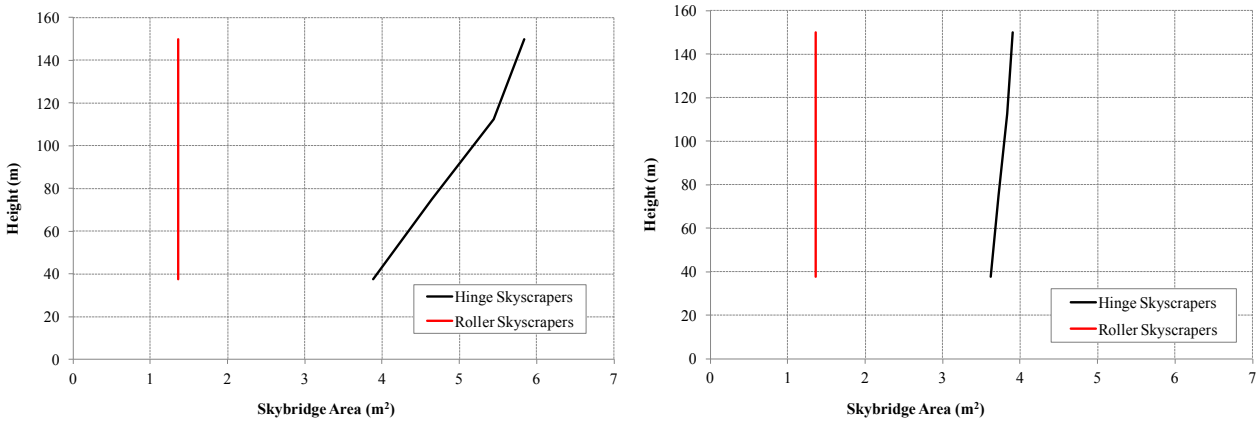

(a) With Envelope (b) No Envelope

Figure 7-8: 16-Skyscraper Box, HWHS Site, Total Skybridge Areas

7.3 64-Skyscraper Box - HWLS Site

The overall lightest design is the hinge system with envelope, see Table 7-7. This is 9.9 percent less than the roller-connected system and 7.7 percent less than the no skybridge system. It is also 11 percent less than without an envelope. This is the most dramatic comparison of all the other connected skyscraper systems. The envelope leads to lower volume for the hinge system, but a higher volume for the roller and no skybridge systems. Figure 7-10 and Figure 7-11 indicate that core, column, and outrigger volumes are more for exterior skyscrapers in the roller system than for the hinge system. The optimal designs of hinge and roller systems without envelope are essentially the same.

Figure 7-12 shows that the hinge system with envelope has larger skybridges than the roller system with envelope. This indicates that the primary difference between the roller system with envelope and the hinge system with envelope is that material is reallocated from the exterior skyscrapers to the skybridges, resulting in a lighter design. The skybridges are at the fourth

interval, and the smallest are at the bottom interval. This is a similar trend to the 16-skyscraper box.

Natural periods are lower for exterior skyscrapers than for the interior skyscrapers, see Table 7-8. Lateral wind displacements, shown in Figure 7-9, indicate that the hinge system with envelope better distributes lateral load to all skyscrapers than does the roller system. The roller interior skyscrapers do not displace at all where exterior skyscrapers displace significantly more than hinge skyscrapers. For systems without envelope, lateral displacements are about the same for all skyscrapers in hinge and roller systems.

Table 7-9 shows that for the hinge case while minimum thickness controls the core and megacolumn design, seismic stress also contributes to their design. Outriggers are controlled by seismic stress and nothing controls skybridge design. Note that wind drift controls the roller and no skybridge cases where it does not for the hinge case, further indicating that hinge skybridges distribute lateral wind load between skyscrapers. In addition, wind drift has a significant effect on the hinge skybridge case without envelope, further indicating that the envelope significantly reduces wind load and overall volume.

Table 7-7: 64-Skyscraper Box, HWLS Site, Optimum Volume Values

Volumes (m^3)	# Sky-scrapers	With Envelope			No Envelope		
		Hinge Skybridge	Roller Skybridge	No Skybridge	Hinge Skybridge	Roller Skybridge	No Skybridge
Exterior Skyscraper Core Vol	28	3,183	3,899	3,924	3,511	3,602	3,613
Exterior Skyscraper Column Vol		2,916	3,568	3,454	3,213	3,296	3,179
Exterior Skyscraper Outrigger Vol		61	371	392	208	214	208
Interior Skyscraper Core Vol	36	3,132	3,133	3,128	3,487	3,482	3,483
Interior Skyscraper Column Vol		2,915	2,910	2,752	3,240	3,235	3,064
Interior Skyscraper Outrigger Vol		55	56	59	193	152	164
Total Skybridge Vol	--	5,834	2,969	--	3,200	2,969	--
Total System Vol	--	398,051	442,002	431,358	446,422	449,403	437,582

Table 7-8: 64-Skyscraper Box, HWLS Site, Optimum Periods

Period(s)	With Envelope			No Envelope		
	Hinge Skybridge	Roller Skybridge	No Skybridge	Hinge Skybridge	Roller Skybridge	No Skybridge
Exterior Skyscraper Period	--	4.819-5.129	4.802-5.116	--	5.377-5.412	5.396
Interior Skyscraper Period	--	6.956	7.066	--	5.668	5.633
System Period	6.879	--	--	5.535	--	--

Table 7-9: 64-Skyscraper Box, HWLS Site, Controlling Constraints

Controlling Constraint	With Envelope			No Envelope		
	Hinge Skybridge	Roller Skybridge	No Skybridge	Hinge Skybridge	Roller Skybridge	No Skybridge
Wind Stress Controls Core/Columns	9%	23%	23%	57%	57%	57%
Seismic Stress Controls Core/Columns	34%	26%	26%	0%	0%	0%
Min Thickness Controls Core/Columns	57%	51%	51%	43%	43%	43%
Nothing Controls Core/Columns	0%	0%	0%	0%	0%	0%
Wind Stress Controls Outriggers	0%	20%	20%	57%	74%	71%
Seismic Stress Controls Outriggers	46%	17%	0%	0%	0%	0%
Outriggers Deleted	0%	17%	34%	0%	0%	0%
Nothing Controls Outriggers	54%	46%	46%	43%	26%	29%
Wind Stress Controls Skybridges	34%	0%	0%	71%	0%	0%
Seismic Stress Controls Skybridges	0%	0%	0%	0%	0%	0%
Gravity Stress Controls Skybridges	0%	100%	0%	14%	100%	0%
Nothing Controls Skybridges	66%	0%	0%	14%	0%	0%
Max Wind Drift / Allowable	0.273	1.000	1.000	0.808	0.908	0.913
Max Seismic Drift / Allowable	0.069	0.070	0.076	0.059	0.060	0.060

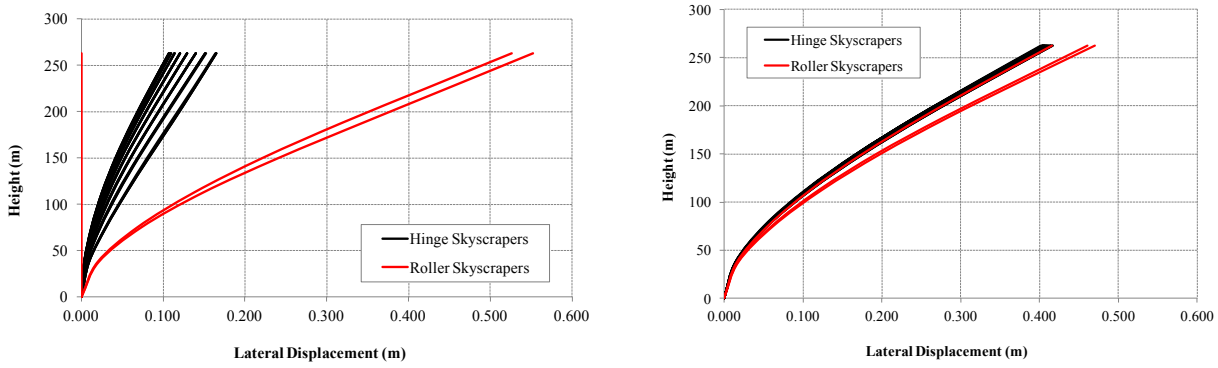

(a) With Envelope (b) No Envelope

Figure 7-9: 64-Skyscraper Box, HWLS Site, Wind Displacements

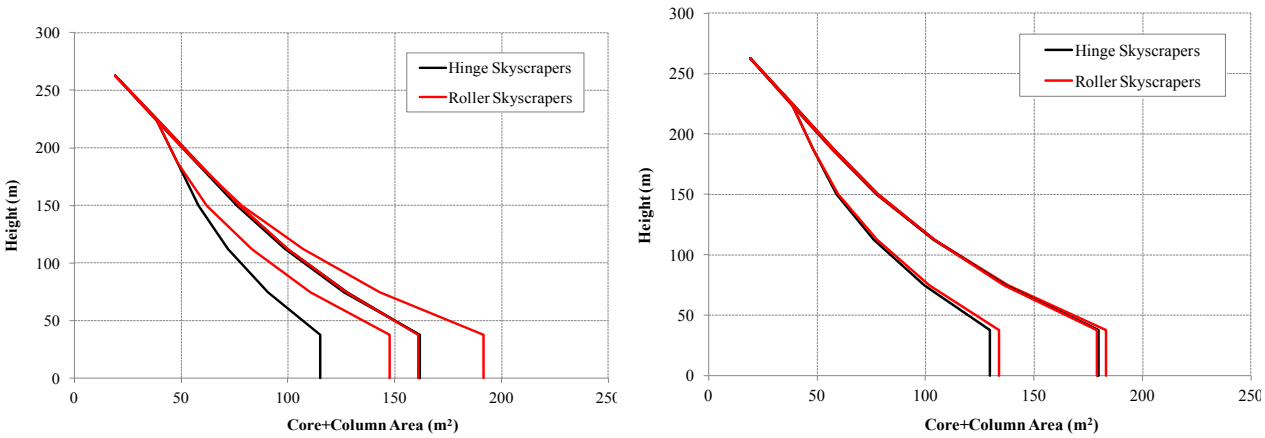

(a) With Envelope (b) No Envelope

Figure 7-10: 64-Skyscraper Box, HWLS Site, Combined Core and Column Areas

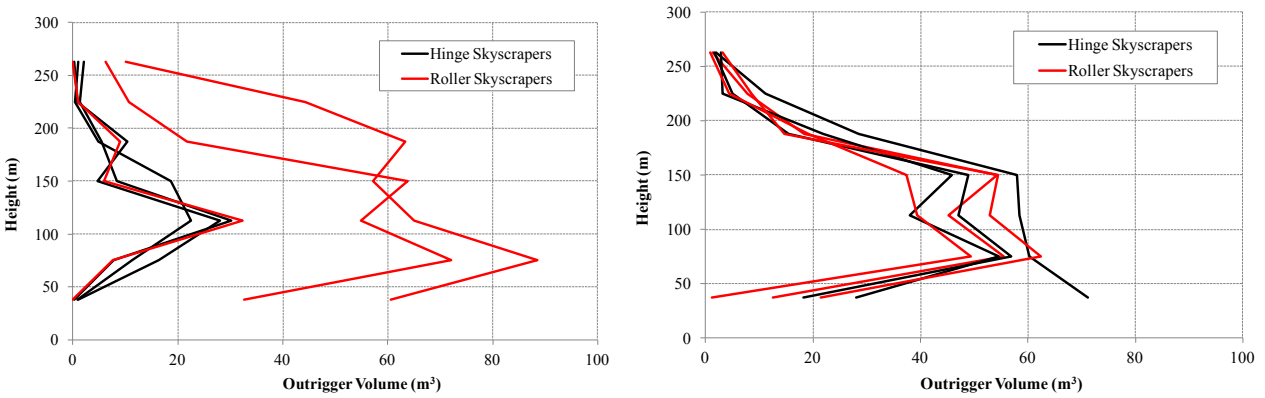

(a) With Envelope (b) No Envelope

Figure 7-11: 64-Skyscraper Box, HWLS Site, Outrigger Volumes

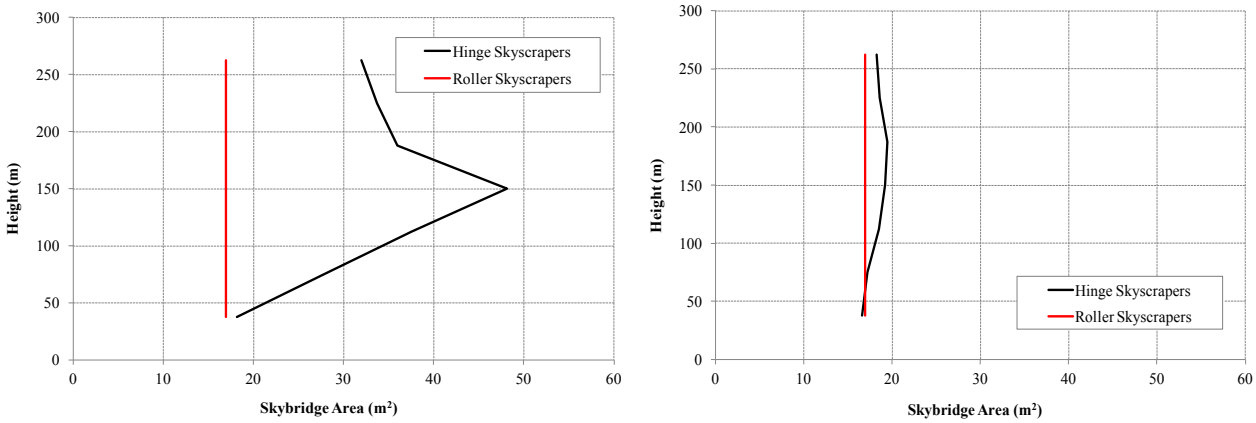

(a) With Envelope (b) No Envelope

Figure 7-12: 64-Skyscraper Box, HWLS Site, Total Skybridge Areas

7.4 64-Skyscraper Box - HWHS Site

From Table 7-10, the overall lightest design is the hinge system with envelope. This design is 6.4 percent less volume than the roller system with envelope. The trend of increasing hinge skybridges to distribute exterior wind load to interior skyscrapers also extends to the high-seismic site (recall, this was not the case for the 16 box HWHS site). An envelope also contributes to reduction in the overall volume of the hinge system. While the difference in volume between hinge and roller is not as great as it was for the low-seismic site, there is still a significant improvement using hinge skybridges and envelope.

Table 7-12 shows that core, megacolumns, and outriggers are controlled by seismic stress. Similar to the low seismic site, nothing controls skybridge design and wind drift controls the roller and no skybridge cases.

Table 7-10: 64-Skyscraper Box, HWHS Site, Optimum Volume Values

Volumes (m^3)	# Sky-scrapers	With Envelope			No Envelope		
		Hinge Skybridge	Roller Skybridge	No Skybridge	Hinge Skybridge	Roller Skybridge	No Skybridge
Exterior Skyscraper Core Vol	28	3,410	3,895	3,936	3,525	3,606	3,618
Exterior Skyscraper Column Vol		3,124	3,565	3,464	3,225	3,299	3,183
Exterior Skyscraper Outrigger Vol		152	372	394	225	212	204
Interior Skyscraper Core Vol	36	3,409	3,411	3,405	3,506	3,492	3,501
Interior Skyscraper Column Vol		3,172	3,168	2,995	3,258	3,244	3,080
Interior Skyscraper Outrigger Vol		149	153	143	194	161	155
Total Skybridge Vol	--	5,236	2,969	--	3,283	2,969	--
Total System Vol	--	434,695	464,570	453,764	449,110	450,504	438,626

Table 7-11: 64-Skyscraper Box, HWHS Site, Optimum Periods

Period(s)	With Envelope			No Envelope		
	Hinge Skybridge	Roller Skybridge	No Skybridge	Hinge Skybridge	Roller Skybridge	No Skybridge
Exterior Skyscraper Period	--	4.82-5.119	4.794-5.116	--	5.361-5.373	5.375
Interior Skyscraper Period	--	5.690	5.725	--	5.558	5.570
System Period	5.688	--	--	5.455	--	--

Table 7-12: 64-Skyscraper Box, HWHS Site, Controlling Constraints

Controlling Constraint	With Envelope			No Envelope		
	Hinge Skybridge	Roller Skybridge	No Skybridge	Hinge Skybridge	Roller Skybridge	No Skybridge
Wind Stress Controls Core/Columns	0%	23%	23%	57%	40%	57%
Seismic Stress Controls Core/Columns	57%	34%	34%	0%	17%	0%
Min Thickness Controls Core/Columns	43%	43%	43%	31%	43%	43%
Nothing Controls Core/Columns	0%	0%	0%	11%	0%	0%
Wind Stress Controls Outriggers	0%	20%	20%	23%	34%	31%
Seismic Stress Controls Outriggers	69%	51%	51%	43%	51%	51%
Outriggers Deleted	0%	0%	0%	0%	9%	0%
Nothing Controls Outriggers	31%	29%	29%	34%	6%	17%
Wind Stress Controls Skybridges	41%	0%	0%	66%	0%	0%
Seismic Stress Controls Skybridges	0%	0%	0%	0%	0%	0%
Gravity Stress Controls Skybridges	0%	100%	0%	0%	100%	0%
Nothing Controls Skybridges	59%	0%	0%	34%	0%	0%
Max Wind Drift / Allowable	0.202	1.000	1.000	0.756	0.875	0.885
Max Seismic Drift / Allowable	0.120	0.120	0.122	0.122	0.121	0.122

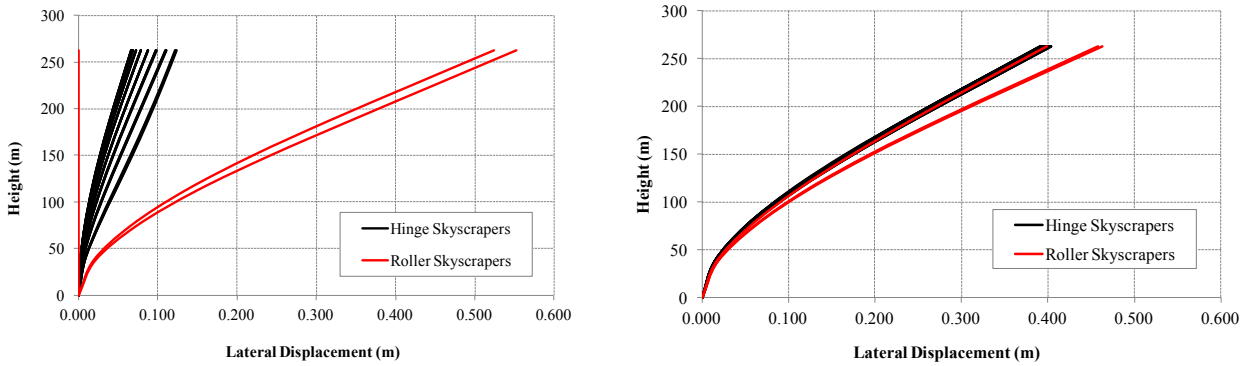

(a) With Envelope (b) No Envelope

Figure 7-13: 64-Skyscraper Box, HWHS Site, Wind Displacements

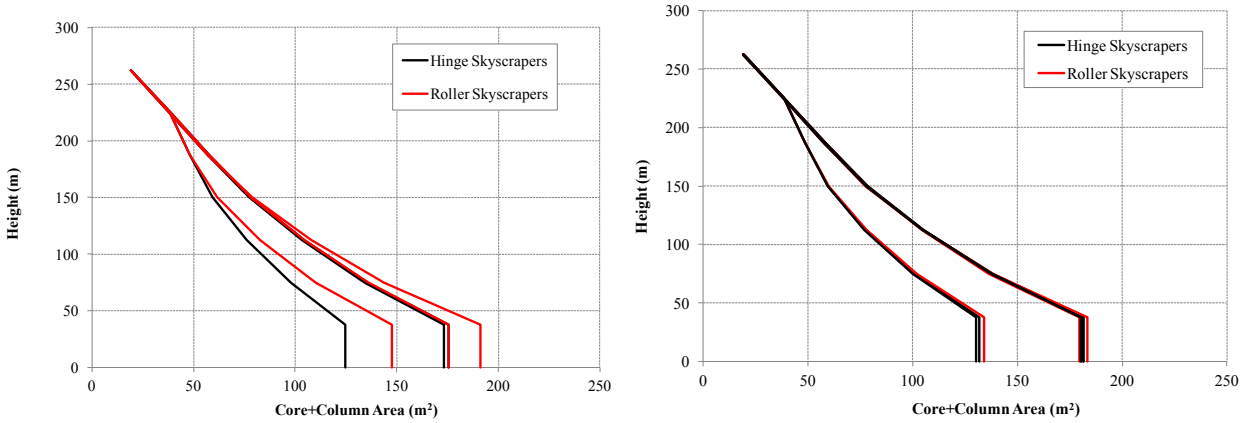

(a) With Envelope (b) No Envelope

Figure 7-14: 64-Skyscraper Box, HWHS Site, Combined Core and Column Areas

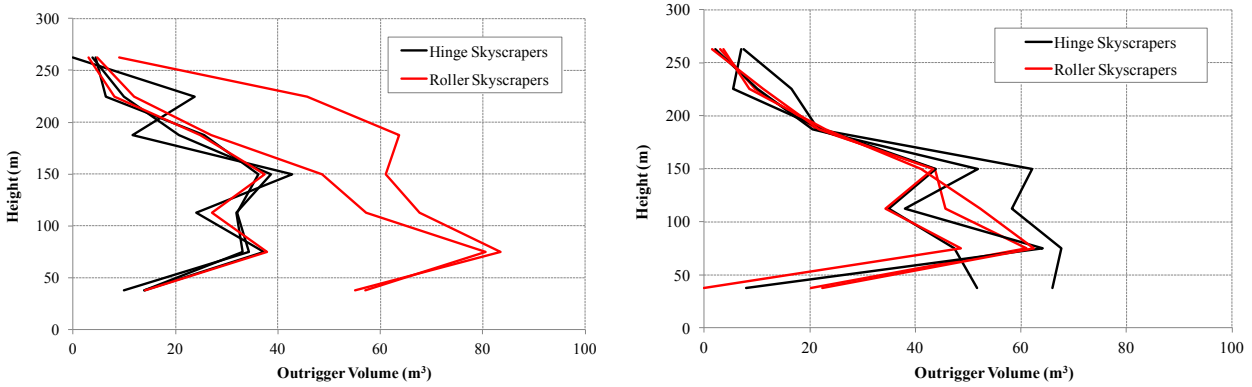

(a) With Envelope (b) No Envelope

Figure 7-15: 64-Skyscraper Box, HWHS Site, Outrigger Volumes

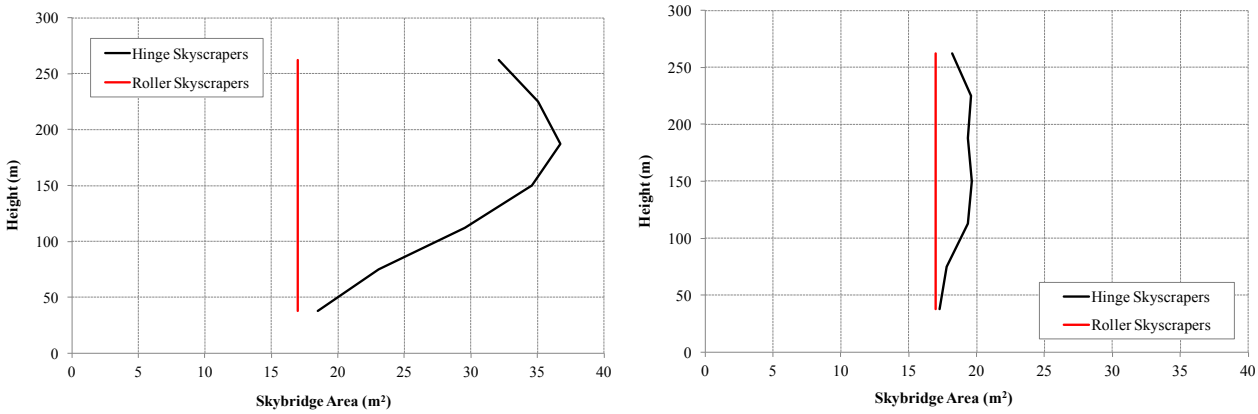

(a) With Envelope (b) No Envelope

Figure 7-16: 64-Skyscraper Box, HWHS Site, Total Skybridge Areas

7.5 25-Skyscraper Pyramid - HWLS Site

The overall lightest design is the design without skybridges and with envelope, as illustrated in Table 7-13. The benefits of large hinge skybridges and lower exterior skyscraper volume in box systems is not as prominent for pyramid systems. Optimized results are very similar between the hinge and roller systems. The difference in volume is only 0.08 percent and 0.13 percent, for with and without envelope, respectively. This small difference can be attributed

to algorithm convergence margins wherein, designs can be assumed to be the same. All skyscraper volumes are very similar if not identical between hinge, roller, with and without envelope cases. The exterior skyscrapers (2-Interval) are the stiffest indicated by the lowest building period and lowest displacement, as illustrated in Table 7-14 and Figure 7-17. Only the skybridges vary between hinge and roller systems, as illustrated in Figure 7-18. The skybridges decrease in height for the hinge system because there are fewer total skybridges at the top of a pyramid than at the bottom.

Table 7-15 shows that core and megacolumns are controlled by minimum thickness, most of the outriggers are deleted altogether, and skybridges are controlled by wind stress. Note that drift does not control any of the designs.

Hinge pyramid systems do not perform as well as hinge box systems because exterior skyscrapers in a pyramid system to not extend to the full height of the overall system. Interior skyscrapers therefore protrude above exterior skyscrapers, making it necessary for them to take some of the lateral load. Therefore, the process of re-distributing volume from skyscrapers to skybridges no longer works to reduce overall volume.

Table 7-13: 25-Skyscraper Pyramid, HWLS Site, Optimum Volume Values

Volumes (m^3)	# Sky-scrapers	With Envelope			No Envelope		
		Hinge Skybridge	Roller Skybridge	No Skybridge	Hinge Skybridge	Roller Skybridge	No Skybridge
2 Interval Skyscraper Core Vol	16	750	750	750	750	750	750
2 Interval Skyscraper Column Vol		685	685	660	685	685	660
2 Interval Skyscraper Outrigger Vol		0	0	0	0	0	0
3 Interval Skyscraper Core Vol	8	1,125	1,125	1,125	1,125	1,125	1,125
3 Interval Skyscraper Column Vol		1,032	1,032	989	1,032	1,032	989
3 Interval Skyscraper Outrigger Vol		0	0	0	0	0	0
4 Interval Skyscraper Core Vol	1	1,515	1,541	1,515	1,515	1,541	1,542
4 Interval Skyscraper Column Vol		1,367	1,391	1,332	1,368	1,391	1,356
4 Interval Skyscraper Outrigger Vol		7	44	18	8	44	44
Total Skybridge Vol	--	390	348	--	375	348	--
Total System Vol	--	43,500	43,542	42,335	43,484	43,542	42,411

Table 7-14: 25-Skyscraper Pyramid, HWLS Site, Optimum Periods

Period(s)	With Envelope			No Envelope		
	Hinge Skybridge	Roller Skybridge	No Skybridge	Hinge Skybridge	Roller Skybridge	No Skybridge
2 Interval Skyscraper Period	--	1.353-1.357	1.345-1.345	--	1.353-1.357	1.345
3 Interval Skyscraper Period	--	2.704-2.711	2.684-2.684	--	2.704-2.711	2.684
4 Interval Skyscraper Period	--	3.214	3.745	--	3.214	3.203
System Period	2.400	--	--	2.401	--	--

Table 7-15: 25-Skyscraper Pyramid, HWLS Site, Controlling Constraints

Controlling Constraint	With Envelope			No Envelope		
	Hinge Skybridge	Roller Skybridge	No Skybridge	Hinge Skybridge	Roller Skybridge	No Skybridge
Wind Stress Controls Core/Columns	0%	0%	0%	0%	6%	6%
Seismic Stress Controls Core/Columns	6%	6%	6%	6%	0%	0%
Min Thickness Controls Core/Columns	94%	94%	94%	94%	94%	94%
Nothing Controls Core/Columns	0%	0%	0%	0%	0%	0%
Wind Stress Controls Outriggers	0%	0%	0%	0%	0%	0%
Seismic Stress Controls Outriggers	13%	19%	19%	6%	0%	0%
Outriggers Deleted	88%	75%	75%	94%	81%	81%
Nothing Controls Outriggers	0%	6%	6%	0%	19%	19%
Wind Stress Controls Skybridges	71%	0%	0%	57%	0%	0%
Seismic Stress Controls Skybridges	0%	0%	0%	21%	0%	0%
Gravity Stress Controls Skybridges	14%	100%	0%	21%	100%	0%
Nothing Controls Skybridges	14%	0%	0%	0%	0%	0%
Max Wind Drift / Allowable	0.087	0.176	0.176	0.263	0.358	0.357
Max Seismic Drift / Allowable	0.052	0.051	0.051	0.052	0.046	0.045

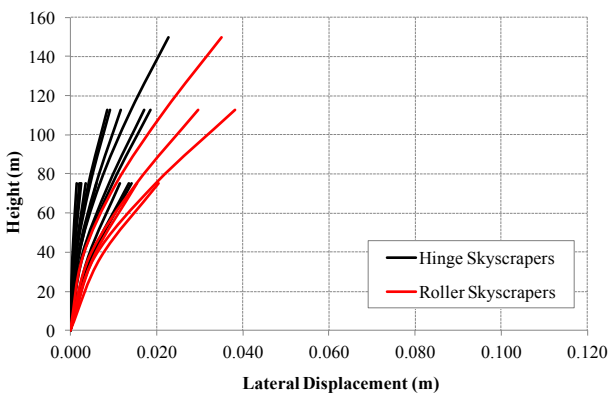

(a) With Envelope

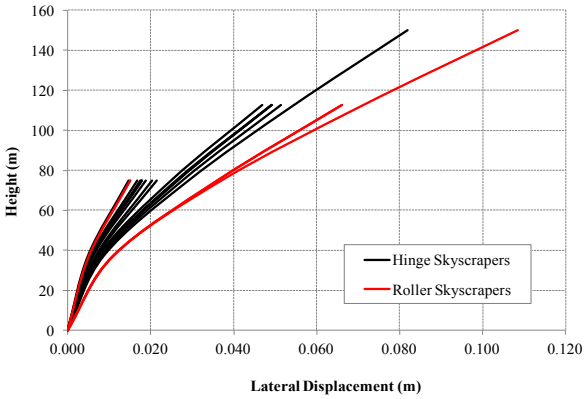

(b) No Envelope

Figure 7-17: 25-Skyscraper Pyramid, HWLS Site, Wind Displacements

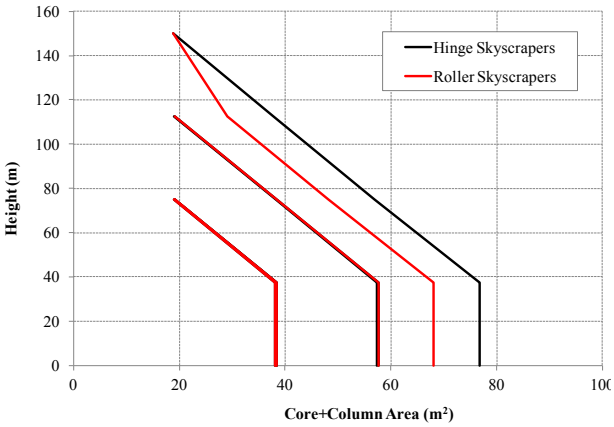

(a) With Envelope

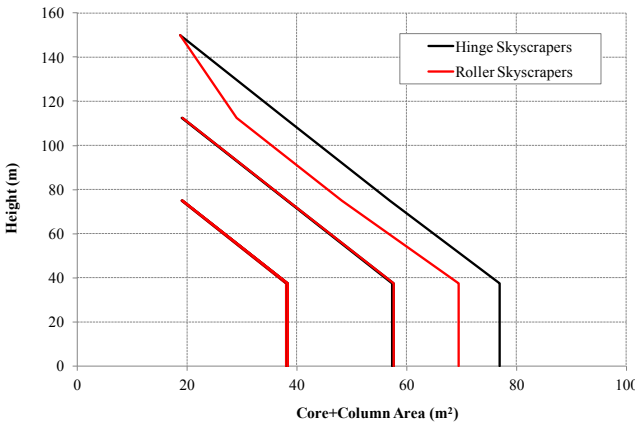

(b) No Envelope

Figure 7-18: 25-Skyscraper Pyramid, HWLS Site, Combined Core and Column Areas

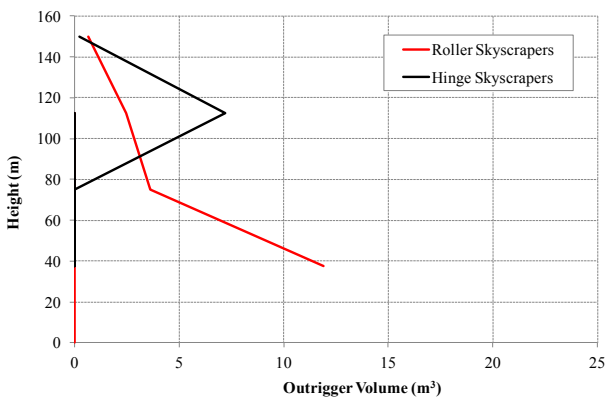

(a) With Envelope

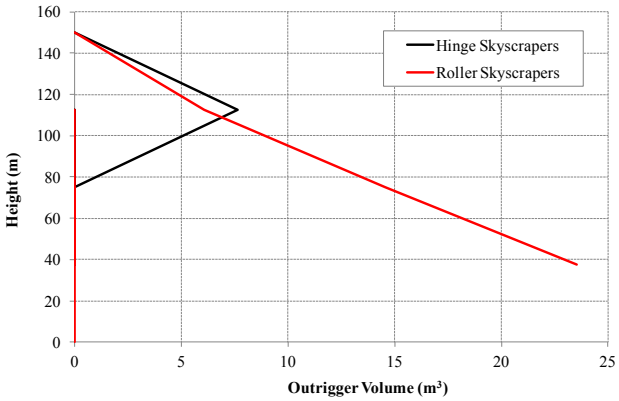

(b) No Envelope

Figure 7-19: 25-Skyscraper Pyramid, HWLS Site, Outrigger Volumes

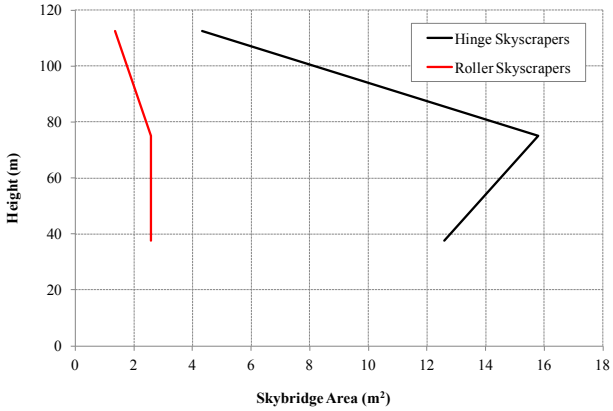

(a) With Envelope

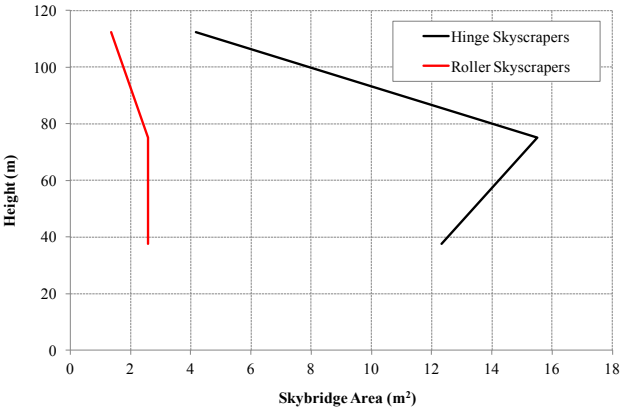

(b) No Envelope

Figure 7-20: 25-Skyscraper Pyramid, HWLS Site, Total Skybridge Areas

7.6 25-Skyscraper Pyramid - HWHS Site

The overall lightest design is the design without skybridges and without envelope, as illustrated in Table 7-16. This design volume is within 2.2 percent of the hinge system with an envelope. Volume differences between the roller and hinge systems for with and without envelope are 0 percent and 0.09 percent, respectively. This is even less of a difference than for

the low-seismic site, further indicating that the designs are identical to each other within algorithm convergence tolerances.

Similar to the low seismic site, Table 7-18 shows that core and megacolumns are controlled by minimum thickness and skybridges are controlled by wind stress. Outriggers, however, are controlled by seismic stress.

Figure 7-22 through Figure 7-24 are similar to those for the low seismic site except that the skyscrapers are heavier for the high-seismic case. It is obvious that the interior skyscrapers of the 25-skyscraper pyramid should be the heaviest since they are the tallest skyscrapers. In addition, they still take some of the wind load at the top of the skyscraper. Similar to the 25 pyramid HWLS site, optimization is not able to re-distribute volume from exterior skyscrapers to skybridges to decrease overall system volume as it could for the box systems.

Table 7-16: 25-Skyscraper Pyramid, HWHS Site, Optimum Volume Values

Volumes (m^3)	# Sky-scrapers	With Envelope			No Envelope		
		Hinge Skybridge	Roller Skybridge	No Skybridge	Hinge Skybridge	Roller Skybridge	No Skybridge
2 Interval Skyscraper Core Vol	16	750	750	750	750	750	750
2 Interval Skyscraper Column Vol		685	685	660	685	685	660
2 Interval Skyscraper Outrigger Vol		7	0	0	7	0	0
3 Interval Skyscraper Core Vol	8	1,125	1,132	1,132	1,126	1,132	1,132
3 Interval Skyscraper Column Vol		1,032	1,038	996	1,033	1,038	996
3 Interval Skyscraper Outrigger Vol		44	57	52	50	57	52
4 Interval Skyscraper Core Vol	1	1,615	1,599	1,600	1,617	1,599	1,543
4 Interval Skyscraper Column Vol		1,459	1,445	1,408	1,461	1,445	1,357
4 Interval Skyscraper Outrigger Vol		90	87	80	77	87	41
Total Skybridge Vol	--	416	348	--	389	348	--
Total System Vol	--	44,259	44,258	43,080	44,294	44,258	42,935

Table 7-17: 25-Skyscraper Pyramid, HWHS Site, Optimum Periods

Period(s)	With Envelope			No Envelope		
	Hinge Skybridge	Roller Skybridge	No Skybridge	Hinge Skybridge	Roller Skybridge	No Skybridge
2 Interval Skyscraper Period	--	1.353-1.357	1.345-1.345	--	1.353-1.357	1.345
3 Interval Skyscraper Period	--	1.9-1.902	1.912-1.912	--	1.9-1.902	1.912
4 Interval Skyscraper Period	--	2.698	2.718	--	2.698	3.195
System Period	1.860	--	--	1.849	--	--

Table 7-18: 25-Skyscraper Pyramid, HWHS Site, Controlling Constraints

Controlling Constraint	With Envelope			No Envelope		
	Hinge Skybridge	Roller Skybridge	No Skybridge	Hinge Skybridge	Roller Skybridge	No Skybridge
Wind Stress Controls Core/Columns	0%	0%	0%	0%	0%	6%
Seismic Stress Controls Core/Columns	6%	19%	19%	13%	19%	13%
Min Thickness Controls Core/Columns	94%	81%	81%	88%	81%	81%
Nothing Controls Core/Columns	0%	0%	0%	0%	0%	0%
Wind Stress Controls Outriggers	0%	0%	0%	0%	0%	0%
Seismic Stress Controls Outriggers	50%	56%	56%	56%	56%	38%
Outriggers Deleted	19%	38%	38%	13%	38%	38%
Nothing Controls Outriggers	31%	6%	6%	31%	6%	25%
Wind Stress Controls Skybridges	71%	0%	0%	21%	0%	0%
Seismic Stress Controls Skybridges	0%	0%	0%	43%	0%	0%
Gravity Stress Controls Skybridges	14%	100%	0%	29%	100%	0%
Nothing Controls Skybridges	14%	0%	0%	7%	0%	0%
Max Wind Drift / Allowable	0.071	0.128	0.128	0.149	0.239	0.349
Max Seismic Drift / Allowable	0.090	0.082	0.082	0.088	0.082	0.068

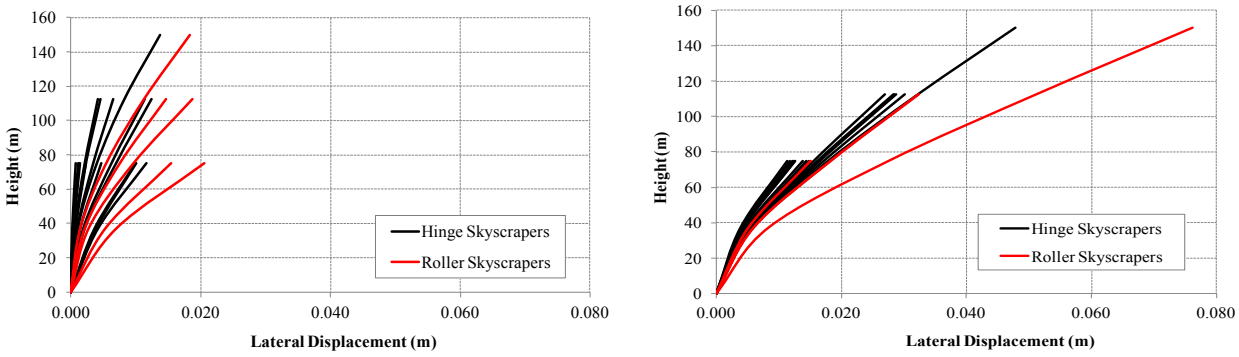

(a) With Envelope (b) No Envelope

Figure 7-21: 25-Skyscraper Pyramid, HWHS Site, Wind Displacements

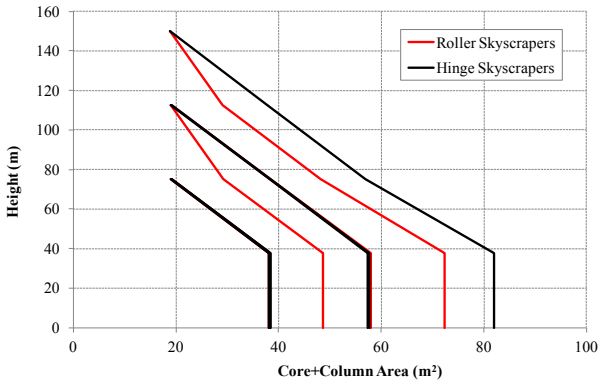

(a) With Envelope

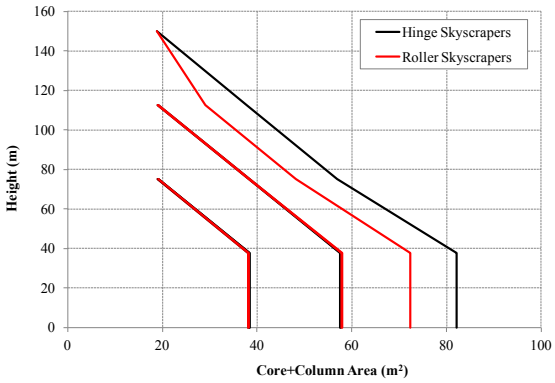

(b) No Envelope

Figure 7-22: 25-Skyscraper Pyramid, HWHS Site, Combined Core and Column Areas

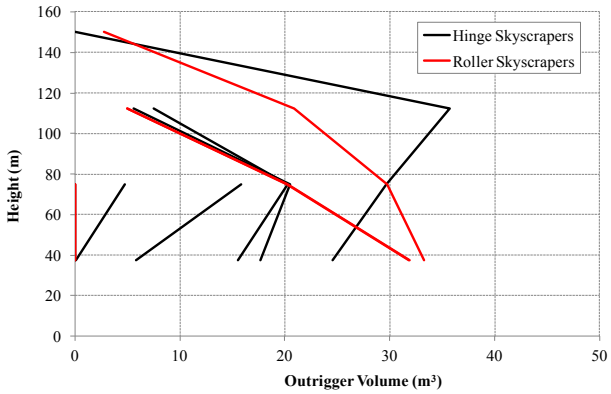

(a) With Envelope

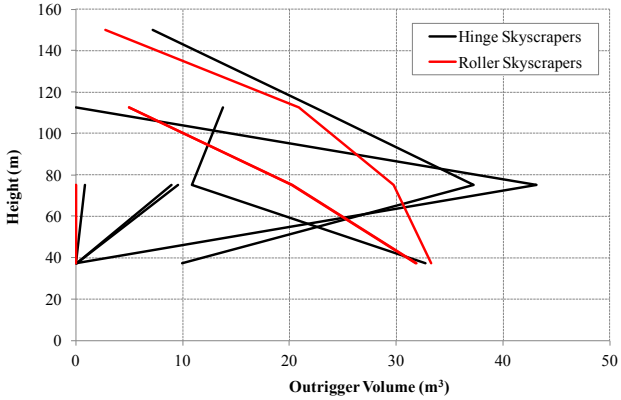

(b) No Envelope

Figure 7-23: 25-Skyscraper Pyramid, HWHS Site, Outrigger Volumes

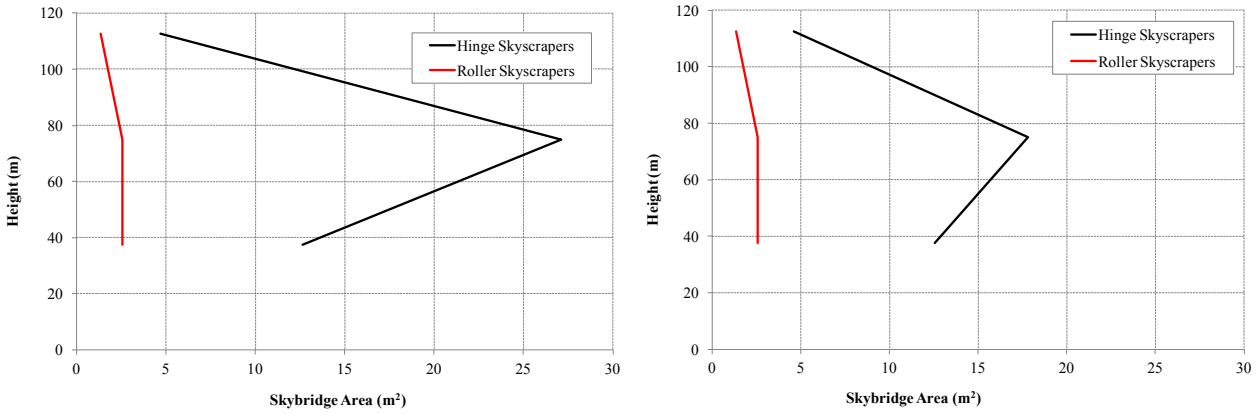

(a) With Envelope (b) No Envelope

Figure 7-24: 25-Skyscraper Pyramid, HWHS Site, Total Skybridge Areas

7.7 100-Skyscraper Pyramid - HWLS Site

The overall lightest design is the no skybridge with envelope system, as shown in Table 7-19. However, the hinge skybridge system is comparable in volume and differs by only 3 percent. Similar to the behavior of the 25-skyscraper pyramid, the overall volume is close if not the same between hinge and roller skybridge systems with a difference of 0 percent and 0.7 percent for with and without envelope, respectively. This can be seen from the close correlation in combined core and megacolumn volumes shown in Figure 7-26. The envelope makes the hinge system lighter by 3.7 percent, the roller system by 4.3 percent, and the no skybridge system by 4.5 percent. The biggest difference between with and without envelope designs can be seen from the large outrigger volumes without envelope in Figure 7-27. Figure 7-28 shows little variation in skybridge areas between with and without envelope cases, but a large difference between hinge and roller cases. The stiffest skyscrapers are the exterior or 3-interval skyscrapers, as shown by the lowest natural period in Table 7-20 and lowest lateral displacement in Figure 7-25.

Table 7-21 shows that core and megacolumns are controlled by minimum thickness, outriggers are not controlled by any dominant constraint, and skybridges are controlled by wind stress. While drift does not control the designs, it does have more of an effect on the no envelope cases.

Table 7-19: 100-Skyscraper Pyramid, HWLS Site, Optimum Volume Values

Volumes (m^3)	# Sky-scrapers	With Envelope			No Envelope		
		Hinge Skybridge	Roller Skybridge	No Skybridge	Hinge Skybridge	Roller Skybridge	No Skybridge
3 Interval Skyscraper Core Vol	36	1,125	1,125	1,125	1,125	1,125	1,125
3 Interval Skyscraper Column Vol		1,030	1,030	989	1,031	1,030	989
3 Interval Skyscraper Outrigger Vol		14	3	3	33	0	0
4 Interval Skyscraper Core Vol	28	1,500	1,516	1,516	1,549	1,541	1,542
4 Interval Skyscraper Column Vol		1,383	1,397	1,334	1,428	1,420	1,356
4 Interval Skyscraper Outrigger Vol		17	18	15	48	45	44
5 Interval Skyscraper Core Vol	20	1,966	1,977	1,977	2,034	2,057	2,059
5 Interval Skyscraper Column Vol		1,814	1,823	1,739	1,878	1,897	1,812
5 Interval Skyscraper Outrigger Vol		7	26	23	13	79	78
6 Interval Skyscraper Core Vol	12	2,528	2,510	2,509	2,623	2,703	2,712
6 Interval Skyscraper Column Vol		2,333	2,315	2,207	2,421	2,494	2,385
6 Interval Skyscraper Outrigger Vol		47	50	49	98	119	113
7 Interval Skyscraper Core Vol	4	3,164	3,134	3,133	3,316	3,499	3,506
7 Interval Skyscraper Column Vol		2,913	2,884	2,755	3,053	3,221	3,084
7 Interval Skyscraper Outrigger Vol		55	54	53	133	154	158
Total Skybridge Vol	--	3,530	2,803	--	4,538	2,803	--
Total System Vol	--	321,962	321,835	312,193	334,265	336,469	326,980

Table 7-20: 100-Skyscraper Pyramid, HWLS Site, Optimum Periods

Period(s)	With Envelope			No Envelope		
	Hinge Skybridge	Roller Skybridge	No Skybridge	Hinge Skybridge	Roller Skybridge	No Skybridge
3 Interval Skyscraper Period	--	2.526-2.701	2.504-2.684	--	2.701-2.709	2.684
4 Interval Skyscraper Period	--	3.754-3.758	3.780	--	3.204-3.22	3.203
5 Interval Skyscraper Period	--	4.812-4.829	4.836	--	3.978-3.984	3.965
6 Interval Skyscraper Period	--	5.792-5.797	5.777-5.81	--	4.767-4.773	4.764
7 Interval Skyscraper Period	--	6.955	6.970	--	5.606	5.603
System Period	4.820	--	--	4.135	--	--

Table 7-21: 100-Skyscraper Pyramid, HWLS Site, Controlling Constraints

Controlling Constraint	With Envelope			No Envelope		
	Hinge Skybridge	Roller Skybridge	No Skybridge	Hinge Skybridge	Roller Skybridge	No Skybridge
Wind Stress Controls Core/Columns	0%	0%	0%	40%	37%	37%
Seismic Stress Controls Core/Columns	30%	26%	28%	0%	0%	0%
Min Thickness Controls Core/Columns	70%	74%	72%	60%	63%	63%
Nothing Controls Core/Columns	0%	0%	0%	0%	0%	0%
Wind Stress Controls Outriggers	0%	0%	2%	33%	42%	0%
Seismic Stress Controls Outriggers	30%	49%	44%	0%	0%	40%
Outriggers Deleted	23%	30%	30%	0%	33%	28%
Nothing Controls Outriggers	47%	21%	23%	67%	26%	33%
Wind Stress Controls Skybridges	90%	0%	0%	78%	0%	0%
Seismic Stress Controls Skybridges	3%	0%	0%	3%	0%	0%
Gravity Stress Controls Skybridges	0%	100%	0%	5%	100%	0%
Nothing Controls Skybridges	8%	0%	0%	15%	0%	0%
Max Wind Drift / Allowable	0.139	0.391	0.391	0.604	0.825	0.842
Max Seismic Drift / Allowable	0.072	0.069	0.070	0.068	0.058	0.058

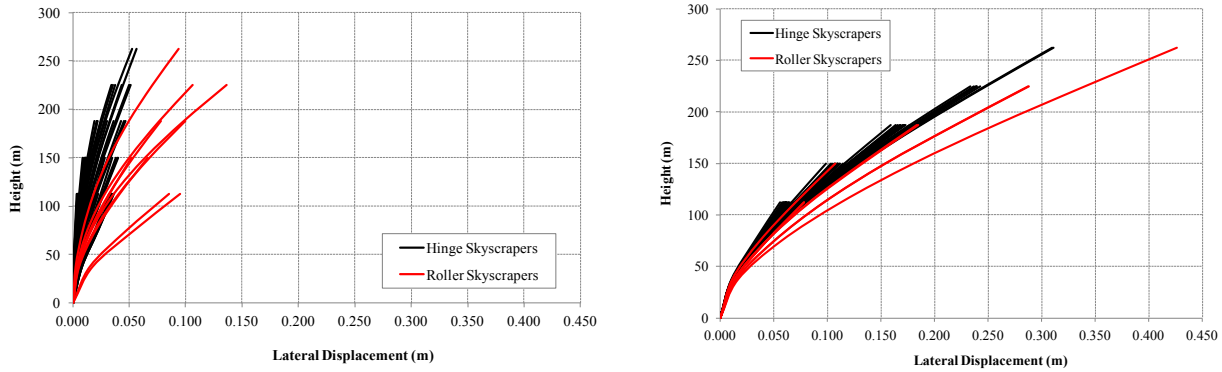

(a) With Envelope (b) No Envelope

Figure 7-25: 100-Skyscraper Pyramid, HWLS Site, Wind Displacements

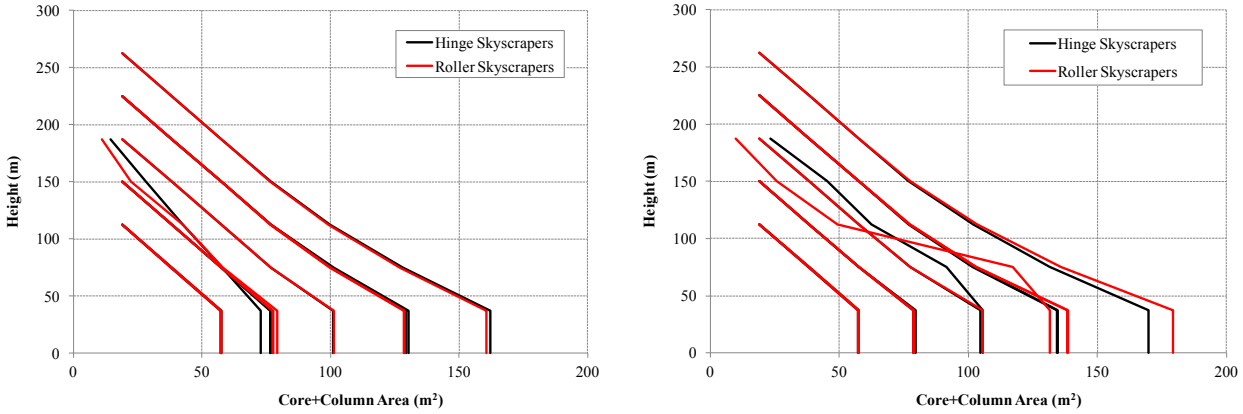

(a) With Envelope (b) No Envelope

Figure 7-26: 100-Skyscraper Pyramid, HWLS Site, Combined Core and Column Areas

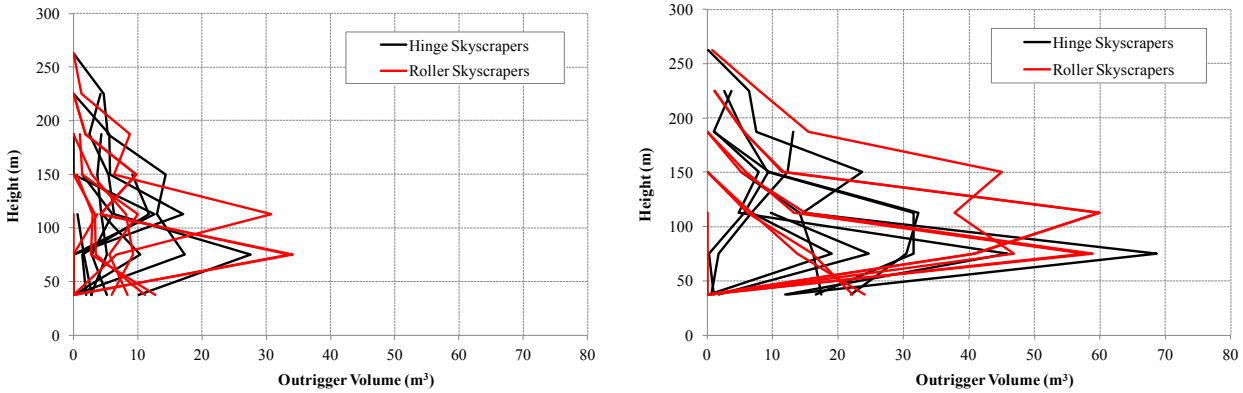

(a) With Envelope (b) No Envelope

Figure 7-27: 100-Skyscraper Pyramid, HWLS Site, Outrigger Volumes

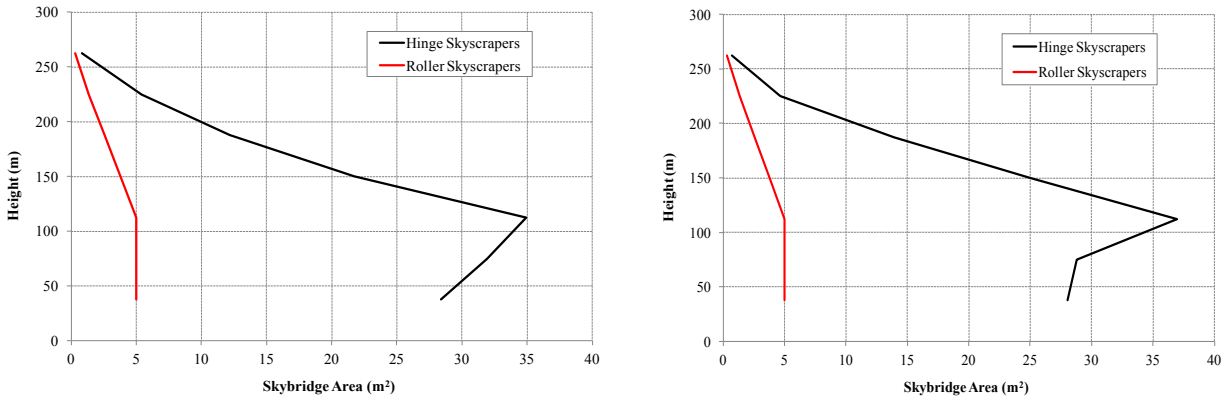

(a) With Envelope (b) No Envelope

Figure 7-28: 100-Skyscraper Pyramid, HWLS Site, Total Skybridge Areas

7.8 100-Skyscraper Pyramid - HWHS Site

The overall lightest design is the no skybridge without building envelope system, as shown in Table 7-22. The hinge skybridge system without envelope is comparable in volume and within 2.9 percent. The same is true for the high-seismic site as it was for low-seismic in that optimal designs between hinge and roller systems are essentially the same. The difference in volume between hinge and roller systems is 0.9 percent and 1.1 percent for with and without envelope, respectively. Figure 7-30 shows that the core and megacolumn areas are less for the roller system than for the hinge system for both with and without envelope. Figure 7-31 shows that the outrigger volumes are at a maximum at the second interval and are about the same in magnitude between with and without envelope. Table 7-24 shows that core and megacolumns are controlled by minimum thickness, outriggers are not controlled by any dominant constraint, and skybridges are controlled by wind stress. Note that drift does not control any of the designs. Neither the hinge skybridge nor the envelope help to reduce overall volume for the 100 skyscraper pyramid.

Table 7-22: 100-Skyscraper Pyramid, HWHS Site, Optimum Volume Values

Volumes (m^3)	# Sky-scrapers	With Envelope			No Envelope		
		Hinge Skybridge	Roller Skybridge	No Skybridge	Hinge Skybridge	Roller Skybridge	No Skybridge
3 Interval Skyscraper Core Vol	36	1,126	1,134	1,131	1,126	1,133	1,132
3 Interval Skyscraper Column Vol		1,031	1,038	995	1,031	1,037	996
3 Interval Skyscraper Outrigger Vol		37	54	55	32	53	52
4 Interval Skyscraper Core Vol	28	1,571	1,599	1,600	1,573	1,599	1,600
4 Interval Skyscraper Column Vol		1,449	1,474	1,408	1,450	1,474	1,408
4 Interval Skyscraper Outrigger Vol		61	87	80	58	87	80
5 Interval Skyscraper Core Vol	20	2,096	2,124	2,122	2,094	2,123	2,122
5 Interval Skyscraper Column Vol		1,934	1,959	1,866	1,932	1,959	1,866
5 Interval Skyscraper Outrigger Vol		19	96	93	21	97	93
6 Interval Skyscraper Core Vol	12	2,720	2,725	2,721	2,743	2,738	2,741
6 Interval Skyscraper Column Vol		2,511	2,515	2,394	2,532	2,526	2,411
6 Interval Skyscraper Outrigger Vol		127	113	109	155	119	115
7 Interval Skyscraper Core Vol	4	3,453	3,407	3,405	3,446	3,507	3,514
7 Interval Skyscraper Column Vol		3,181	3,136	2,995	3,174	3,228	3,091
7 Interval Skyscraper Outrigger Vol		156	151	143	160	161	160
Total Skybridge Vol	--	5,306	2,803	--	5,139	2,803	--
Total System Vol	--	342,979	346,031	335,406	343,405	347,089	336,816

Table 7-23: 100-Skyscraper Pyramid, HWHS Site, Optimum Periods

Period(s)	With Envelope			No Envelope		
	Hinge Skybridge	Roller Skybridge	No Skybridge	Hinge Skybridge	Roller Skybridge	No Skybridge
3 Interval Skyscraper Period	--	1.904-1.979	1.906-1.908	--	1.91-2.018	1.912
4 Interval Skyscraper Period	--	2.704-2.707	2.718	--	2.704-2.707	2.718
5 Interval Skyscraper Period	--	3.634-3.641	3.654	--	3.637-3.639	3.654
6 Interval Skyscraper Period	--	4.652-4.653	4.675	--	4.614-4.616	4.629
7 Interval Skyscraper Period	--	5.681	5.725	--	5.534	5.545
System Period	3.831	--	--	3.835	--	--

Table 7-24: 100-Skyscraper Pyramid, HWHS Site, Controlling Constraints

Controlling Constraint	With Envelope			No Envelope		
	Hinge Skybridge	Roller Skybridge	No Skybridge	Hinge Skybridge	Roller Skybridge	No Skybridge
Wind Stress Controls Core/Columns	0%	0%	0%	0%	9%	12%
Seismic Stress Controls Core/Columns	42%	42%	42%	37%	33%	30%
Min Thickness Controls Core/Columns	35%	58%	58%	37%	58%	58%
Nothing Controls Core/Columns	23%	0%	0%	26%	0%	0%
Wind Stress Controls Outriggers	0%	0%	0%	0%	0%	5%
Seismic Stress Controls Outriggers	56%	79%	84%	47%	79%	79%
Outriggers Deleted	0%	12%	9%	0%	12%	5%
Nothing Controls Outriggers	44%	9%	7%	53%	9%	12%
Wind Stress Controls Skybridges	45%	0%	0%	38%	0%	0%
Seismic Stress Controls Skybridges	8%	0%	0%	15%	0%	0%
Gravity Stress Controls Skybridges	0%	100%	0%	3%	100%	0%
Nothing Controls Skybridges	48%	0%	0%	45%	0%	0%
Max Wind Drift / Allowable	0.106	0.228	0.236	0.472	0.778	0.801
Max Seismic Drift / Allowable	0.124	0.121	0.122	0.126	0.121	0.122

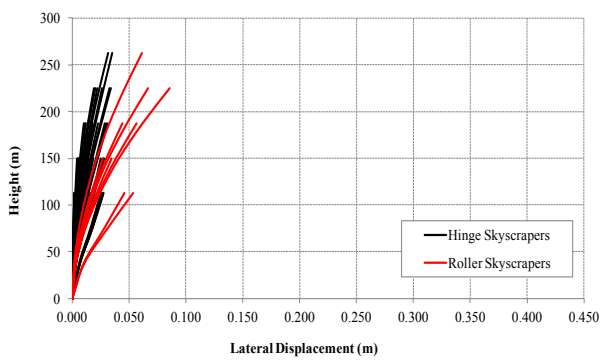

(a) With Envelope

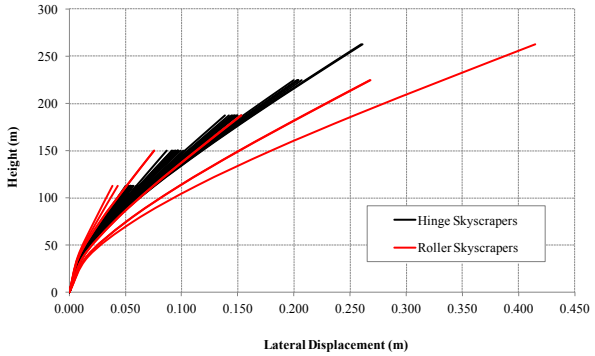

(b) No Envelope

Figure 7-29: 100-Skyscraper Pyramid, HWHS Site, Wind Displacements

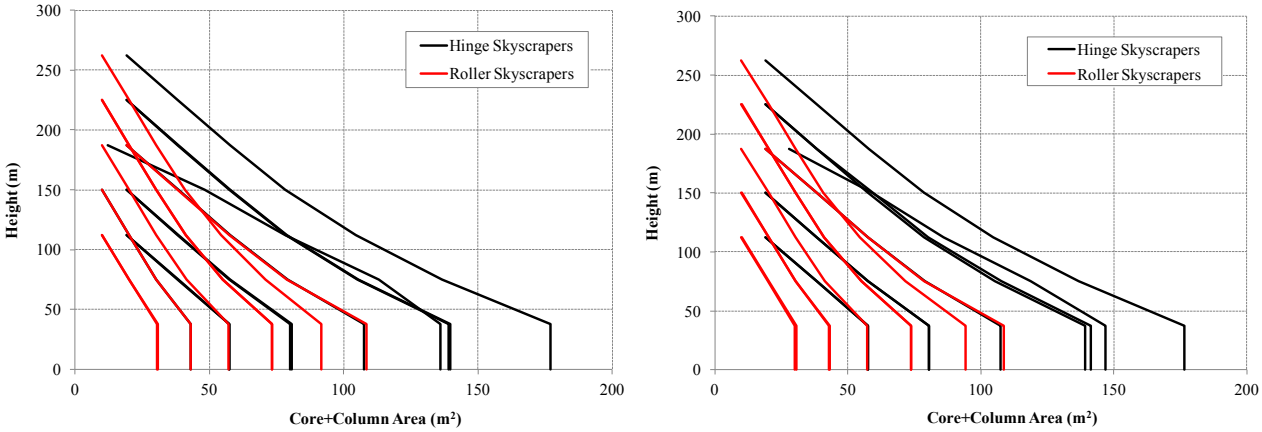

(a) With Envelope (b) No Envelope

Figure 7-30: 100-Skyscraper Pyramid, HWHS Site, Combined Core and Column Areas

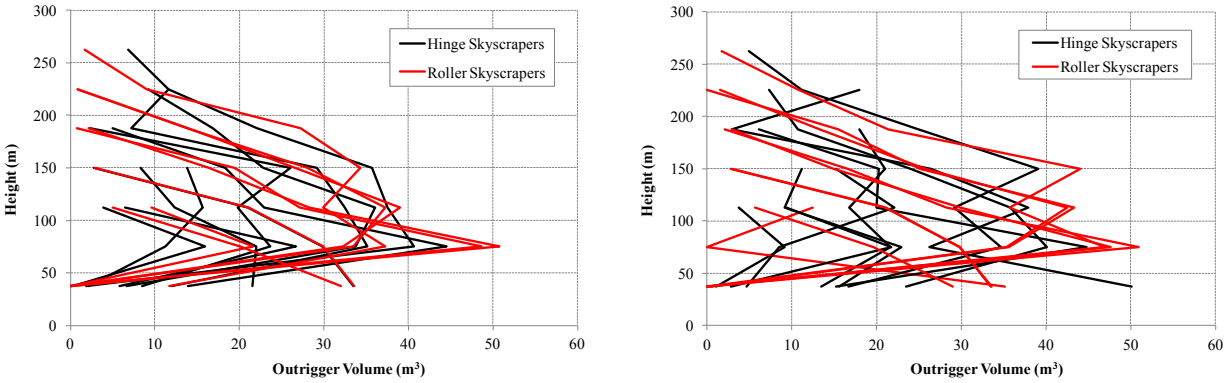

(a) With Envelope (b) No Envelope

Figure 7-31: 100-Skyscraper Pyramid, HWHS Site, Outrigger Volumes

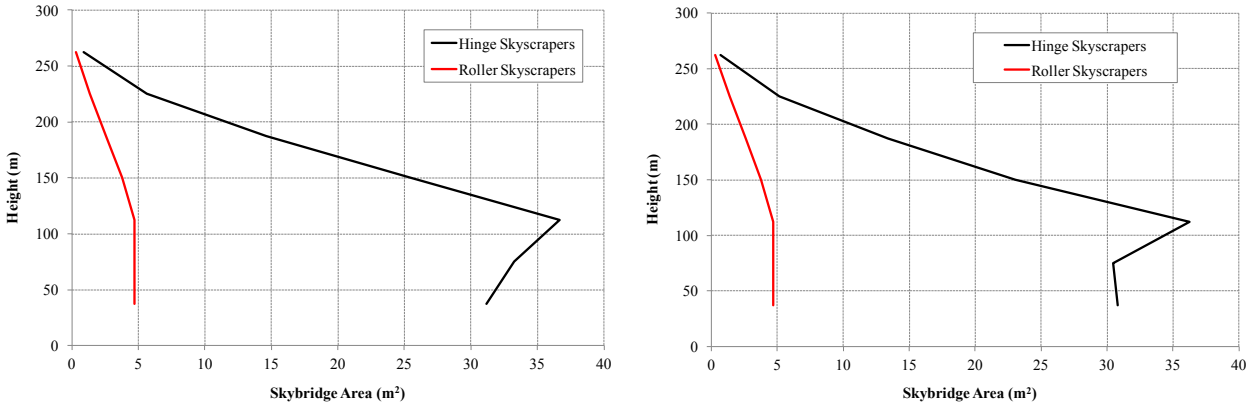

(a) With Envelope (b) No Envelope

Figure 7-32: 100-Skyscraper Pyramid, HWHS Site, Total Skybridge Areas

7.9 Summary

A summary of optimum volume results have been collected in Table 7-25 for all optimization problems. Note that the no skybridge volumes are between 2 percent and 3 percent less than the roller skybridge volumes in every case. This difference is attributable to the additional volume of the skybridges, and the additional volume in the skyscrapers that must support skybridge weight. In comparing roller skybridge volumes to hinge skybridge volumes, the difference is less than 1 percent except for three cases: 1) 16-skyscraper box with envelope at the HWLS site where hinge skybridge is 4.4 percent less than roller skybridge, 2) 64-skyscraper box with envelope at the HWLS site where hinge skybridge is 9.9 percent less than roller skybridge, and 3) 64-skyscraper box with envelope at the HWHS site where hinge skybridge is 6.4 percent less than roller skybridge. These three hinge skybridge with envelope cases will be referred to as the ideal cases, which are bold in Table 7-25. Note that for these ideal cases, the optimum volumes are even less than the no skybridge cases.

It was reported in Chapter 5 that the envelope reduced the total wind load on the system by 57 percent for the 16-skyscraper box, 78 percent for the 64-skyscraper box, 69 percent for the 25-skyscraper pyramid, and 85 percent for the 100-skyscraper pyramid. Note that these dramatic wind load reductions did not lead to reduced optimum volumes at the HWHS site except for the ideal case (64-skyscraper box with envelope and hinge skybridge). Indeed, the difference in optimum volume between no-envelope and with-envelope was less than 1 percent at the HWHS site for all cases except for the 64-skyscraper box cases where there was an increase of 3.4 percent for the no skybridge case, an increase of 3.1 percent for the roller skybridge case, and a decrease of 3.8 percent for the ideal hinge skybridge case. All this suggests that at the HWHS site, seismic lateral loading generally controlled over wind lateral loading. At the HWLS site, the envelope had more effect on reducing optimum volume for the larger systems. The volume reduction due to the envelope was between 3 percent and 5 percent for the 100-skyscraper pyramid, and between 1 percent and 2 percent for the 64-skyscraper box except for the ideal hinge skybridge case where the reduction was 10.8 percent, significantly larger than other cases. For smaller systems at the HWLS site, the volume change due to envelope was less than 1 percent for the 25-skyscraper pyramid, and increased by 1.9 percent for the 16-skyscraper box except for the ideal hinge skybridge case where it decreased by 2.1 percent.

Table 7-25: Optimum Volumes of all Optimization Problems

HWLS Site				
		No SB	Roller SB	Hinge SB
16 Box	No Env	47,580	48,852	48,584
	With Env	48,468	49,755	**47,550**
64 Box	No Env	437,582	449,403	446,422
	With Env	431,358	442,002	**398,051**
25 Pyramid	No Env	42,411	43,542	43,484
	With Env	42,335	43,467	43,500
100 Pyramid	No Env	326,980	336,469	334,265
	With Env	312,193	321,835	321,962
HWHS Site				
		No SB	Roller SB	Hinge SB
16 Box	No Env	49,367	50,786	50,827
	With Env	49,586	50,936	50,945
64 Box	No Env	438,626	450,504	449,110
	With Env	453,764	464,570	**434,695**
25 Pyramid	No Env	42,935	44,258	44,294
	With Env	43,080	44,258	44,259
100 Pyramid	No Env	336,816	347,089	343,405
	With Env	335,406	346,031	342,979

CHAPTER 8. CONCLUSIONS

The need for this work was to build sustainable cities that are friendly to people, planet, and prosperity. Skybridges and atria satisfy this need. Skybridges and atria between buildings are becoming popular, and there is a need to understand their effect on structural behavior and design. The purpose of this work was to understand the behavior and design of skyscrapers connected with skybridges and atria. To do so, it was necessary to develop a fast and accurate approximate model for analyzing connected skyscraper systems. It was also necessary to formulate appropriate optimization problems, and to develop an efficient optimization strategy. A specific objective was to understand the effect of hinge-connected skybridges on optimal design. Another specific objective was to investigate whether it was possible to reduce total structural material with skybridges and atria. All of these objectives have been accomplished and resulting contributions will now be elaborated.

A significant contribution of this work was to establish an understanding of the behavior and design of skyscrapers connected with skybridges. The optimum total volume of roller skybridge systems were generally between two and three 3 percent more than for no skybridge systems, which can be attributed to the weight of the skybridges. The difference in optimum total volume between roller skybridge systems and hinge skybridge systems was less than 1 percent except for three ideal cases: 1) 16-skyscraper box with envelope at the HWLS site where hinge skybridge is 4.4 percent less than roller skybridge, 2) 64-skyscraper box with envelope at the HWLS site where hinge skybridge is 9.9 percent less than roller skybridge, and 3) 64-skyscraper

box with envelope at the HWHS site where hinge skybridge is 6.4 percent less than roller skybridge. In these ideal cases, the optimum total volumes were even less than those of the no skybridge cases.

Also established was an understanding of the behavior and design of skyscrapers connected with atria. The envelope reduced total system wind load dramatically (up to 85 percent), but this did not make much difference in the optimum total volumes at the HWHS site, except for the ideal case mentioned in the previous paragraph. At the HWLS site, the atria resulted in reduction of optimum total volume for the larger systems, particularly for the aforementioned ideal cases.

Another contribution was the discovery of when and why it is possible to reduce total structural material with skybridges and atria. Clearly, the envelope and hinge skybridges significantly reduced the optimum total volume for the three ideal cases. In these cases, the hinge-connected skybridges distributed the envelope-reduced wind load among all the skyscrapers, and the volume and stiffness of the skyscrapers were uniform throughout the system. For roller-connected skybridges and no skybridges with envelope, the perimeter skyscrapers were much bigger and stiffer to resist the wind load. In the ideal cases, material was effectively transferred from the perimeter skyscrapers to the skybridges. The efficiency of the ideal cases was greater for the HWLS site than for the HWHS site, and greater for systems where the proportion of the number of exterior skyscrapers to the number of interior skyscrapers was low. All of the ideal cases were box systems. For large pyramid systems, the envelope led to reduced volume at the HWLS site, but the hinge-connected skybridges did not lead to volume reductions over roller-connected skybridges. This is because the perimeter skyscrapers were shorter and smaller, and were not resisting as much wind load as in the box systems.

This work developed the SSSM, which dramatically reduced computational time and computer memory requirements over the FEM. For the 16-skyscraper box, the number of DOF's was reduced by a factor of 41, the number memory bytes was reduced by a factor of 4,323, and the number of computational FLOPS was reduced by a factor of 115,403. These reductions made possible the optimization of the large systems of up to 100 skyscrapers considered in this work. The accuracy of the SSSM compared against the FEM was within 3 percent for displacements and 6 percent for stresses in cores, megacolumns, and skybridges. For outrigger stress, the maximum difference between the SSSM and FEM was 17 percent for one particular outrigger member, but the average difference in outrigger stress was 7 percent.

Another contribution was the formulation of appropriate optimization problems. Four skyscraper systems at two sites with and without envelope, and with roller-connected skybridges, hinge-connected skybridges, and no skybridges were optimized for a total of 48 optimization problems. Skyscrapers and skybridges were grouped into classes and divided vertically into intervals, and design variables were assigned to each class, each interval, and each component (core, outrigger, and skybridge). The total volume of concrete in the core, megacolumns, outriggers, and skybridges was minimized, and constraints on lateral drift and stress in each component were satisfied. The optimum volume of material in the core and megacolumns was constrained to monotonically decrease with height. The optimum volume of material in outriggers varied with height and from class to class with no apparent trend. The optimum volume of material in skybridges was constant at the minimum bound for roller-connected skybridges, and was generally greatest at medium height for hinge-connected skybridges, and the smallest volumes were at the top of pyramid systems and at the bottom of box systems.

Also contributed was the development of efficient optimization strategies. The optimization of systems without skybridges and systems with roller-connected skybridges was decomposed into a series of single-skyscraper optimization subproblems, each of which could be efficiently solved with a single execution of the GRG gradient-based algorithm in a matter of seconds. Such decomposition could not be made for systems with hinge-connected skybridges because of the structural interaction between skyscrapers under lateral loading. The optimization strategy consisted of a series of executions of the SQP algorithm, followed by executions of the GRG algorithm, followed by executions of a discrete genetic algorithm. The genetic algorithm made significant progress for the large systems.

As the use of skybridges and atria between skyscrapers continues to increase, the impact of this work will also increase. Future work should involve the investigation of systems with skyscrapers that are more slender than those in this investigation. Skyscraper slenderness increases the effect of wind-controlled design, and hinge-connected skybridges and atria could produce even greater reduction in total material volume. Future work could also include investigation of systems with a variety of skyscrapers with different heights, plan shapes and dimensions, and structural configurations beyond the core-megacolumn-outrigger configuration. Future work could also investigate nonlinear and dynamic effects as well as rigid-connected skybridges.

REFERENCES

Abada, G. (2004). "2004 On Site Review Report: Petronas Office Towers, Kuala Lumpur, Malaysia."

AISC (2013). "City Creek Center Retractable Roof." *13 Structural Steel Buildings That Dazzle*, <http://www.bdcnetwork.com/13-structural-steel-buildings-dazzle>. (September 10, 2013, 2013).

Anderson, C. (2011). "Connective Atrium." *Design By Many*, <http://www.designbymany.com/project/connective-atrium>. (September 10, 2013, 2013).

Architect (2009). "Shanghai World Financial Center." *architectmagazine.com*, S. W. F. Center, ed., Hanley Wood, LLC.

Architectism (2011). "Highlight Towers." *architectism.com.* Munich, Germany.

Architen, L. (2008). "Radclyffe School." <http://www.architen.com/projects/radclyffe-school>. (September 10, 2013, 2013).

Architen, L. (2011). "Trinity Walk Shopping Centre, ETFE Roof." <http://www.architen.com/projects/trinity-walk-shopping-centre-etfe-roof>. (September 10, 2013, 2013).

ASCE (2010). *Minimum Design Loads for Buildings and Other Structures*, Reston, VA.

Balling, R. J. (1991). *Computer Structural Analysis* BYU Academic Publishing, Provo, UT.

Bessey, R. P. (2012). "Structural Design of Flexible ETFE Atrium Enclosures Using a Cable-Spring Support System." MS, Brigham Young University, Provo.

Bharti, S. D. (2010). "Seismic response analysis of adjacent buildings connected with MR dampers." *Engineering Structures*, 32(8), 2122-2133.

Boggs, D. W., and Hosoya, N. (2001). "Wind-Tunnel Techniques to Address Structures with Multiple Coupled Interactions." *Proceedings of the 2001 Structures Congress & Exposition.* Washington D.C.

Chan, C.-M., and Wong, K.-M. (2008). "Structural topology and element sizing design optimisation of tall steel frameworks using a hybrid OC–GA method." *Struct Multidisc Optim*, 35(5), 473-488.

CTBUH (2007). "Nina Tower." *The Skyscraper Center*, <http://skyscrapercenter.com/hong-kong/nina-tower/421/>. (April 30, 2013, 2013).

CTBUH (2011). "Kingdom Centere." *The Skyscraper Center*, <http://www.skyscrapercenter.com/building.php?building_id=494>. (April 29, 2013, 2013).

CTBUH (2013). "Kajima Corporation Buildings-Demolition Method." <http://www.ctbuh.org/TallBuildings/FeaturedTallBuildings/FeaturedTallBuildingArchive2012/KajimaCorporationBuildingsDemolitionMethod/tabid/3870/language/en-GB/Default.aspx>. (May 1, 2013, 2013).

Davis, J. G. (2012). "New GSA Federal Office Building." <http://www.davisconstruction.com/datasheetpage.aspx?ProjectID=974746>. (September 10, 2013, 2013).
Emporis (2008). "Shanghai World Financial Center." <http://www.emporis.com/building/shanghaiworldfinancialcenter-shanghai-china>. (April 29, 2013, 2013).
Emporis (2012). "Highlight Munich Business Towers." <http://www.emporis.com/complex/highlight-munich-business-towers-munich-germany>. (May 1, 2013, 2013).
Engineers, (2010). "The Pinnacle@Duxton." *The Singapore Engineer*, Jun 2010.
Foiltec, V. (2013). "The Avenues of Kuwait." <http://www.archello.com/en/project/avenues-kuwait>. (September 10, 2013, 2013).
Haklar, T. (2009). "10 Fascinating Skybridges." <http://www.theworldgeography.com/2013/08/skybridges.html>. (September 3, 2013, 2013).
Hartley-Parkinson, R. (2011). "And the trophy goes to... China's silliest supertower build in a village of 2,000 farmers." *Rueters*, H. Tower, ed., Associated Newspapers Ltd.
Holl, S. A. (2009). "Linked Hybrid." <http://www.stevenholl.com/project-detail.php?id=58>. (May 1, 2013, 2013).
IBC (2006). *International Building Code*, Country Club Hills, IL.
Johnson, B. (2008). "Failsworth School, Oldham: ETFE Roof Steelwork." <http://www.belljohnson.com/projects.html>. (September 10, 2013, 2013).
Kundu, S., Seto, K., and Sugino, S. (2002). "Genetic algorithm application to vibration control of tall flexible structures." *Proc., Electronic Design, Test and Applications, 2002. Proceedings. The First IEEE International Workshop*, 333-337.
Lee, J. S. (2013). "Accuracy of a Simplified Analysis Model for Modern Skyscrapers." M.S., Brigham Young University, Provo.
Liang, B., and Liu, J. (2009) "A New Approach to Determine the Optimum Structure System for Tall Buildings Using Artificial Neural Networks and PSO Algorithms." *Proc., Natural Computation, 2009. ICNC '09. Fifth International Conference*, 181-185.
Lim, J. (2007). "Wind-induced response of structurally coupled twin tall buildings." *Wind and Structures, An International Journal*, 10(4), 383-398.
Lim, J., Bienkiewicz, B., and Richards, E. (2011). "Modeling of structural coupling for assessment of modal properties of twin tall buildings with a skybridge." *Journal of Wind Engineering and Industrial Aerodynamics*, 99(5), 615-623.
Liu, D. K., Yang, Y. L., and Li, Q. S. (2003). "Optimum positioning of actuators in tall buildings using genetic algorithm." *Computers & Structures*, 81(32), 2823-2827.
Lu, X. (2009). "Shaking table model tests on a complex high-rise building with two towers of different height connected by trusses." *Structural Design of Tall and Special Buildings*, 18(7), 765-788.
Luco, J. E. (1998). "Control of the seismic response of a composite tall building modelled by two interconnected shear beams." *Earthquake Engineering and Structural Dynamics*, 27(3), 205-223.
Luong, A., and Kwok, M. (2012). "Finding Structural Solutions by Connecting Towers." *CTBUH Journal*(III), 26-31.

Mettler, L., Gregg, T., and Schaffer, H. (1988). *Population Genetics and Evolution*, Prentice Hall, Englewood Cliffs, NJ.
Ming, L. J., Suan, T. P., and Toh, W. (2010). "HDB's next generation of eco-districts at Punggol and eco-modernisation of existing towns." *The IES Journal Part A: Civil & Structural Engineering*, 3(3), 203-209.
Mu, Z. (2011). "Analysis of stress response for the super high rise double-tower connected structure with the trusses of changing rigidity." *Advanced Materials Research*, 291-294(PAGE), 1559-1563.
NewScientist (2006). "No way out?" *New Scientist*, 189(2538), 40-43.
Nishimura, A. (2011). "Base-isolated super high-rise RC building composed of three connected towers with vibration control systems." *Structural Concrete*, 12(2), 94-108.
Nordenson, G. a. A. (2010). "Linked Hybrid." <http://www.nordenson.com/project.php?l=name&offset=495&id=17>. (May 1, 2013, 2013).
NSC (2011). "Network Rail HQ, Milton Keynes." *Steelwork Just the Ticket*, <http://www.newsteelconstruction.com/wp/wp-content/uploads/digi/NSCNov11/index.html#/22/>. (September 10, 2013, 2013).
Parkinson, A. R. (2010). *Optimization-Based Design*, BYU Academic Publishing, Provo.
Parkinson, A. R., and Balling, R. J. (2002). "The OptdesX design optimization software." *Struct Multidisc Optim*, 23(2), 127-139.
Patel, C. C. (2010). "Seismic response of dynamically similar adjacent structures connected with viscous dampers." *IES Journal Part A: Civil & Structural Engineering*, 3(1), 1-13.
Roaf, S., Crichton, D., and Nicol, F. (2005). "Adapting Buildings and Cities for Climate Change: A 21st Century Survival Guide." Architectural Press, Oxford.
Safdie (2008). "Bureau of Alcohol, Tobacco, Firearms, and Explosives Headquarters." <http://www.msafdie.com/#/projects/bureauofalcoholtobaccofirearmsandexplosivesheadquarters>. (September 19, 2013, 2013).
SkyscraperCity (2013). "Gate of the Orient." <http://www.google.com/cse?cx=partner-pub-2024614554274860:paf3j4-c0bw&ie=ISO-8859-1&q=gate+of+the+orient&sa=Search&ref=#gsc.tab=0&gsc.q=gate%20of%20the%20orient&gsc.page=1>. (Decemeber 6, 2013, 2013).
SkyscraperPage (2013). "East Pacific Business Center." *SkyscraperPage.com*, <http://skyscraperpage.com/cities/?buildingID=34159>. (April 30, 2013, 2013).
Smith, B. S., and Salim, I. (1981). "Parameter Study of Outrigger-Braced Tall Building Structures." *Journal of the Structural Division*, 107(10), 2001-2014.
Spence, S. M. J., and Gioffrè, M. (2011). "Efficient algorithms for the reliability optimization of tall buildings." *Journal of Wind Engineering and Industrial Aerodynamics*, 99(6–7), 691-699.
Speyer, T. (2013). "Tower Place." <http://www.tishmanspeyer.com/properties/tower-place#!/properties/tower-place>. (September 10, 2013, 2013).
Toronto, U. (2009). "Hong Kong Supertall Update: Nina Tower." <http://urbantoronto.ca/forum/showthread.php/8824-Hong-Kong-Supertall-Update-Nina-Tower>. (September 3, 2013, 2013).
WikiArquitectura (2010). "Umeda Sky Building." *Buildings of the World*, <http://en.wikiarquitectura.com/index.php/Umeda_sky_building>. (May 1, 2013, 2013).
Wikipedia (2010). "Island Tower Sky Club." *Wikimedia Commons*, wikipedia.org.

Wikipedia (2013). "Union Square." <http://en.wikipedia.org/wiki/Union_Square_(Hong_Kong)#cite_note-skyscraperpage-23>. (September 3, 2013, 2013).
Wood, A. (2003). "Pavements in the sky: the skybridge in tall buildings." *Arq: Architectural Research Quarterly*, 7(3-4), 325-332.
Wood, A. (2013). "PhD for CTBUH Executive Director, Antony Wood." *CTBUH* <http://www.ctbuh.org/NewsMedia/PR_1009_AWPhD/tabid/1702/language/en-US/Default.aspx>. (April 30, 2013, 2013).
Xiaohua, S. (2009). "It's Platinum for Beijing." <http://www.chinadaily.com.cn/bw/2009-05/04/content_7739510.htm>. (July 28, 2013, 2013).
Xie, J., and Irwin, P. A. (1998). "Application of the force balance technique to a building complex." *Journal of Wind Engineering and Industrial Aerodynamics*, 77–78(0), 579-590.
Yuan, W. (2011). "Influence of connection location on dynamic characteristics of three-towers-connected high-rise building." *Advanced Materials Research*, 243-249(PAGE), 419-425.
Zhou, Y. (2011). "Study on the seismic performance of a multi-tower connected structure." *Structural Design of Tall and Special Buildings*, 20(3), 387-401.
Zimbres, E. (2006). "National Congress Complex of Brasilia." *Wikipedia.org*, B. N. Congress, ed.